

# **Heating, Ventilation and Air Conditioning Multivariable Control System with Least Energy Dissipation**

التحكم بنظام تنقية وتكييف الهواء متعدد المتغيرات مع أقل تبديد للطاقة

by

**BASIM TOUQAN**

**A thesis submitted in fulfilment**

**of the requirements for the degree of**

**DOCTOR OF PHILOSOPHY IN ARCHITECTURE AND  
SUSTAINABLE BUILT ENVIRONMENT**

at

**The British University in Dubai**

**March 2019**

## DECLARATION

I warrant that the content of this research is the direct result of my own work and that any use made in it of published or unpublished copyright material falls within the limits permitted by international copyright conventions.

I understand that a copy of my research will be deposited in the University Library for permanent retention.

I hereby agree that the material mentioned above for which I am author and copyright holder may be copied and distributed by The British University in Dubai for the purposes of research, private study or education and that The British University in Dubai may recover from purchasers the costs incurred in such copying and distribution, where appropriate.

I understand that The British University in Dubai may make a digital copy available in the institutional repository.

I understand that I may apply to the University to retain the right to withhold or to restrict access to my thesis for a period which shall not normally exceed four calendar years from the congregation at which the degree is conferred, the length of the period to be specified in the application, together with the precise reasons for making that application.

*Basim Touqan*

---

Signature of the student

## **COPYRIGHT AND INFORMATION TO USERS**

The author whose copyright is declared on the title page of the work has granted to the British University in Dubai the right to lend his/her research work to users of its library and to make partial or single copies for educational and research use.

The author has also granted permission to the University to keep or make a digital copy for similar use and for the purpose of preservation of the work digitally.

Multiple copying of this work for scholarly purposes may be granted by either the author, the Registrar or the Dean only.

Copying for financial gain shall only be allowed with the author's express permission.

Any use of this work in whole or in part shall respect the moral rights of the author to be acknowledged and to reflect in good faith and without detriment the meaning of the content, and the original authorship.

## **Abstract**

The highest energy consumption in building sector is caused by building's services such as lighting units and thermal comfort systems. Heated Ventilated Air Conditioning (HVAC) system consumes approximately 50% of the total building energy bill. Many measures have been proposed to achieve energy efficient buildings. Accurate HVAC mathematical models, as well as suitable HVAC control system that leads to optimised energy consumption and improved system performance are part of the engineering efforts to achieve greater efficiency. This study is part of such engineering efforts. It concentrates on employing a ready developed reliable HVAC system mathematical model, namely hybrid distributed-lumped parameter model which handles HVAC as spatially and dimensional dispersed systems for specific HVAC components such as ventilated volume. Other components, such as fan motors, inlet and exit impedances, have physical properties that treated as concentrated lumped mass elements without compromising on the accuracy. Applying an appropriate automatic control strategy to achieve improved HVAC system performance associated with least control energy consumption is one of the major research objectives. This objective has been achieved by adopting and applying a multivariable Least Effort (LE) control technique to regulate a multivariable three inputs-three outputs HVAC system model that employs output feedback, passive compensators and proportional gains, avoiding employment of active integrators. Direct Nyquist Array (DNA), as an alternative multivariable control technique, was employed to compare with the LE performance in terms of system performance and proportional control energy cost. Contrasting the straightforward procedure used to decouple the interaction between the outputs in the LE controller, the identification of decoupling matrix in the DNA controller was based on a trial and error approach, which was very time consuming. After decoupling the plant transfer function matrix, the DNA controller was able to regulate and control the HVAC

multivariable system based on using PID loop control, but on the price of consuming higher proportional control energy cost which contravenes with global efforts to minimize energy consumption inside buildings. The ratios of proportional control energy cost between LE and DNA at the time 900 seconds following disturbance unity changes on the system outputs are 4.4/100, 39/100 and 22/100 for three different disturbance scenarios. LE controller has shown also better system performance than DNA which at the end makes it superior to the DNA control solution based on the consideration of the simplicity of each controller, the system behaviour under closed loop control and the control energy dissipation.

## خلاصة البحث

يعد قطاع المباني الأعلى استهلاكاً للطاقة بسبب خدمات المباني التي تستهلك طاقة عالية، مثل وحدات الإضاءة وأجهزة التكييف والتدفئة. ويستهلك نظام تنقية وتكييف وتدفئة الهواء لوحده حوالي ٥٠ ٪ من إجمالي فاتورة طاقة المبنى. وبهذا الخصوص تم اقتراح العديد من التدابير لتحقيق المباني الموفرة للطاقة حيث تعد النماذج الرياضية الدقيقة لأنظمة تنقية وتكييف وتدفئة الهواء وكذلك نظام التحكم المناسب المطبق عليها والذي يمتاز باستهلاك أقل للطاقة وأداء نظام محسن، جزءاً مهماً من الجهود الهندسية لتحقيق كفاءة أكبر. هذه الدراسة هي ترجمة لتلك الجهود حيث تركز على استخدام نموذج رياضي محكم لنظام تنقية وتكييف وتدفئة الهواء تم تطويره مسبقاً من قبل بعض الباحثين، وهو نموذج مختلط يجمع بين النمذجة ذات العوامل المتكثلة والعوامل المنتشرة الذي يتعامل مع بعض مكونات نظام تنقية وتكييف وتدفئة الهواء كنظم ذات خواص فيزيائية منتشرة مكانياً مثل المساحات الواسعة المطلوب تهويتها في حين تعامل بعض المكونات الأخرى للنظام، مثل المحركات الكهربائية لمراوح التهوية، وموانع دخول وخروج الهواء، تعامل كعناصر ذات عوامل فيزيائية متكثلة ومركزة دون المساس بالدقة. يعد تطبيق استراتيجية التحكم الآلي المناسبة لتحقيق أداء محسن لنظام تنقية وتكييف وتدفئة الهواء المرتبط بأقل استهلاك للطاقة هو أحد تيسير لا فادهاً لهذه الدراسة حيث تم تحقيق هذا الهدف بالفعل من خلال اعتماد وتطبيق ما يسمى تقنية التحكم ذات جهد التحكم الأدنى متعدد المتغيرات لتنظيم عمل نموذج رياضي لنظام تنقية وتكييف وتدفئة الهواء ذات ثلاث مداخل وثلاث مخارج والذي يستخدم تغذية المخارج العكسية ومعوذات التحكم الخاملة، كما ويتجنب استخدام عناصر تكامل نشطة. و بنفس الوقت، تم استخدام مصفوفة نيكويست المباشرة متعددة المتغيرات، كطريقة تحكم بديلة، للمقارنة مع أداء تقنية التحكم ذات جهد التحكم الأدنى هذه من حيث أداء النظام وتكلفة طاقة التحكم النسبية. فعلى النقيض من الإجراء الصريح المستخدم لفصل الارتباط بين المخرجات في تقنية التحكم ذات جهد التحكم الأدنى، اعتمدت طريقة إيجاد مصفوفة فصل الارتباط بين المخرجات في تقنية مصفوفة نيكويست المباشرة على نهج التجربة والخطأ، والتي استهلكت وقتاً طويلاً للغاية. فبعد النجاح في إيجاد مصفوفة الفصل هذه أصبحت تقنية تحكم مصفوفة نيكويست المباشرة قادرة على التنظيم والتحكم بنظام تنقية وتكييف وتدفئة الهواء متعدد المتغيرات استناداً إلى استخدام تقنية التحكم المعروفة بنسبي تكامل مشتق، ولكن على حساب استهلاك طاقة تحكم عالية والتي تتعارض مع الجهود العالمية لتقليل استهلاك الطاقة داخل المباني. لقد توصلت هذه الدراسة أن نسبة طاقة التحكم المستهلكة في تقنية التحكم ذات جهد التحكم الأدنى إلى الطاقة المستهلكة في تقنية تحكم مصفوفة نيكويست المباشرة بعد مرور ٩٠٠ ثانية على عمل النظام للتعامل مع ثلاث سيناريوهات مختلفة للتشويش على عمل النظام هي ٤,٤ / ١٠٠، ٣٩ / ١٠٠، ٢٢ / ١٠٠ ومنها يمكن الاستنتاج بسهولة أن أداء تقنية التحكم ذات

جهد التحكم الأدنى هو الأفضل استنادًا إلى مراعاة بساطة تصميم كل تقنية تحكم وسلوك نظام تنقية وتكييف وتدفئة الهواء وتبديد

طاقة التحكم في كلتا تقنيتي التحكم.

**Dedication**

To the memory of my father (Abdul Khaleq Touqan), who always dreamed that I get a degree of doctorate in engineering. "You are gone but your belief in me has made this journey possible and the dream achievable."

To my wife (Dr. Mona Salameh) who was always motivating me to go in this academic journey

To my siblings who feel happy with this certificate and proud of such achievement.

## **Acknowledgments**

I would like to express my deep gratitude to my research supervisor Professor Alaa Abdul-Ameer for his patient guidance, encouragement and useful critique of this research work.

I would like also to sincerely thank Professor Robert Whalley (deceased), who started the journey with me coaching and guiding. Although he is no longer with us, he continues inspiring me by the innovative researches he published and the dedication to his students

Special thank is extended to Engineer Khalid Karajeh from SIEMENS UAE who offered valuable contribution to this research work.

## Table of Contents

List of Notations and Abbreviations: .....	v
List of Figures .....	x
Chapter One .....	1
Introduction.....	1
1.1 Research Background .....	1
<b>1.1.1 HVAC Systems Overview</b> .....	3
<b>1.1.1 HVAC System Major Components</b> .....	6
<b>1.1.2 HVAC Systems Performance Challenges</b> .....	8
<b>1.1.3 Physical fundamentals Governing HVAC System Operations</b> .....	12
1.2 Research Problem.....	15
1.3 Research Significance .....	16
1.4 Research Aims and Objectives: .....	17
<b>1.4.1 Research Aims</b> .....	17
<b>1.4.2 Research Objectives</b> .....	18
1.5 Research Organization.....	18
Chapter Two.....	21
Literature Review .....	21
HVAC System Mathematical Modelling.....	21
2.1. Physics-Based Modelling: .....	23
2.2. Data-Driven Modelling.....	31
2.3. Grey Box Modelling.....	37
2.4. HVAC Distributed Parameter Modelling .....	40

2.5. Summary of HVAC System Modelling Techniques .....	41
2.6. Mathematical Model to be Employed in the Study .....	43
2.7. Chapter Summary.....	47
Chapter Three.....	49
Literature Review .....	49
HVAC Control Techniques.....	49
3.1 Classic Control Techniques.....	50
3.2 Advanced Control Techniques .....	51
3.3 Multivariable System Control .....	55
3.4 Least Effort Multivariable Control Technique .....	57
Chapter Four .....	63
HVAC Mathematical Modelling and Control Techniques Approaches.....	63
4.1 HVAC Hybrid Distributed-Lumped Parameter model.....	63
4.2 Deriving the Air Conditioning System Transfer Function Matrix.....	71
4.2.1 Fast Forier Transform (FFT) .....	72
4.2.2 System Identification Toolbox .....	73
4.3 Air Conditioning Multivariable Open Loop Responses .....	76
4.4 Control Objectives .....	80
4.5 LE Control Theory.....	81
4.5.1 Closed Loop Plan .....	81
4.5.2 Inner Loop Analysis.....	85
4.5.3 Optimization of the Gains.....	88
4.5.4 Disturbance Rejection Calibrator for LE control technique.....	91

<b>4.5.5</b>	<b>Stability of the System with LE Control</b> .....	91
4.6	Direct Nyquist Array (DNA).....	92
<b>4.6.1</b>	<b>System Decoupling</b> .....	93
<b>4.6.2</b>	<b>Direct Nyquist Array Stability Theorem</b> .....	95
Chapter Five	.....	97
HVAC System Model Simulation Results and Discussions.....		97
5.1	LE Controller.....	98
<b>5.1.2</b>	<b>Inner Loop Configuration</b> .....	100
<b>5.1.3</b>	<b>Root Locus Design</b> .....	104
<b>5.1.4</b>	<b>Performance Index</b> .....	106
<b>5.1.5</b>	<b>Multivariable Performance Index Equation Solution</b> .....	109
<b>5.1.6</b>	<b>System Performance Analysis under the LE Controller</b> .....	118
<b>5.1.7</b>	<b>Disturbance Rejection Analysis Under LE Controller.</b> .....	123
5.2	Direct Nyquist Array.....	128
<b>5.2.1</b>	<b>Decoupling compensators</b> .....	129
<b>5.2.2</b>	<b>Gershgorin Circles</b> .....	130
<b>5.2.3</b>	<b>System Stability Test</b> .....	134
<b>5.2.4</b>	<b>System Performance Analysis under DNA Controller</b> .....	138
<b>5.2.5</b>	<b>Disturbance Rejection Analysis for DNA control technique</b> .....	141
Chapter Six	.....	146
LE and DNA Control Techniques Comparison .....		146
6.1	Mathematical and Algebraic Operations.....	146
6.2	The Controller Simplicity .....	147
6.3	Closed Loop Responses and Disturbance Rejection.....	148
6.4	Control Energy Consumption.....	154
Chapter Seven	.....	158
Conclusion and Recommendations for Future Work .....		158

7.1 Conclusion.....	158
7.2 Recommendations for Future Work .....	162
References.....	164
Appendix.....	171
8.1 Performance Index Equation .....	171
8.2 Partial differential Equation of ( $J$ ) in respect to ( $n_1$ ). .....	172
8.3 Partial differential Equation of ( $J$ ) in respect to ( $n_2$ ). .....	175
8.4 Script file to find list of roots pairs .....	177
8.5 List of roots pairs.....	177
8.6 Script file : roots making $J(n_1, n_2)$ only local minimum: .....	180
8.7 Script file : Proper compensators to decouple $G(s)$ :.....	182
8.8 Script file for Executing Newton Raphson Algorithm .....	185

### List of Notations and Abbreviations:

AHU	Air Handling Unit
ARMAX	Autoregressive Moving Average with External Inputs
ARX	Autoregressive with External Inputs
ASHRAE	American Society of Heating, Refrigeration, and Air Conditioning Engineers
BJ	Box–Jenkins
BMS	Building Management Systems
CBR	Case-Based Reasoning
EEV	Electronic Expansion Valve
FCU	Fan Coil Unit
FE	Finite Element
FFT	Fast Forier Transform
GA	Genetic Algorithm
GSC	Gain Scheduling Control
HVAC	Heating, Ventilation and Air Conditioning
IAQ	Indoor Air Quality
KB	Knowledge Base
LE	Least Effort
LQG	Linear quadratic Gaussian
MAE	Mean Absolute Error
MAPE	Mean Absolute Percentage Error
MIMO	Multiple Inputs Multiple Outputs
MLP	Multi-Layer Perceptron
MPC	Model Predictive Control
MSE	Mean Squared Error
NN	Neural Network
OE	Output Error
PDF	Probability Density Functions
PID	Proportional-Integral-Derivative
PMV	Predicted Mean Vote
PPD	Predicted Percentage of Dissatisfaction

SI	International System of Units
SISO	Single Input Single Output
SIT	System Identification Toolbox
Std_AE	Standard Deviation of Absolute Error
Std_APE	Standard Deviation of Absolute Percentage Error
TEV	Thermostatic Expansion Valve
TRV	Temperature-Regulating Valve
VFD	Variable Frequency Drive
VAV	Variable Air Volume
$(r^2)$ .	Coefficient of determination
(G)	Goodness of fit

#### **Notations of thermal energy transfer principles**

$(Q)$	Heat flow per unit time
$(\phi)$	Heat rate transferred per unit cross sectional area
$H$	heat energy transferred from hotter to a cooler system
$C$	Heat Capacitance
$C_p$	Specific heat capacity
$c_p$	Specific heat
$T_1$	Temperature of the first material ( $^{\circ}C$ )
$T_2$	Temperature of the second material ( $^{\circ}C$ )
$A$	Material surface area through which the heat is transferred ( $m^2$ )
$d$	Thickness of the material through which the heat is transferred ( $m$ )
$h$	Heat transfer coefficient or the heat admittance coefficient ( $W/m^2 \cdot ^{\circ}C$ )
$\varepsilon$	Emissivity that indicates the ability of a material to emit radiation. It is a dimensionless
$k$	The thermal conductivity of the material ( $W/m \cdot ^{\circ}C$ )

$\sigma$  Stefan- Boltzmann Constant (  $5.6703 \times 10^{-8} W/m^2 K^4$ )

### Notations of LE Control technique Equations

$a_{ij}(s)$	Element of $A(s)$ matrix
$a_{j,j}, b_{i,j}, \dots, \gamma_{i,j}$	coefficients of $a_{ij}(s)$
$A(s)$	Numerator of $G(s)$
$b(s)$	polynomial
$b_0, b_1, \dots, b_{m-1}$	coefficients of $b(s)$
$d(s)$	Denominator of $G(s)$
$G(s)$	HVAC open loop transfer function matrix (input/output)
$g_{ij}(s)$	Transfer function element of $G(s)$
$G_{hyb}(s)$	Hybrid distributed-lumped parameter transfer function
$G_{red}(s)$	HVAC open loop reduced-order transfer function matrix (input/output)
$G_{ol}$	Open loop transfer function matrix in the DNA control design
$G_{cl}$	Closed loop transfer function matrix in the DNA control design
$h$	feedback path gain
$h(s)$	feedback path transfer function
$H(s)$	feedback path compensator
$I_m$	Identity array
$J$	Performance Index
$k$	Forward path gain
$k(s)$	Forward path transfer function
$k \gg h$	outer product of $k$ and $h$
$\langle kh \rangle$	inner product of $k$ and $h$
$K(s)$	forward path controller model (pre-compensator)
$(l_1)$	The ventilated volume length

$L(s)$	left (row) factors
$n_1, n_2, \dots, n_{m-1}$	gain ratios
$P$	pre-compensator array
$Q$	Coefficient array
$r(s)$	transformed reference input
$\bar{r}(s)$	transformed inner loop reference input
$(2r_1)$	Ventilated Volume diameter
$L(s)$	Left (column) factors
$R(s)$	Right (column) factors
$S(s)$	Sensitivity array
$S_s$	Steady-state array
$u(s)$	Transformed input
$y(s)$	Transformed output
$\Gamma(s)$	Finite time array
$\delta(s)$	Transformed disturbance signal
$Q(t)$	Atmospheric ambient heat transfer
$v_1(t)$	Voltage at inlet fan motor
$v_2(t)$	Voltage at exit fan motor
$v_{wp}(t)$	Voltage at the chilled water pump
$P_1(t)$	Air pressure at the inlet of the ventilated volume
$q_1(t)$	Volume Air Flow Rate at the inlet of the ventilated volume
$T_1(t)$	Air stream temperature at the inlet of the ventilated volume
$P_2(t)$	Air pressure at the exit of the ventilated volume
$q_2(t)$	Volume Air Flow Rate at the exit of the ventilated volume
$T_2(t)$	Air stream temperature at the exit of the ventilated volume
$F$	Feedback outer loop gains diagonal matrix
$f_{ii}$	Element of F diagonal matrix
$E(t)$	Control Energy (Effort)

### Notations of Direct Nyquist Array Control Technique

$R(s)$	Inputs vector
$Y(s)$	Outputs vector
$G(s)$	HVAC open loop transfer function matrix (input/output)
$g_{ij}(s)$	Transfer function element of $G(s)$
$K(s)$	Decoupling compensators matrix
$C(s)$	Diagonal transfer function controllers
$N_i$	Number of encirclements of the point $(-1, 0j)$ in the complex plane
$Q(s)$	Diagonal dominant decoupled transfer function matrix
$q_{ij}(s)$	Elements of $Q(s)$
$H(s)$	HVAC open loop transfer function in DNA control technique
$h_{ij}(s)$	Transfer functions $H(s)$ of elements
$p_0$	Number of the open loop transfer function $H(s)$ poles located in the right-hand side of s-plane

## List of Figures

- Figure 2.1 Superposition of Building Thermal Model
- Figure 2.2 Equivalent electrical circuits for thermal sources of outdoor
- Figure 2.3 Schematic diagram of HVAC system showing the major components including ventilated volume, the ducting network, the chilled water pump, the ambient heat transfer into the ventilated volume and the inlet and exhaust fans.
- Figure 3.1 Block diagram of tradition multivariable control technique
- Figure 4.1 The transmission line as of distributed element
- Figure 4.3 Time domain pressure response when 1% step change in the voltages  $v_1(t)$  and  $v_2(t)$  applied on the inlet and exit fan motors
- Figure 4.4 Time domain pressure responses when 1% step change in the voltage  $v_{wp}(t)$  is applied at chilled water pump.
- Figure 4.5 Time domain pressure responses when 1% step change in the ambient heat transfer  $Q(t)$  is applied.
- Figure 4.6 Open loop Air Conditioning complete block diagram in transfer function form.
- Figure 4.7 Time and frequency domain pressure responses when 1% step change in the voltages  $v_1(t)$  and  $v_2(t)$  applied on the inlet and exit fan motors.
- Figure 4.8 Time and frequency domain pressure responses when 1% step change in the voltage  $v_{wp}(t)$  is applied in the chilled water pump.
- Figure 4.9 Time and frequency domain pressure responses when 1% step change in the ambient heat transferr  $Q(t)$  is initiated
- Figure 4.10 Block diagram of LE Controller showing the HVAC model, inner loop and outer loop
- Figure 4.11 HVAC multivariable closed loop control with (DNA) controller
- Figure 4.12 Graphical Example of diagonal dominance for a row or a column of square matrix
- Figure 5.1 a Responses of original and reduced order models for  $g_{11}(s)$
- Figure 5.1 b Responses of original and reduced order models for  $g_{21}(s)$

Figure 5.1 c.	Responses of original and reduced order models for $g_{31}(s)$
Figure 5.1 d	Responses of original and reduced order models for $g_{12}(s)$
Figure 5.1 e	Responses of original and reduced order models for $g_{22}(s)$
Figure 5.1 f	Responses of original and reduced order models for $g_{32}(s)$
Figure 5.1 g	Responses of original and reduced order models for $g_{31}(s)$
Figure 5.1 h	Responses of original and reduced order models for $g_{32}(s)$
Figure 5.1 i	Responses of original and reduced order models for $g_{33}(s)$
Figure 5.2	Root locus plot showing two poles are overlapping with the two zeros while the third pole is going to infinity.
Figure 5.3	Graphical representation of multivariable function with minimum function value shown with corresponding zero plane slob in both variables' direction.
Figure 5.4	Inner loop system responses in comparison with the open loop responses
Figure 5.5	Block diagram of LE Controller showing the inner and the outer loop with forward and feedback gains
Figure 5.6	LE Control closed loop system output responses following unity step input change on $r_1(t)$ at different values of $f = 0.1$ , 0.5 and 0.8
Figure 5.7	LE Control closed loop system output responses following unity step input change on $r_2(t)$ at different values of $f = 0.1$ , 0.5 and 0.8
Figure 5.8	LE Control closed loop system output responses following unity step input change on $r_3(t)$ at different values of $f = 0.1$ , 0.5 and 0.8
Figure 5.9	LE Control closed loop system output responses following unity disturbance step input change on $\delta_1(t)$ at different values of $f = 0.1$ , 0.5 and 0.8

Figure 5.10	LE Control closed loop system output responses following unity disturbance step input change on $\delta_2(t)$ at different values of $f = 0.1$ , 0.5 and 0.8
Figure 5.11	LE Control closed loop system output responses following unity disturbance step input change on $\delta_3(t)$ at different values of $f = 0.1$ , 0.5 and 0.8
Figure 5.12 a	Gershgorin band and Nyquist diagram for matrix element $q_{11}(s)$
Figure 5.12 b	Gershgorin band and Nyquist diagram for matrix element $q_{22}(s)$
Figure 5.12 c	Gershgorin band and Nyquist diagram for matrix element $q_{33}(s)$
Figure 5.13 a	Gershgorin bands centered about the diagonal elements of $h_{11}(s)$ and with radii equal to the summation of the off-diagonal elements for the row $h_{11}(s)$
Figure 5.13 b	Gershgorin bands centered about the diagonal elements of $h_{22}(s)$ and with radii equal to the summation of the off-diagonal elements for the row $h_{22}(s)$
Figure 5.13 c	Gershgorin bands centered about the diagonal elements of $h_{33}(s)$ and with radii equal to the summation of the off-diagonal elements for the row $h_{33}(s)$
Figure 5.14	Direct Nyquist Array closed loop system output responses following a unity step change at $r_1(t)$ and zero change at $r_2(t)$ and $r_3(t)$
Figure 5.15	Direct Nyquist Array closed loop system output responses following a unity step change at $r_2(t)$ and zero change at $r_1(t)$ and $r_3(t)$
Figure 5.16	Direct Nyquist Array closed loop system output responses following a unity step change at $r_3(t)$ and zero change at $r_1(t)$ and $r_2(t)$
Figure 5.17	System air pressure, volume airflow rate and temperature responses at the inlet of the ventilated volume following

unity step disturbance change at  $\delta_1(t)$  while the change on the other disturbance inputs  $\delta_2(t)$  and  $\delta_3(t)$  remain zero.

Figure 5.18 System air pressure, volume airflow rate and temperature responses at the inlet of the ventilated volume following unity step disturbance change at  $\delta_2(t)$  while the change on the other disturbance inputs  $\delta_1(t)$  and  $\delta_3(t)$  remain zero.

Figure 5.19 System air pressure, volume airflow rate and temperature responses at the inlet of the ventilated volume following unity step disturbance change at  $\delta_3(t)$  while the change on the other disturbance inputs  $\delta_1(t)$  and  $\delta_2(t)$  remain zero.

Figure 5.20 Block diagram of Direct Nyquist Array controller

Figure 6.1 System responses under both controllers techniques when unity change is applied on the  $r_1(t)$  representing the voltage on the inlet and exit motor fans, and with zero change at  $r_2(t)$  and  $r_3(t)$ .

Figure 6.2 System responses under both controllers techniques when unity change is applied on the  $r_2(t)$  representing the voltage on the chilled water pump, and with zero change at  $r_1(t)$  and  $r_3(t)$ .

Figure 6.3 System responses under both controllers techniques when unity change is applied on the  $r_3(t)$  representing the ambient heat transfer, and with zero change at  $r_1(t)$  and  $r_2(t)$ .

Figure 6.4 System responses following unity step change  $\delta_1(t)$  on the Pressure output, while there is no disturbance change at  $\delta_2(t)$  and  $\delta_3(t)$  and no change at all reference inputs  $r_1(t)$ ,  $r_2(t)$  and  $r_3(t)$ .

Figure 6.5 System responses following unity step change  $\delta_2(t)$  on the Volume Air Flow Rate output, while there is no disturbance change at  $\delta_1(t)$  and  $\delta_3(t)$  and no change at all reference inputs  $r_1(t)$ ,  $r_2(t)$  and  $r_3(t)$

Figure 6.6 System responses following unity step change  $\delta_3(t)$  on the Volume Air Flow Rate output, while there is no

disturbance change at  $\delta_1(t)$  and  $\delta_2(t)$  and no change at all reference inputs  $r_1(t)$ ,  $r_2(t)$  and  $r_3(t)$ .

Figure 6.7

Proportional control energy cost

# Chapter One

## Introduction

### 1.1 Research Background

Buildings sector constitutes the third-largest major energy consumer worldwide with a percentage of 27% of total energy consumption (Nejat et al., 2015). Building services such as lighting and thermal comfort systems are consuming significant amount of energy. Meanwhile, Human Beings are spending a greater quantity of time indoors, especially in the home which cause more energy consumption (Noh, Jang and Oh, 2007). Thermal comfort is one of the major aims of building services. According to the international standard EN ISO 7730, thermal comfort is: "...that condition of mind which expresses satisfaction with the thermal environment". Simply, it is the comfortable condition where a person is not feeling too hot or too cold (Thermal Comfort, 2018). In addition to acoustic, visual and indoor air quality, indoor thermal comfort is a factor that is directly connected with human wellbeing (Allen, 2016).

The outcome of many studies found that feeling comfortable in an interior space impacts directly on people's mood and can have a significant impact on their health and comfort. In office buildings, working in optimal conditions enables people to think and work better; thermal comfort in particular is not only influences people's satisfaction, but also impacting work productivity (Crahmaliuc, 2018). Thermal comfort in indoor spaces is a key indicator of a well-designed building. Good building design not only improves indoor comfort, it can also reduce buildings energy consumption. Well-designed buildings with reduced energy consumption contribute actively to the global efforts of implementing sustainable technology in the buildings (Nicol and Humphreys, 2002).

The Heating, Ventilation and Air Conditioning (HVAC) system is an integral part of a buildings' services. The main purpose of installing HVAC systems is to provide thermal comfort and acceptable indoor air quality. The design of HVAC systems is based upon the principles of fluid mechanics, thermodynamics and heat transfer fundamentals, which aims to build HVAC equipment that provides indoor thermal comfort. HVAC systems have become an essential part of building services. They can be found in facilities such as apartment buildings, villas, hotels, medium to large industrial and office buildings, low/ high rise buildings, ships and submarines; anywhere that humans are sheltered and need to feel thermally comfortable and enjoy a healthy environment. Today's advanced HVAC systems provide high indoor quality comfort but consume significant energy.

HVAC systems are classified as high energy consumers because of the active components that they comprise of, such as fans, heaters, pumps and compressors. They are one of the main energy consumers inside a building. Pérez-Lombard, Ortiz and Pout (2008) reported that in 2004, buildings in the EU had a total energy consumption of 37%, whilst in the US, it was 41%. Lighting as well as HVAC systems consume the most energy in buildings, with HVAC systems alone account for approximately 50% of building energy consumption (Pérez-Lombard, Ortiz and Pout, 2008). Upon addressing energy efficiency when designing new facilities, the most important decision to be taken is the type of heating and cooling system to install. They must comply with local regulations relating to energy efficiency.

Globally, commercial and residential buildings consume large amounts of energy; HVAC systems contribute significantly to this consumption; therefore, it is important that buildings are monitored, and efforts are made to reduce energy usage.

### 1.1.1 HVAC Systems Overview

Since prehistoric times, people were working persistently to improve the thermal comfort of their shelters. The ancient Egyptians used techniques such as hanging wet reeds in windows as primitive air conditioning. In the Roman period, water was circulated through aqueducts inside the walls of specific houses to cool them. Wind towers were widely used in some hot and arid regions of Persia and the Arabian Gulf to capture breezes to cool the indoor spaces (Bahadori, 1978). In colder climates, water was heated to produce steam which warmed the indoor spaces during winter. A similar technique was used in the Great Mosque of Cordoba at the period of old Andalusia in the tenth century.

The first modern air condition system was invented in 1902 by Willis Carrier when he was tasked to find a system to create humidity to enhance the production quality of an industrial process. By 1903, Carrier had designed a system of chilled coils that maintained a constant, and comfortable humidity of 55%. In 1914 he has been hired to install his invented cooling unit in a millionaire's mansion. Carrier carried on his creativity by inventing the centrifugal refrigeration machine, which was called "chiller". His invented system was used in 1925 at the Rivoli Theatre in the US, exposing the movie theatre patrons to their first taste of indoor "cool comfort". During the next five years, Carrier installed his chiller cooling unit in 300 movie theatres across America. Throughout the next few decades the air conditioning system were manufactured at commercial volume using the ammonia as a coolant. By the year 2007, 86% of residences in the US, were installed with Air condition systems (Palermo, 2014). HVAC system were previously considered as luxurious building equipment; however, they have now become a necessary part of today's building services in this quickly changing civilized society, (Pita, 2008).

According to HVAC systems function, thermal energy has to be either extracted, so that the system is acting as heat sink in summer, or supplied to the conditioned space, so it acts as a heat source in winter. Based on the working fluid used in the thermal transportation process, HVAC can be classified into four major systems (Gheji et al., 2016):

**a. All Air Systems:** In this system, the air is used as the fluid medium to transport the thermal energy. It is supplied to the conditioned space and re-circulated using fans, blowers and ducts. During the circulation, the air passes through the Air Handling Unit (AHU) where a cooling coil extracts the heat. In the heating function, a heating coil is used to warm the circulated air. The AHU is accommodated in a packaged cabinet comprising dampers, filters, mixing chambers, cooling/heating coils, fans, blowers and humidifiers. In All Air HVAC systems, enough fresh air is always supplied to maintain the required ventilation and the indoor air quality (IAQ). A thermostat can be installed in the conditioned area to monitor and control the amount of heat that should be extracted or supplied to the conditioned space. The amount of heat can be controlled using a valve that adjusts the flow rate of chilled or hot water in the cooling/heating coil. All Air systems are installed as single duct systems, or dual duct systems. In the single duct system, either the cooling or heating function can be entertained, but not both. However, in advanced All Air HVAC systems both functions can be provided by mixing both cooled and heated air using dual ducts, one for heating and the other for the cooling function.

**b. All Water Systems:** Here, water is used as the fluid medium to transport the thermal energy. In the case of the cooling function, chilled water is transported through a circulation flow between the terminal unit and the conditioned area, whilst hot water is transported and circulated when heating conditioning is required. Fresh air to maintain the ventilation and indoor air quality is supplied by a separate system.

The water transportation process takes place by either a 2- pipe or a 4-pipe system. In the 2- pipe system, one pipe is used for supplying the water whilst the other is returning it. In this system either the cooling or heating function can be used but not both. The flow of hot or chilled water is regulated by a flow control valve, which is controlled by a zone thermostat that feeds back the thermal gain information and adjusts the water flow rate accordingly. In the 4- pipe system, two pipes are used to supply hot and cold water respectively. Before it is supplied, both hot and cold water are mixed in a certain proportion, corresponding with the temperature set point of the conditioned area. One of the remaining two pipes is used for returning the cold water and the other for returning the hot water.

The terminal unit can be one of following types:

- **Fan Coil Unit (FCU)**, which is a small unit located inside the conditioned space and consists of air filter, blower, cooling or heating coil, louvers and condensation drain tray and pipe. The water is circulated through the coil integrated in the FCU. Air is drawn from the conditioned area and flows over the coil before being returned. The air in this process exchanges the heat between the conditioned area and FCU through the conduction heat transfer process.

- **Convectors** are used mainly for heating function. The hot water is circulated through the heating coil which heats the conditioned area through the thermal convection heat transfer process.

- **Radiators** are also used for heating function only. Heating the conditioned area takes place through the radiation heat transfer process. Chilled beam technology can also be used in conjunction with radiators for cooling.

**c. Air-Water Systems:** Incorporating the best features of All Air and All water systems, an Air-Water system is a compact system where both air and water are cooled or heated in the

central plant in order to condition the indoor space. Air ducting and fans are utilized to transport the cooled/heated air from the central plant, as is the case in All Air systems, whilst water pipes are utilized to transport cooled/ heated water to the terminal unit as is the case in All Water function systems.

**d. Unitary Air Conditioning:** This is a compact air conditioning unit which is configured with an individual refrigeration system and is factory assembled and tested. It varies in its capacity, fulfilling several thermal loads. They can be manufactured for heating function as well. Either the cooling compressor or heat pump is combined with a set of fans, a filter, a condensation tray with pipe and a control system, which form the major components of the system configuration. It is available as a window or split unit as well as other types of unitary based systems. The process of switching OFF the refrigerator unit and keeping the fan's operation ON can be used in certain cases to obtain the ventilation function only. Drainage of the water created as a result of the cooling and condensation processes, is handled by a dedicated tray and pipe, spilling the water to the drainage or out of the conditioned area.

### **1.1.1 HVAC System Major Components**

HVAC is a system designed to provides thermal comfort and indoor air quality based on sub-discipline of mechanical engineering and employing the principles of thermodynamics, heat transfer and fluid mechanics. The system has many inputs such as power supply at the motor fans, chilled water pump, heat transferred from ambient environment. It has also many outputs as well such as air pressure, air flow and indoor temperature. The internal coupling inside HVAC system functions is significant so that when one of the inputs is altered, all the outputs will be affected accordingly which creates complexity in its structure under the open loop performance. The complexity is magnified in big scale buildings such as theatres, shopping

malls and high-rise buildings. HVAC system complexity can be recognized by reviewing its components which are listed as follows:

**a. Furnace:** This key component is the largest one and requires a substantial area. It is responsible for providing heated water for the purpose of warming the indoor spaces. The heating process can be undertaken by several heat sources such as electrical resistance, heat pump combustion and solar energy.

**b. Thermostat:** It is a sensing component that measures the exact value of the indoor space temperature and feeds back the reading to the HVAC control unit to be processed, so that the control output command can be decided accordingly, i.e. opening the valve of chilled/hot water pipe enabling warming or cooling process. The thermostat is designed as part of the HVAC system to keep the indoor space temperatures at the desired value.

**c. Heat exchanger:** This component is working in conjunction with the furnace to produce warm air during winter. It pulls the cold air from the ventilated volume, exchanges the heat with it, then circulates the warm air into the ventilated spaces through the vents and ducts.

**d. Condensing Unit:** The condensing unit is assembled along with the compressor and installed outside the building, so that when the compressor pressurizes the refrigerant into a hot liquid, which passes through many coils inside the condenser, the heat is allowed to escape out through the condenser fins to the outside. At the end of the refrigerants journey over the coils it becomes cool but is still under high pressure. The liquid continues its route through a valve to the evaporator coil in the form of mist and vaporizes into a cool gas inside the evaporator.

**e. Evaporator Coil:** This element operates in an opposite function to the Heat Exchanger and works in summer by pulling the warm air from the ventilated volume, exchanges the heat with it, then blows the cool air into the ventilated spaces through the vents and ducts.

**f. Refrigerant Lines:** These are special narrow pipes used for the refrigerant cycle from the condenser to the evaporator and back again to the condenser. They are made from materials such as copper or aluminum that are durable and resistant to heat exchange.

**g. Air Ways and Ducts:** It is a network of air ways that carry the warm or cool air to the indoor spaces in the building and pulling the warm or cool air from the ventilated volume back, completing the air circulation. They are made from lightweight materials such as aluminum steel, fiberglass or polyurethane.

**h. Fans:** Fans are facilitating the heat exchange process between the evaporator and the heat exchanger pumping the warm or cooled air into the indoor spaces. Other fans are also installed to suck the air from the indoor spaces so enabling the air circulation process.

It is worth mentioning that the HVAC system model employed in this study will be HVAC system with cooling function only (Air Conditioning System) that consists of chilled water pump, inlet and exit fans, airways and ducts network and ventilated volume

### **1.1.2 HVAC Systems Performance Challenges**

It is recommended to design a building with passive cooling or heating techniques in order to avoid active HVAC system operations that consume energy. However, providing good filtration, indoor air quality and thermal comfort often necessitates the need to install HVAC systems as part of the building services. Nevertheless, a badly designed HVAC system is a source of never-ending suffering for users in terms of performance, maintenance and energy consumption. The main concern for building executives is to control the power consumption of HVAC systems to reduce operational costs and system maintenance. Many actions can be adopted to control the cost of HVAC system operations and maintenance. For instance, set points for desired indoor temperature value enhance efficient system operation and environmental control. Setting clear operational schedules will make sure that the system is

running only when needed. Opting for preventive routine maintenance programs will ensure that HVAC system components are running at the highest efficiency. However, despite of all these procedures, there might be some factors embedded in the system design, which can limit the systems efficient performance. Such situation limits building executives' options for solutions unless significant design changes are implemented in the system. In most of the cases, cost of those changes is expensive, disruptive and not always successful. Therefore, ensuring optimum HVAC system energy consumption and operation efficiency from the beginning and throughout its life cycle, requires focus on the system design. The following steps must be examined at the design phase (Piper, 2004):

**a. Appropriate Sizing:** Efficient HVAC system operations are strongly related to the sizing of the correct load capacity of all the components, including chillers, heaters, water pumps, inlet and outlet fans, etc. On one hand, if the system capacity is too small it will lead to the occupants feeling uncomfortable and will extend the system working time and prevent it from reaching the appropriate set point temperature, thus consuming more energy. On the other hand, oversizing the capacity unnecessarily to lower indoor thermal loads will consume more energy than is required. It is worth mentioning that HVAC system capacity sizing can be done after considering thermal load reductions, which can be achieved by installing high-efficiency glazing, so reducing the solar thermal gain. Selecting lighting units with least thermal load can be also considered before sizing the HVAC system. However, the practicality of HVAC design must consider a small margin of excess capacity to allow minor thermal load changes and unavoidable HVAC equipment depreciation over the time; this requires the system to be oversized with 25%.

**b. High-Efficiency Equipment:** Significant improvements have been achieved in the operating efficiencies of HVAC equipment over the last two decades. Boilers and

centrifugal chillers now offer high efficiency with full load performance. Therefore, selecting such highly efficient equipment should be of the utmost importance. They are financially expensive, but this can be recovered through savings in the power consumption. Part-load should not be overlooked when considering an efficient operation. It is very important to realize that operating the HVAC equipment at part load decrease the performance and the efficiency of equipment. For example, chillers at full load work at 0.5 kW per ton, but at 75% of the full load they work at 0.65 kW per ton, so consuming more energy. Meanwhile the operation of electric motors has become more efficient with the incorporation of a variable frequency drive (VFD) powering the electric motor, that is coupled with the chillers, pumps and fans so that such VFD can improve the part-load performance. This can be achieved by reducing the voltage and the frequency of the power supply, aiming to keep part-load operating efficiencies at near-full-load ratings over a wide range of loads. In this way, power consumption can be optimized.

c.           **Efficient Controls:** This is a very important aspect related to efficient HVAC system operations. Indoor spaces can be wisely divided into zones and each zone can be air conditioned separately according to actual thermal load and zone occupancy. HVAC efficient controls can regulate the amount of ventilated air. Sometimes the amount of external ventilated air is set by the operator without any knowledge of what this should be and is based on guesswork only. This is often set at a higher rate than the ventilated space requires. Alternatively, Carbon Dioxide sensors can be installed and linked to the ventilation air dampers, which can control and minimize the rates of outdoor air ventilation. Flexibility of control systems design can overcome any incorrect assumption made at design stage. It should also be flexible enough to accommodate any changes required by the occupants, such as shifting hours of operation. Failing to incorporate flexible control systems will lead to

compromises on the reliability performance of the HVAC system that will reduce the HVAC operations efficiency, thus leading to more power consumption.

**d. Designing for Maintenance:** Even when the HVAC system equipment is properly sized and selected, it can only perform well when it is subjected to an appropriate routine maintenance programs in order to keep components' operating efficiently. Meanwhile, a lot of items designed in the system deteriorate over the time and some components might completely fail, these components must be installed in some accessible areas to enable repair and maintenance work. Therefore, unless the components are easily accessible with enough space to work, proper maintenance and repairs will not be achieved and thus efficiency is likely to suffer.

**e. Static Pressure:** This is an air pressure that can affect the HVAC performance significantly. In order to get air flowing properly through the ducts and the ventilated volumes during HVAC operations, it needs the pushing force to be greater than the flow resistance, otherwise air will not flow. Static pressure represents in this case the flow resistance. There are some scenarios that create improper static pressure, some of them are related to system design issues such as a pleated filter, poor duct design or installation and insufficient fan power, while other reasons are related to a lack of periodic maintenance, such as blocked filters and dirty components, etc. If the static pressure is too high, this will require the unit to work with greater power to overcome the air resistance and will affect the system reaching work efficiency. In this situation, some areas in the indoor space will be left too hot or too cold depending on the HVAC function, so reducing thermal comfort. This leads to more stress on the system components. One consequence of more stress on the components will be increased wear and tear.

### 1.1.3 Physical fundamentals Governing HVAC System Operations

The building envelope including ceilings, walls, floors, windows, thermal gains, indoor space air as well as HVAC elements, such as cooling and heating units, thermal exchange unit, fan blowers and air ducts are the main components to be considered when a HVAC thermal system mathematical representation based on thermodynamic principles is required. Non-equilibrium thermodynamics behavior is the basis of the mathematical Equations utilized to derive the HVAC mathematical model. Heat transfer driving force is the difference in the temperature, which is like the voltage difference in the case of electrical circuit current flow. The two major forms of energy concerned with thermodynamics are the heat and temperature. Using the International System of Units (SI), heat is the energy that is transferred from hotter to a cooler system measured by (*Joule*) and denoted by (*H*) while temperature refers to the kinetic energy of the atoms or molecules in the system measured by (*Celsius*) or (*Kelven*) and denoted by (*T*). Heat Capacitance (*C*) measured by (*Joule / Celsius*) is the amount of heat that substance either gains or loses per unit temperature, while specific heat capacity (*c<sub>p</sub>*) measured by (*Joule / Celsius / kg*) is the amount of heat that substance either gains or loses per unit mass, per unit temperature. The major governing Equation describing the heat energy absorbed or released in a substance that has the specific heat (*c<sub>p</sub>*) *J / kg°C* and mass (*m*) *kg* can be expressed as:

$$H = m \times c_p \times \Delta T, \quad (1.1)$$

where ( $\Delta T$ ) is the difference between the hotter and colder substances that heat is transferred and exchanged (Lienhard, J., 2017).

Since the concern of the heat transfer energy is represented by the rate heat transfer, so that heat flow per unit time denoted by ( $Q$ ) indicates how fast the heat energy is transferring from an object to other and measured by (*Joul per sec or Watt*) and expressed as:

$$Q = \frac{dH}{dt} = m \times c_p \times \frac{dT}{dt} = C \times \frac{dT}{dt}. \quad (1.2)$$

Heat flux is defined as the heat rate transferred per unit cross sectional area and measured as  $W / m^2$  (Watt per square meter) and denoted by ( $\phi$ ) (Lienhard, J., 2017).

The heat transfer by conduction can be described by the heat transferred between two different objects that have physical contact with each other, with different temperatures between both. In HVAC field, conduction is used to calculate the thermal load that can be established by the heat transferred through walls and ceiling. The governing Equation describing the heat conduction between the two objects with different temperature values is expressed as follows (Lienhard, J., 2017):

$$Q = kA \frac{(T_1 - T_2)}{d}, \quad (1.3)$$

where:

$Q$  is heat energy transferred between the two objects (*Joule*)

$T_1$  is temperature of the first material ( $^{\circ}C$ ),

$T_2$  is temperature of the second material ( $^{\circ}C$ ),

$k$  is the thermal conductivity of the material ( $W/m. ^{\circ}C$ )

$A$  is material surface area through which the heat is transferred ( $m^2$ )

$d$  is thickness of the material through which the heat is transferred ( $m$ )

Material thermal conductivity is an indication of the ease of heat transfer in the material. Heat lost from an object to its surroundings represents negative heat quantity and is positive heat quantity when it gains heat from its surrounding.

Convection is the second way of heat transfer; it is a thermal transfer process where the heat is carried from one location to another, through a fluid carrier travelling away from the heat source. In HVAC systems, the heat transfer process is a forced convection mechanism through a fan blower aiming to cool or heat the indoor space more efficiently. The governing Equation describing the convection heat transfer process through the fluid carrier is expressed as:

$$Q = hA(T_1 - T_2), \quad (1.4)$$

where:

$h$  is heat transfer coefficient or the heat admittance coefficient ( $W/m^2 \cdot ^\circ C$ )

$T_1$  is temperature of the first material ( $^\circ C$ )

$T_2$  is temperature of the second material ( $^\circ C$ )

$A$  is material surface area ( $m^2$ )

The third heat transfer process is radiation where the heat is transferred and emitted in the space without the need for any mass or medium. Warm objects with a temperature greater than absolute zero emit infrared radiation in the form of electromagnetic waves of thermal energy. In the application of HVAC, the thermal load created by the sun's radiation through the window, as well as heat emitted by occupants, appliances and furniture must be calculated and modelled based on thermal radiation process.

Ganji, D., Sabzehmeidani, Y. and Sedighiamiri, A., (2018) have described the heat transfer equation through the radiation process as:

$$Q = \varepsilon \times A_h \times \sigma \times (T_h^4 - T_c^4), \quad (1.5)$$

where:

$\varepsilon$  : Emissivity that indicates the ability of a material to emit radiation. It is a dimensionless parameter value, varying between one and zero.

$\sigma$  : Stefan- Boltzmann Constant ( $5.6703 \times 10^{-8} W/m^2 K^4$ )

$A$ : Area of material that emits thermal energy ( $m^2$ )

$T_h$ : Hot body absolute temperature in *Kelvin*

$T_c$ : Cold surroundings absolute temperature in *Kelvin*

## 1.2 Research Problem

HVAC is designed to provide indoor thermal comfort so that HVAC plant components as mentioned in section 1.1.2 must work together simultaneously and are required to operate under continuously dynamic environmental conditions, which in turn adds more complexity to the system design and operation. HVAC systems can be formed of large scale, spatially and dimensional dispersed systems such as components of airways, long slender air shaft and indoor volumes where the physical properties of the object are distributed and not lumped mass elements. Other components such as fan motors, inlet and exit impedances and valves have physical properties that can be treated as a concentrated lumped mass element without compromising on the accuracy. Failing to realize and to tackle such physical properties of the system in the design stage, will degrade the accuracy of the system model, thus leading to unreliable system performance

HVAC systems with such structures and components need a realistic multi-variable mathematical model, which can be the basis for a more robust control strategy. The problem gets more complicated when the control system design is required to achieve multiple objectives by means of operating multiple actuators. This induces a situation where the operation of each of these actuators influences the other process variables. Hence one of the aims of the proposed process controller is to balance the activation of all actuators simultaneously (VanDoren, 2017). The design complexity increases significantly when the number of inputs and outputs to be regulated increases, leading to extensive and complicated mathematical procedures. Control system robustness is an important requirement when

designing HVAC systems, so that system parameter uncertainties cease to affect the HVAC system performance. The Control system should also enable disturbance suppression and recovery of the system operations to normal performance in a relatively short time. Reliable system response predictions in terms of pressure, temperature and airflow rate throughout all system conditions is necessary. Therefore, the reliability of the control system is a major requirement when operating the HVAC system under input changes, disturbance effects and fault conditions with the aim of assuring cost effective, safe and efficient system operations.

Consequently, the research problem can be summarized in the following points:

- i. Actual HVAC system has a multi-variable system nature.
- ii. The HVAC system has dispersed components such as ventilated volume where lumped modeling is not the right option
- iii. The actual operating conditions of such systems have many disturbances effecting system robustness and performance.
- iv. Any control strategy developed for these kinds of systems must be capable overall of saving system integrity, system robustness and disturbance suppression with minimum energy consumption and the least maintenance effort.

### **1.3 Research Significance**

There are some of points that give significance to the study. HVAC system is considered in the research as multiple inputs multiple outputs where many variables related to the thermal comfort such as volume air flow rate, air pressure and indoor temperature need to be manipulated simultaneously aiming to reach the desired values of the indoor comfort. The multivariable model structure produces complexity in the way how to reach such desired output values because of the internal connection between the manipulated variables. In HVAC systems, where the internal interaction is obvious, lowering the air temperature in the indoor

space for example lowers also the air pressure. Therefore, the required balance of having lower temperature with maintained air pressure can be challenging to determine. Consequently, the significance in the research is perceived herein by employing a multivariable control technique that able to meet all the control objectives successfully through reaching desired variable values with several different combinations of control requirement. The combination of control requirement incorporates decoupling the internal interaction between the internal loops of the system to minimum levels, reducing the steady state error of the desired outputs values and implement acceptable disturbance rejections. One more important significance of the study can be realized from the least control efforts spent on achieving the control targets and especially while rejecting the disturbance applied on the system outputs. The Performance Index (PI) Equation which is part of the general control energy expression and can be calculated by finding the integral of the summation of squared control signals is employed to optimize the control energy consumption. The control technique used in this study is Least Effort Control where it uses specific values of forward and feedback gains that correspond with the minimum values of the Performance Index Equation. The least effort control can be an advantage in saving power consumption and achieving least actuator activity, least heat and least wear and maintenance cost minimization without sacrificing the system performance under the proposed control strategy.

#### **1.4 Research Aims and Objectives:**

##### **1.4.1 Research Aims**

The major aim of this research is to develop a reliable, robust, least control energy dissipation multivariable control strategy for a complete HVAC system in order to obtain improved system performance associated with least energy consumption and effective disturbance rejection. In order to secure improved multivariable HVAC system performance, a reliable multivariable

mathematical model is a mandatory prerequisite to achieve the major research aim. Hence identifying a reliable multivariable mathematical HVAC system model that is close to reality is one of the main research's aims

#### **1.4.2 Research Objectives**

The aims and the overall intentions of the research are revealed in the previous section, therefore the following detailed objectives of how to reach the research aims are listed in the below points:

- i. Obtaining and examining, in time domain, different responses of the hybrid distributed-lumped parameter HVAC systems mathematical model developed by Whaley R. and Abdul-Ameer A. (2011), to obtain the dynamical characteristics of the system.
- ii. Obtaining the required necessary frequency domain transfer functions employing MATLAB Toolbox to handle and process HVAC system time domain mathematical model responses developed in (i) and building-up 3 input and 3 outputs multi-variable transfer function matrix.
- iii. Developing the HVAC system control strategy based on the Least Effort (LE) control technique outlined by Whalley R. and Ebrahimi M. (2004) to achieve minimized control system energy dissipation, adequate disturbance suppression and improved system performance in terms of integrity and closed loop stability.
- iv. For the theoretical validation, a detailed comparison will be explored between the Direct Nyquist Array multivariable control technique with the adopted LE Control Strategy.

#### **1.5 Research Organization**

This thesis is structured into seven chapters, which can be summarized as follows:

##### **Chapter 1:**

In chapter one an introduction to the research topic incorporating the research background and

highlighting the global environmental problem including the contribution of HVAC system to global warming. An overview about the HVAC system types, structures, design gaps and challenges is part of the chapter. Research problem, significance and aims of the research are highlighted also in the chapter.

### **Chapter 2:**

The chapter will present in detail the literature review of HVAC system mathematical modelling contributions showing the excellence and limitation of previous HVAC system models. The chapter will show at the end the most suitable HVAC mathematical system model representation that is close to HVAC system reality and bridging the gap that has arisen from previous model's limitations.

### **Chapter 3:**

This chapter will address the literature review of the control strategies employed to regulate the HVAC systems, highlighting the characteristics and advantages of the proposed control strategy in this study over the others previously employed.

### **Chapter 4:**

Obtaining the transfer function matrix extracted from the time domain HVAC system mathematical model as well as reviewing the control techniques theories applications to be employed in the study are highlight in this chapter. The stability criteria for each control technique will be also reviewed in the chapter

### **Chapter 5:**

This section will represent the research methodology and review HVAC system model simulation, responses results and discussions under the open loop system as well as simulation, results and discussions for closed control loop configuration responses for both LE and Direct Nyquist Array control strategies.

**Chapter 6:**

HVAC control strategies comparisons will be undertaken in this chapter demonstrating the closed loop HVAC system responses under both main and alternative control strategies, comparing their performances at the dynamic period characteristics as well as disturbance rejection and control energy dissipation.

**Chapter 7:**

The chapter will report the research works detailed conclusions, research limitations and recommendations for further future research work.

## **Chapter Two**

### **Literature Review**

#### **HVAC System Mathematical Modelling**

Regardless what type of HVAC system is installed, it consists of many active components that consume significant energy. Consequently, optimizing the energy consumption of HVAC systems is a key measure in achieving building energy efficiency. The “American Society of Heating, Refrigeration, and Air Conditioning Engineers” (ASHRAE) is an internationally recognized organization and has been established to care about developing sustainable technology pertaining to indoor air conditioning, air quality and energy efficiency. There are many measures that have been studied to achieve energy efficient buildings. Apart from the measures used in architectural design and measures of increasing building envelope insulation, integrating the operation of the HVAC system into the Building Management Systems (BMS) so that it is linked with the spaces occupancy has also been approached. However, there are other engineering measures that can be proposed to optimize the operation of HVAC systems within energy efficient buildings. Reliable and accurate HVAC mathematical models as well as a suitable control strategy are part of the efforts to achieve greater efficiency.

Mathematical models are widely used in many disciplines, such as engineering, ecology, agriculture, medicine and economics, aiming to predict and control the performance of the actual related discipline process (Homod, 2013). Furthermore, they are also used for other reasons, such as operator training, simulation and fault diagnosis, as well as for some industrial processes that cannot be constructed within laboratories in order to measure and analyse their behaviour. Typically, HVAC systems are too large for laboratory studies because of the size of components; for instance long airways and large ventilated volumes (Whalley and Abdul-

Ameer, 2014). A practical solution would be to model the system mathematically. However, the accuracy for the model representation is vital to obtaining reliable predicted results. Therefore, a modelling process is essential for a system representation by specifying the set of mathematical Equations or input-output relationships describing the system arrangement.

Due to the nonlinearity and the different time lags and inertia, which are inherent characteristics of HVAC systems, it is a challenging exercise to develop an accurate mathematical model describing the real HVAC process over a wide operating range (Mirinejad *et al.*, 2012). In the meanwhile, modelling building envelopes as mentioned in Homod (2013) is a complicated procedure when including HVAC system components in the modelling process. The complexity is caused by the fact that modelling any building is not confined to construction components, such as walls, floor, ceiling, windows, etc., but it also includes the consideration of the internal thermal loads, such as lighting, furniture, behaviour and number of people accommodated in the space so that a comprehensive system model can be achieved. Comprehensive HVAC models can be built by incorporating the principle covering mathematical operation of HVAC processes, which incorporates electrical and mechanical components combined with the thermodynamics and fluid mechanics Equations describing the heat transfer between the building's envelop and the indoor space; finally, this also includes the thermal load in the final system model. Although complexity increases when such a comprehensive model is considered in the design study, it offers higher system representation accuracy and leads to more reliable system dynamical behaviour analysis. Nonetheless, it is normally difficult for HVAC system models to be completely comprehensive and consequently most of the models built in this domain are fragmented into sub-models reducing the work complexity (Homod, 2013).

The literature will review most of the contributions presented to model HVAC systems, which has shown that lumped/point wise modelling was the dominant technique. But even when the authors were intending to include the dispersed nature of the system in the model, they have modelled the HVAC system as a series or parallel interconnected point-wise lumped elements employing the mass and energy conservation Equations.

Based on the modelling contributions reviewed for HVAC systems, it has also been noticed that there are three different HVAC mathematical modelling approaches which have been reviewed by many researchers, such as Afram and Janabi-Sharifi (2014a) and Homod (2013). These approaches are (i) physics-based model or white box, (ii) data driven model or black box and (iii) mixed approach using a data driven and physics-based model or what is called grey box.

One more observation also obtained from the literature is that many researches developed building envelope models only, while others confined the HVAC model's development to active machinery components, and very few modelled comprehensive HVAC systems that combine the building envelop with the HVAC mechanical and electrical components integrating their thermal interaction with building interior and exterior.

### **2.1. Physics-Based Modelling:**

This modelling methodology is known in many references as white box and leads to deterministic and continuous models. The detailed knowledge of the process is necessary in this modelling technique. Some of the white box models usually end with dynamic model realization, while others end with static realization and both can be employed for HVAC subsystems. On one hand, dynamic models are realized generally by describing slow physical processes, such as zone humidity and temperature, as well as cooling and heating water temperature variations. On the other hand, static models are generally presented by describing

fast physical processes, such as mixing box handling mixed air temperature, air flow rate through dampers and hot or cooled water flow through valves.

Generally, thermodynamics models are forms of thermal-network equivalent to electrical network where voltage and current are equivalent to temperature and heat flux respectively while thermal capacitance is equivalent to electrical capacitance and the substance thermal resistance corresponds to the resistor in the electrical circuit.

HVAC physics-based models usually employ mass and energy conservation, as well as heat transfer Equations taking into important consideration the full knowledge of the concerned process (Afram and Janabi-Sharifi, 2014). The physics of mass and energy conservation and heat transfer Equations have been reviewed briefly in Chapter one.

The major advantage of the physics-based modelling process is the provision of accurate system prediction and output estimation. Nevertheless, it has a disadvantage, as the modelling process requires intensive computation operations and significant efforts to be developed (Yiu and Wang, 2007). Homod (2013) has talked about the white box modelling technique and mentioned that it is based on two different approaches, lumped and distributed parameters. Lumped methodology has a major advantage in that it is an easy model derivation and easy algebraic mathematical operation in comparison with the distributed parameters technique. However, distributed parameters modelling provides more model accuracy and reliable system behavioural prediction results.

Typically, HVAC modelling processes end with high order nonlinear differential Equations and dynamic models associated with high thermal inertia, lag time and uncertain disturbance signals. Provided that the HVAC nonlinearity of models are linearized through specific techniques, they can be also derived through differential Equations with either time domain in the state space representation or frequency domain in the transfer function representation.

Many researchers have followed physics-based modelling techniques to model the thermal behaviour in indoor spaces. For example, Lü (2002) worked on deriving a model of coupled moisture and heat transfer through walls of a building intending to predict the indoor thermal conditions. A model like this can be employed to apply a control strategy in order to reach indoor thermal comfort. For the building envelope, conservation Equations including the mass, momentum and energy as well as the constitutive Equations as described by laws of Darcy (law of water flow), Fick (law of gaseous flow) and Fourier (law of heat flow) were employed to derive the model. Modelling the indoor space air was also included in the final model employing the Equations of heat and moisture from the building envelope. The set of derived Equations were solved using numeric methodology through the finite element method. The derived model has been verified by the specially designed test box and real test house that have given high model accuracy. However, inclusion of HVAC system components in the model was not considered, rather, the model has used the energy conservation and thermodynamics Equations sufficiently so it can be the basis of more comprehensive HVAC system-related models.

Based on thermodynamic non-equilibrium characteristics of building thermal behaviour and applying first principles and the constitutive laws, Ghiaus and Hazyuk (2010) were able to derive a dynamic building model through a set of algebraic and differential Equations. The output of the model represented by the indoor temperature was impacted by external heat sources, (i.e., heat flux generated by outdoor air temperature and solar radiation on the walls). Internal heat resources (i.e., heat flux from thermal gains, such as occupants, appliances, and heat flux from solar radiation into the indoor zone) also have affected indoor temperature. Ventilation and infiltrations, which are also sources of heat, were considered as constant values and proportional to the difference between the outdoor and indoor temperatures, hence the

researchers did not consider them as separate sources. They assumed linearity in the heat transport process and the building thermal model is built by a network of three thermal sources, as per Figure 2.1 below, that can be in superposition form,  $\theta_o$  is the input of the model representing outdoor air temperature while  $\theta_z$  is the output of the model which represents indoor temperature,  $\dot{Q}_g$  is the lumped internal thermal sources which acts as disturbance and  $\dot{Q}_s$  is the solar radiation thermal source on the walls and acts as a disturbance too. Each source in the network needs to be converted to an equivalent electrical circuit, as showed in Figure 2.2. Therefore, based on the second Kirchhoff law, its Equations can be derived and set by the input output relationship and transformed into Laplace representation.

In Figure 2.2, the voltage and electric current in the thermal network converted into equivalent

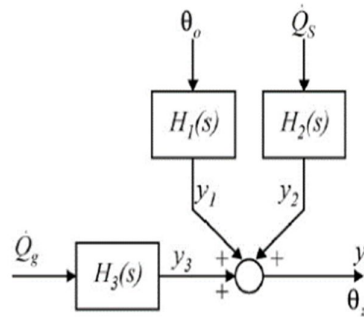


**Figure 2.1.** Superposition of building thermal model (Ghiaus and Hazyuk, 2010, pg 4)

electrical network are equivalent to temperature and heat flux respectively while thermal capacitance is equivalent to electrical capacitance and the substance thermal resistance corresponds to the resistor in the electrical circuit.

The mathematical model Equations can afterwards be derived from second Kirchhoff law for each circuit. At the end, the dynamic model of each circuit can be introduced by state-space representation. To reach such a simple thermal model, the authors have considered some major assumptions that can reduce the accuracy of the final thermal model, such as the assumption of linear relation of the heat transfer process and constant value of heat flux generated from ventilation and infiltrations air. However, the model in such representation is indeed a simple one but can be problematic for further control procedures that aim to contribute to low energy consumption buildings.

Modelling Air Handling Units (AHU) and room zone have been approached by Wang, Zhang and Jing (2007), who considered the model consists of two parts, the air handling unit where cooling and heating processes are incorporated, and the indoor room required to be air-conditioned. Both parts are connected with each other by airshaft. The injected air into air-conditioned space is a mix of fresh air with the recycled air and handled through the heat exchanger and humidifier in the AHU. Using thermal balance Equations based on the conservation of energy law, the mathematical model was derived.

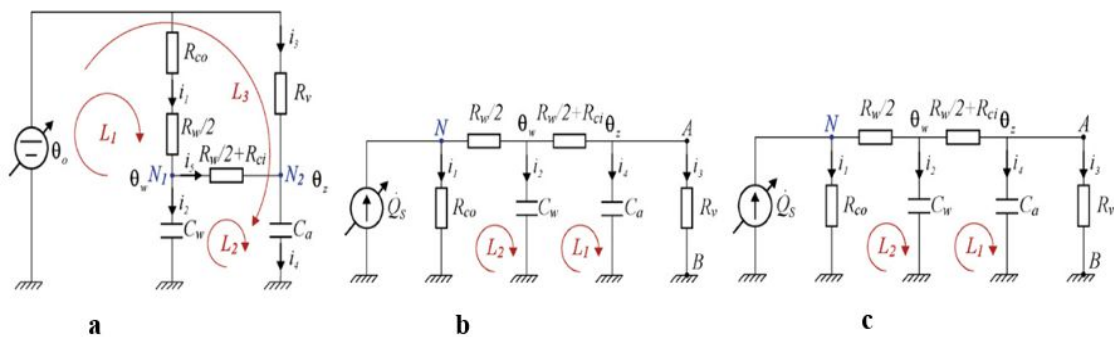


**Figure 2.2.** Equivalent electrical circuits for thermal sources of **a**: outdoor, **b**: solar radiation on the walls and **c**: internal building gains (Ghiaus and Hazyuk, 2010, pg 4)

The derived model for both the heat exchanger and the air-conditioned space was of first order so the final system transfer function was of second order with single input single output simple

representation. There are some assumptions considered in the model by the researchers that might weaken the accuracy of the model, for example they did not include the ventilation and the infiltration air that can ingress from outdoor, which can be considered as a real thermal disturbance, into the model. They also assumed homogenous temperature in the room, moreover, the internal thermal gains that can be caused by the occupant, appliances and the heat through windows were neglected and the temperature of heat exchanger surface was considered equal to the temperature after the heat exchanger.

Tashtoush, Molhim and Al-Rousan (2005) mentioned that due to the distributed system parameters and the multivariable nature of the HVAC system, it is extremely difficult to develop an exact and accurate HVAC mathematical model. Therefore they did not consider the dispersed nature of the system and developed a dynamic model based on Equations of energy and mass balance incorporating HVAC system components, such as room zone, cooler, heater, fan, humidifier, dehumidifier and ducts. These Equations were used also to model the whole HVAC plant so that the final dynamic model was with two outputs, i.e., zone temperature and humidity while the inputs were the supplied air mass flow rate, supplied air temperature and supplied air humidity. The authors have assumed that air inside the entire room is homogeneous and its temperature is distributed so that the room can be considered as a lumped thermal capacitance model. They assumed also that room pressure loss or drop is neglected. It is worth mentioning that considering lumped modelling for dispersed parameter elements is not enhancing final model accuracy.

An energy balance Equations approach was the basis of the HVAC models built by many other researchers. House and Smith (1995) used energy and mass conservation Equations to build their model for the thermal indoor space, which neglects humidity effects and the spatial

features of the space volume. They also modelled the indoor space as a lumped capacitance despite its dispersed features.

Aiming to model and control indoor thermal comfort and air quality with the purpose to save energy consumption, Yang and Wang (2012) built their model based on two major laws related to heat and energy balance Equations. At first, they did employ the Equations of heat transfer between indoor space and three heat sources in the form of either reducing or gaining heat effects. These are the occupants' heat, adjacent zones heat and the heat blown by cooling or heating fans to the indoor space. The second was the major principles of the thermodynamics used to calculate the power that can be consumed by the air supply fan, air return fan, cooling coil and heating coil. This model was important due the efforts aimed to realise comprehensive HVAC system model. However, dispersed nature HVAC system was also not considered in the model that deteriorates the model accuracy.

Tahersima *et al.* (2010) worked on modelling and controlling a thermal radiator as well as a temperature-regulating valve (TRV). The authors derived a hybrid model so that the room that interacts thermally with the radiator was modelled using lumped capacitance based on a set of heat transfer Equations. A room modelling was based on a network incorporating the parameters of thermal capacitances and transmittance. Kirchhoff's current law was employed at each node of the network to derive the Equations. In the meanwhile, the radiator was modelled as a lumped thermal capacitance using the heat transfer Equations for the system. However, the lumped capacitance model of the radiator did not consider the heat transfer time delay. Neglecting the time delay was always confirmed based on the assumption of high-water flow rate, but once the water flow becomes low and the thermal transfer demand high, the time delay will be an inherent process, thus the accuracy of the model declines. Therefore, the authors presented an alternative model for the radiator in the form of a discrete element for

which the time delay is considered separately for each discretized radiator element. The problem in discrete-element modelling is that there is no clear rule regarding how many discrete-elements should be considered to reach a high system model accuracy. Meanwhile, more discrete elements will lead to many Equations adding complexity to the system model.

Homod *et al.* (2012) divided the building modelling process into four sections employing the physics-based modelling technique. The technique was based on mass and energy conservation and heat transfer Equations. The indoor space and furniture are the first section handled as thermal capacitance and having the same temperature. The so-called opaque building surfaces, such as walls, doors and roofs that exchange heat between the indoor space envelope and its neighbourhood, formed the second structure modelling. The third was modelling the building transparent fenestration surfaces related to windows, skylights and glazed doors that also exchange heat between the indoor space envelope and its neighbourhood. The fourth was modelling the exchanging and storing of heat between the indoor envelope and the building slab floor layers. In order to complete the derived HVAC model, the researchers developed a unique model reference signal based on the evaluation of the indoor thermal comfort to be combined with the four structure-based models. For this purpose, they did use the indicators of Predicted Percentage of Dissatisfaction (PPD) combined with Predicted Mean Vote (PMV). By this technique of referencing they replaced the traditional temperature reference signal which affects the thermal comfort but is not the core comfort measure. The outcome model was also important but neglected the inclusion of the HVAC electrical and mechanical components in the final model that weaken the comprehensiveness of HVAC system model. Focusing on the dynamics of the air handling unit (AHU) including the fan, heat and mass transfer in the cooling coil and the air distribution system with each relevant zone, Thosar, Patra and Bhattacharyya (2008) built their mathematical dynamic model. Modelling the

components of AHU have been considered as lumped thermal capacitance employing mass and energy conservation Equations. The accuracy of the model was affected by several assumptions imposed in the model. The researchers neglected the special and transient effect of air handled by the AUH components. They also assumed a constant heat transfer coefficient in all heat transfer processes and air velocity and temperature are regarded as constants throughout the indoor space.

Baldi *et al.* (2016) proposed a comprehensive HVAC model by employing mass and heat transfer Equations to model each HVAC component. The authors offered a modular model so that depending on the complexity, the designer can regard or disregard HVAC components. All the components synthesized the HVAC system, including chillers, pumps, fans, pipes, air ducts, boilers, radiators, heat pumps, air-handling units and thermal zones were incorporated. They employed a classical controller for each component while an upper layer controller can perform the operating point. They used the thermal energy Equations employing partial differential heat and mass exchange and discretized Equations for the space so that ordinary differential Equations could finally be used. Although the authors modelled all the HVAC components individually, the internal interaction between the components was not incorporated in the study.

Physics-based models can provide good generalization. A challenge might arise from the large number of parameters that needs to be identified to calibrate the final developed physics-based models. Furthermore, physics-based models require mathematical Equations based on detailed system information that is too hard to find most of the time.

## **2.2. Data-Driven Modelling**

Due to the complex structure of HVAC systems, which involve so many parameters governing their performance, it is sometimes difficult to model the HVAC system using physics-based

techniques; hence the data-driven or black box modelling methodology is sometimes preferred as it is a simple and easy procedure for deriving HVAC system models. In some references, the data-driven methodology is called the pattern recognition process, wherein there is no need to understand and analyse the internal physics interactions. Data-driven or black box modelling is a technique that observes the performance of the system through the procedure of testing the system variables to obtain the data that is indexed in the order of time and characterizing the system performance. Based on the obtained data, the input-output relationship of the system model can be derived by employing certain mathematical techniques (e.g., statistical regression through mathematical operation).

Without employing knowledge of internal thermal laws of physics related to the industrial process, Probability Density Functions (PDF) is a statistical prediction method that addresses the probability distribution pertaining to a continuous random variable of a process. It is black box related modelling technique and has been employed to model HVAC systems in many studies, such as Ma, Matusko and Borrelli (2015), Hong and Jiang (1995) and Zlatanović *et al.*, (2011). The main concern in this technique is to predict the weather and the room occupancy by using the PDF technique to identify the building thermal load. Based on the calculated probability of the identified thermal load, an appropriate control strategy can be employed so energy saving can be also anticipated and achieved. The researchers have used measured data adequately to validate the developed model.

Many researchers have worked on modelling processes that have certain patterns indexed with time. Bi *et al.* (2000) developed a HVAC model based on the black box concept and without involving the knowledge of the system's internal physics relations or underlying process. During the training procedure, they used a step test in their model identification process acting as inputs for the plant process and employed a tuner algorithm controlling the testing span

based on the obtained data from the inputs and the outputs of the plant process that are in turn fed directly to the tuner algorithm. This procedure can be repeated at any values of testing span. When the test is complete, the obtained data are analysed so that the process input-output model can be realized and subjected to an appropriate control strategy, which is mostly PID controller.

Mustafaraj, Chen and Lowry (2010) offered a statistical regression mathematical operation to derive linear parametric office building models. The office building was in London in which each zone was equipped with two sensors for zone temperature and relative humidity. Their research offered a prediction of zone temperature and relative humidity employing black-box models, such as the Box–Jenkins method (BJ), autoregressive with external inputs (ARX), Autoregressive Moving Average with External inputs (ARMAX) and Output Error (OE). In order to identify model parameters that describe the zone temperature and relative humidity to validate the trained models, the authors extracted the required data from the existing Building Management System (BMS) sensors for a duration of nine months incorporating summer, fall and winter. The extracted data pertained to the following parameters: (i) indoor and outdoor temperature and relative humidity, (ii) supply air flowrate from the AHUs flowing through FCUs and its temperature as well as relative humidity for the zones and (iii) chilled and hot water temperatures. The validation procedures incorporated the calculation of the performance measures for all identified linear parametric models through the formulas of Goodness of fit (G), Mean Squared Error (MSE), Mean Absolute Error (MAE) and coefficient of determination ( $r^2$ ). The results of the study showed that BJ models can offer a more accurate predicted result over the ARX and ARMAX models. The drawback of such a modelling technique is that if there are any changes in the indoor thermal loads, for example by adding more equipment or the measured disturbances are significantly changed, the overall thermal model will significantly change. This modelling gap can appear by observing the PID control

performance deterioration, which was tuned on the original building thermal model. However, ARX, ARMAX and BJ models can adapt the changes in the parameters by re-modelling the plant based on the new changes and then a new PID tuning procedure can be performed.

Following the statistical models' approach, Yiu and Wang (2007) studied ARMAX modelling for (Variable Air Volume) VAV in the AHU system for Single Input Single Output (SISO) as well as for Multiple Inputs Multiple Outputs (MIMO) models. The authors have investigated to what extent ARMAX could be used to describe an air conditioning system. The results showed more accurate ARMAX MIMO prediction results against SISO models.

Virk and Loveday (1994) reviewed a statistical HVAC modelling technique based on the black box concept too. They selected a specific room to be a domain for the study and determined a HVAC system as a multivariable system with three inputs (i.e., cooling, heating and humidifier) and two outputs (i.e., room temperature and room relative humidity). In order to predict the thermal behaviour of the room, the authors employed several testing procedures to build a numerical model. The room plant was subjected to single input tests as well as multiple input tests in order to obtain the output signals with internal coupling effect. The model was derived by employing a statistical method, namely least squares minimization, that can be understood as a method of proposing a regression line which can be positioned between the obtained data values considering least summation of squared distances of the points from the regression line. The model has been validated by the comparison between the actual measurements and model predictions.

A data mining algorithm is part of the data-driven modelling or black box technique; it is a technique defined by Hughes (2017) as "... the process of sorting through large data sets to identify patterns and establish relationships to solve problems through data analysis". Kusiak, Li and Zhang (2010) employed data mining techniques to develop a daily steam load model.

They used a case study of a major power plant that produces steam that can be supplied to more than 100 buildings for the purpose of heating in winter and operating chillers in summer where the patterns of weather influence the total consumption of the steam. Both the steam load and weather data were stored from 2004 to 2007 and obtained for predicting the steam load for the future. The authors studied ten different data-mining algorithms. They found that neural network (NN) ensemble with five MLPs (multi-layer perception) was the best mapping algorithm.

Kusiak and Xu (2012) developed a HVAC system predictive model employing data mining algorithms. Data from weather and data values of 300 thermal related parameters sampled at 1-minute intervals were collected between 31<sup>st</sup> of July to 15<sup>th</sup> of August 2010 and from 21<sup>st</sup> of September to 7<sup>th</sup> of October 2010. Eliminating most of the parameters in order to acquire quality parameters data values, the researcher qualified 21 parameters only. They employed the “Boosting Tree” which is a learning algorithm for ranking the importance of parameters for prediction. The authors used a Multi-Layer Perception (MLP) ensemble data mining algorithm, which outperformed the other data mining algorithms to build predictive models pertaining to energy consumption and indoor room temperature. They validated the model by four matrices, i.e., Mean Absolute Error (MAE), the Standard deviation of Absolute Error (Std\_AE), the Mean Absolute Percentage Error (MAPE) and the Standard Deviation of Absolute Percentage Error (Std\_APE). Using this model, the authors managed to optimize the HVAC system controllable set points to provide savings in energy consumption and to maintain the room temperature within an acceptable range.

Another group of black box models are the state space models, which directly use the measurements data into state space model representation. A (4SID) model derivation technique has been followed in Ferkl and Jan Siroky (2010). State space system matrices can be obtained

from many input and output data measurements. Since Henkel matrix is an integral part of the model derivation process, the (4SID) technique requires one important parameter that is the block rows number of Henkel matrix for model tuning, which can be provided by the user. The authors compared the (4SID) with the statistical method ARMAX model and found that (4SID) is easier and faster to implement, while the ARMAX model can offer better results. It is worth mentioning that the performance of the 4SID methodology becomes poor when the noise signal process has properties that change over time.

Constructed with the use of cognitive and artificial intelligence science, Case-Based Reasoning (CBR) models can be followed to model processes based on the reasoning concept driven by memory of events, which in turn can customise solutions for such processes to fit new needs. Afram and Janabi-Sharifi (2014a) reviewed black box related modelling techniques, including CBR, which is an algorithm that reviews analogous past data cases to determine the most appropriate model for future operation. This modelling methodology has been used in Watson (2001) as well. CBR has a major weakness as it does not consider the problems that can be associated with unseen or unrecorded cases which deteriorate the model's accuracy.

The data-driven or black box modelling methodology is a simple solution and a good alternative to the difficulties that arise from the physics-based technique. Although the data-driven or black box modelling technique is simple and easy to implement for modelling HVAC systems, it has a major weakness in that when the original system conditions or training data of a HVAC system that were considered at the time of deriving the model change, the accuracy of the model will significantly deteriorate. Accuracy deterioration can be reflected on the employed controller performance leading to indoor thermal discomfort, more maintenance efforts, more component wear-and-tear and more energy consumption. Consequently, it cannot be employed to predict the system performance beyond the training data range. HVAC might

be pushed to work beyond the training data due to the change that might take place over the time in the physical properties of the HVAC system components, such as air filter blockage, contamination in the ducts, change in time constants of some actuators, etc. One more limitation is that models based on the data-driven approach cannot be generalised for more industrial applications and can only be specific for certain processes. As a result, the black box modelling technique generally has poor performance. Performance in this context is defined by thermal comfort so that the well obtained thermal comfort matches good performance and bad thermal comfort matches poor performance.

### **2.3. Grey Box Modelling**

The procedure in the grey box is to use the physics-based Equations to build the process model while the parameters values can be identified by the measured data which can be obtained by the manufacturer's operational data included in the catalogue or through a system commissioning procedure. Therefore, both knowledge of the physics laws of the underlying process, as well as the appropriate parameters values, are the primary basis of the grey box modelling technique. It provides generalization capability and good accuracy superior to other modelling techniques (Afram and Janabi-Sharifi, 2014a).

Wu and Sun (2012) developed their HVAC model using the Equations of thermodynamics to determine the model structure and its order, so that these Equations are plugged in a general Autoregressive Moving-Average (ARMA) relation description. The ARMA coefficients can be identified by the specifications of the room volume, thickness of walls and windows, as well as coefficients of heat conduction and convection processes. The authors carried out extensive measurements for 109 days in order to validate the realized model. The weakness in this modelling technique is that if the operation profile is changed or any changes occur in the

HVAC equipment, such changes will lead to counter changes in system dynamics and then the model needs to be updated but using the same mathematical procedure.

Jin *et al.* (2011) focused only on modelling the cooling coil unit. They employed heat transfer as well as mass and energy balance Equations. The model used six parameters that managed to trace out the nonlinearity features of the unit so that calibration of the system becomes simple. These parameters can be obtained either from the manufacturer's catalogue or experimentally. In order to get a practical model, the researchers linearized the model by utilizing Jacobian matrix techniques.

Li *et al.* (2010) have developed a HVAC dynamic model through mathematically modelling the indoor zone based on the physics laws and theory of electrical circuits. The zone model has been inferred from mass and energy balance Equations explained by electrical circuit theory where the walls are represented by thermal resistances and indoor space air as thermal capacitance. The authors also worked on finding the optimal parameters of the zone model, such as thermal walls resistance and room capacitance that mostly correspond to the measured data. For this purpose, they employed a Genetic Algorithm (GA), which is inspired by the biologist Charles Darwin's theory of natural evolution that has been used also for engineering and in many applications. The GA is executed by implementing certain steps including general evolutionary algorithm, fitness function and rule combination. The developed model was not comprehensive and was limited only to the indoor zone while modelling the heat exchanger was left for future study.

Balan *et al.* (2011) used a simplified thermal model for an indoor zone that consists of two dynamic thermal nodes, which are mainly the heat transfer into the indoor zone and the heat transfer through the zone structure employing the heat balance Equations. In order to identify the values of the model parameters, which are basically five parameters related to the thermal

capacitance and the thermal conductance, are estimated from the building physical data. However, since it is difficult to obtain such data from already built building, employing parameter identification techniques could be a better solution. In their study, the authors reviewed different methodologies for identifying the model parameters.

Lopes dos Santos, Ramos and Martins de Carvalho (2012) modelled a major HVAC system component, namely the Air Handling Unit (AHU), based on the white box technique employing physics-based relations and Equations, while the coefficients of the model were estimated based on the black box model consideration identifying the actual data measurements.

Hariharan and Rasmussen (2010) used physics based thermal Equations to model Electronic Expansion Valve (EEV), Thermostatic Expansion Valve (TEV) and the HVAC compressor where their parameters were identified through nonlinear least squares and simplex search algorithms, which can be easily found in the MATLAB software data package.

System parameters identification, as well as knowledge of the governing physical Equations along with the underlying process that are complicated in modelling HVAC systems, are the main processes of developing grey box HVAC models. Grey box models have proved good accuracy and can provide capability of better generalization against the data driven models. However, they require intensive computation and can result in significant efforts. However, in particular cases this difficulty can be mitigated by today's software packages. In some cases, the input-output data are not available which makes the grey box models difficult to develop. It is worth mentioning that the identified system parameters in the grey box models need to be reviewed and verified in the case where the operation conditions deviate aiming to maintain the model accuracy.

#### **2.4. HVAC Distributed Parameter Modelling**

Looking thoroughly to the nature of HVAC plant components, it can be recognised that some parts of the plant are slender and have high ratio value of length to diameter. Considering this distinction of such components is an important fact to realise an accurate HVAC mathematical model. Whalley (1990) mentioned that large scale and slender elements that constitute dispersed system can be usually described obtaining increasing model accuracy through way of a series of interconnected spatially distributed elements system models. Each dynamical element can be represented through a set of algebraic, differential equations. These equations can be solved giving system response prediction following a stochastic inputs or disturbances. Since accuracy of HVAC mathematical model is a vital requirement to secure improved system performance under variant reference input changes and very often occurred disturbance influence, distributed parameter modelling is a considerable option to define the appropriate and accurate HVAC mathematical model which can be the basis for control design, investigation and analysis.

Liu and He (1994) studied the topic of optimizing the thermal comfort level for HVAC system by considering the conditioned space as a distributed parameter system avoiding the traditional treatment of the conditioned space as homogeneous thermal properties. This approach provided an accuracy on the derived model, which can be a reliable basis for system performance investigation and analysis.

The Finite Elements (FE) modelling technique can deal with the spatial nature of industrial processes where the dispersed distributed parameters are represented by replicated multiple lumped parameter models, so that each element incorporates the thermal capacitance, inductance and resistance associated with mass and energy conversation Equations. Lü (2002) used the finite element method for modelling the indoor space air based on differential

Equations of heat and moisture transferred from the building envelope, which were solved using a numeric methodology.

The (FE) methodology might employ Navier–Stokes Equations that embody all the fluid flow and heat transfer effects arising from the heating, ventilation and air conditioning physics related operations. Commercial software packages, such as Computational Fluid Dynamics (CFD), can be employed to validate the design where the parameters can be configured, and dimensions can be adjusted in order to accommodate the changes in temperature, pressure and airflow conditions (Whalley R. and Abdul-Ameer A., 2011). For example, Kim, Kato and Murakami (2001) studied indoor cooling/heating load analysis employing CFD software. Hiyama and Kato (2011) also followed the approach of optimizing the air conditioning response using CFD analysis. However, considering the (FE) Modelling procedure is not preferable because this approach does not provide clear guidance on how many elements to incorporate in the final model. The model itself does not have any dimensional information and all the effects of the multiple thermal capacitance, inductance and resistance elements exist at undefined points in the space. Moreover, the model generates dimensionally large matrix models and the accuracy of the model relies on how many lumped elements must be used with no guidance for the number of elements to be incorporated.

## **2.5. Summary of HVAC System Modelling Techniques**

The outcome from reviewing the previous literature concerning HVAC modelling techniques reveals the scale and the complexity of the problem. Most of the HVAC models were fragmented to one or more individual components so that a HVAC model represents a single loop model or multiple independent loops each with one controlled variable. This is not a practical approach as it does not adequately include all the HVAC system components in a single comprehensive model. Failing to adhere to such an approach will not achieve the major

objectives of building energy efficiency or high indoor air quality and thermal comfort. Such demands cannot be attained without involving a HVAC model that embodies the modelling of a building envelope, indoor space, and HVAC electrical and mechanical components so it becomes comprehensive plant and reliable model. Being comprehensive, the HVAC model will lead to include many inputs and many outputs so that interaction between the outputs is a familiar performance. The interaction between the outputs is caused by a situation where every input change, in general, affects all the output results in models having multivariable structures. Despite the difficulties and the extensive mathematical operations used to decouple the interaction between the system outputs caused by a multivariable system, it can provide a model that can be, along with a compatible control strategy, the basis to secure improved HVAC system performance.

The evaluation in the previous section indicates that Physics-based models can provide good generalization but with a challenge that might arise from the large number of parameters that needs to be identified to calibrate the final developed physics-based models. Furthermore, physics-based models require mathematical Equations based on detailed system information that is too hard to find most of the time. The data-driven or black box modelling methodology which could be alternative to Physics-based models is a simple modelling solution, but it has a major weakness in that when the original system conditions or training data of a HVAC system that were considered at the time of deriving the model change, the accuracy of the model will significantly deteriorate. Accuracy deterioration can be reflected on the employed controller performance leading to indoor thermal discomfort, more maintenance efforts, more component wear-and-tear and more energy consumption. Grey box models have proved good accuracy and can provide capability of better generalization against the data driven models, but they require intensive computation and can result in significant efforts, however it can be mitigated

by today's software packages. Moreover In some cases, the input-output data are not available which makes the grey box models difficult to develop and the identified system parameters in the grey box models need to be reviewed and verified in the case where the operation conditions deviate aiming to maintain the model accuracy.

Looking at the slenderness effect of some HVAC system components where the ratio of length to diameter is high causing a dispersed system nature so they can be modelled based on a distributed parameters technique, will be beneficial to derive a robust and accurate HVAC system model. Neglecting such system distinctiveness will not help to realize a reliable nor robust HVAC system model, thus fragile system design and poor performance can be encountered.

Having such advanced model incorporating above accurate model arrangements can ensure building energy efficiency, indoor air quality, thermal comfort and improved HVAC system performance. It will also be an appropriate solution for a never ending suffer represented by an expensive, time-consuming and long trial and error calibration procedure required by the HVAC maintenance crew at the time of HVAC system's commissioning and lifecycle maintenance.

## **2.6. Mathematical Model to be Employed in the Study**

Due to its accuracy and being close to actual system representation as mentioned by Whalley (1990), considering the distributed parameter modeling technique will be the one of the most practical HVAC models to be subjected to multivariable control technique and aiming to obtain improved system performance. A hybrid distributed parameter-lumped model developed by Whalley R. and Abdul-Ameer A. (2011) would be an adequate practical approach to mathematically represent a general HVAC system enabling compact modelling of large-scale HVAC systems. As the authors have considered slenderness effect of some HVAC

system components such as the ventilated volume, where the ratio of length to diameter is high that causes a dispersed system, an accurate model that is close to the reality of the system can be obtained. This model incorporates distributed parameters elements as well as concentrated lumped point-wise elements. It enables constructing the analytical model realizations that integrate all the dispersed salient dynamics of the system including the finite time delay. The authors started from the fact that some areas and components of a ventilation system are spatially dispersed and the accuracy of lumped modelling of such components declines when the ratio of the length to diameter increases, therefore the model considers the inclusion of an infinite number of series inductance and resistance, as well as shunt capacitance and conductance. In the meantime, without affecting the accuracy, lumped modelling is quite appropriate for duct terminals, such as inlet and exit fan motors, as well as water pump motors due to their physical nature. It is worth mentioning that time delays are incorporated in the final model that make it difficult to apply some control strategies.

As mentioned in the previous section, due to its accuracy and the proximity to the reality of HVAC system among several reviewed models, Hybrid Distributed Lumped Parameter Model is the acknowledged mathematical model to be used in this study. A ready derived model is found in Whalley R. and Abdul-Ameer A. (2011). Figure 2.3 illustrates a schematic diagram of ventilation and air conditioning system for the Hybrid Distributed Parameter-Lumped Model addressed by the authors. It shows the ventilated volume, the ducting network, the chilled water pump, the ambient heat transfer into the ventilated volume and the inlet and exhaust fans. The inlet and exhaust fans are modelled through lumped parameter realizations. However, the dimensions of the ventilated volume dictate modelling it through a distributed parameter method. More energy efficiency can be achieved through re-cycling the filtered cooled supplied air.

- Air shaft as distributed parameter module
- Impedance lumped/ point wise modules, inlet fan and outlet fan.
- - Hybrid lumped distributed parameter model.

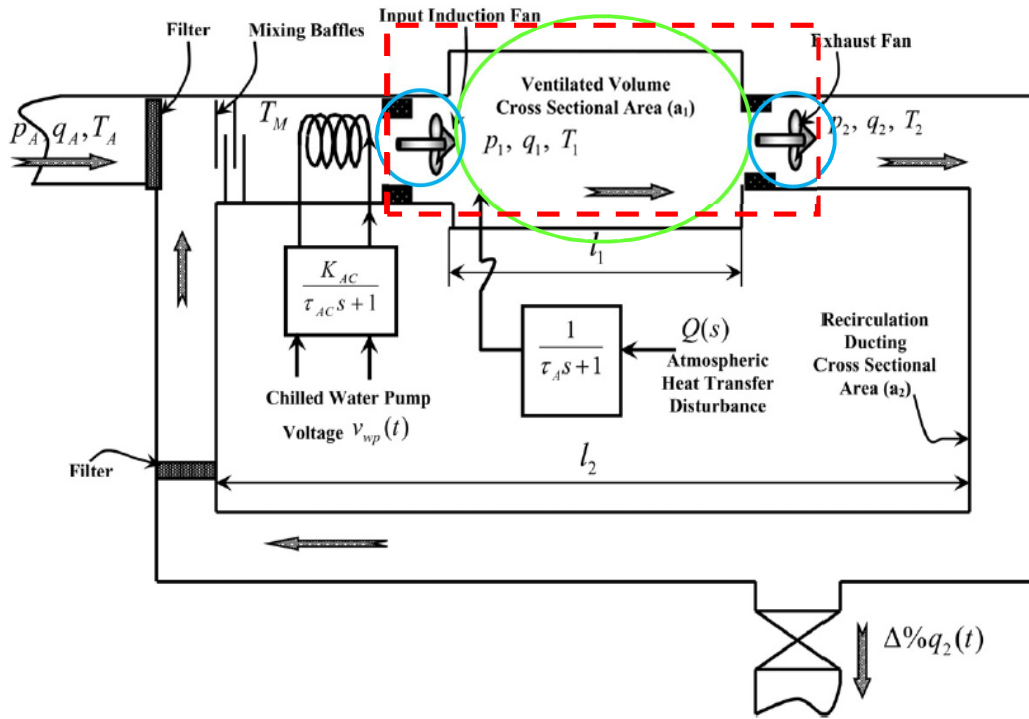


**Figure 2.3**, Schematic diagram of HVAC system showing the major components including ventilated volume, the ducting network, the chilled water pump, the ambient heat transfer into the ventilated volume and the inlet and exhaust fans. (Walley R. and Abdul Ameer A. 2011, pg 3)

This can be achieved by the installation of a re-circulation duct reducing the thermal load on the cooling unit. Through such HVAC system structure, air is filtered, chilled water and temperature control units are used to get the recycled air conditioned after mixing it with atmospheric air and before it is supplied to the ventilated space.

Dual ventilation fans are integrated in the model so that the inlet air fan supplies the cooled air to the ventilated volume while the exit fan enables the air to be returned so that proportion of the return air is expelled to the atmosphere as exhaust air. The remaining proportion is mixed with external air so that the mixture is passed through a filtration process, after which it flows over the cooling coil enabling an air re-circulation process and providing indoor air quality and thermal comfort. The exhaust fan is configured quite often in the HVAC plant serving to keep the ventilated volume static pressure at a constant level relative to the ambient atmospheric pressure.

Additional performance efficiency can be achieved by handling variable air flow based on demand and through operating the exhaust and supply air fans individually. This process can be enhanced by employing VFD fulfilling part-load conditions so that such regulation will be reflected on energy saving implementation. Beside the airflow rate and inlet air pressure, the temperature of the air supplied to the indoor space is the ideal controlled variables.

The final model is an integration of the mathematical Equations that govern the variations of air stream temperature with the mathematical hybrid lumped distributed parameter representation in Figure 2.3. These air stream temperature mathematical Equations are adequately explained in Whalley R. and Abdul-Ameer A. (2011). The temperature variations occur when the HVAC system operates causing changes in air stream pressure and air flow rate and can be caused by external environmental changes so that such temperature variations lead to transient heat transfer effects. In addition, for expressing the transient heat transfer responses, the governing Equations are employed for variations in steady state airflow conditions. These temperature variations are caused by (i) changes in pressure and airflow at the inlet to the ventilated volume, (ii) temperature changes caused by circulation and air conditioning effects, (iii) temperature changes caused by changes in airflow at the outlet from

the ventilated volume. The model has also considered the typical losses related to steady state frictional, dynamic impedance, circulation network and ducting.

With the open loop multivariable system responses, significant complications arise with the variations in system inputs, such as variations in the voltage supply at the inlet and outlet fans, chilled water or airflow temperature, and atmospheric ambient heat transfer affecting many outputs, such as volumetric airflow, air pressure and ventilated volume temperature. In addition to these complications, an interaction between the system outputs in such a manner that a change in each input impacts all the outputs, leading to multivariable structures as an inevitable result.

Adopting an accurate HVAC mathematical model such as the Hybrid Distributed Lumped Parameter along with application of a scientific, systematic, multivariable control strategy is a mandatory requirement in order to achieve energy efficient HVAC operations and improved performance.

## **2.7. Chapter Summary**

The literature has revealed some limitation in HVAC modelling techniques that can lead in inadequacy in the HVAC system performance. Fragmenting the HVAC system into separate components so each one can be modelled individually is one of the limitations. Neglecting the dispersed nature of some HVAC components added more challenges on the HVAC system models.

Learning from such limitations, and based on the guidance that showed how to get accurate and close to reality model, this study will explore the hybrid distributed-lumped parameter approach detailed in the last section and modelled by Whalley R. and Abdul-Ameer A. (2011) as an already derived HVAC system due to its accuracy and proximity to HVAC actual system. Based on the variation of voltages at the inlet and exhaust fan motors, which represent system

inputs, the system outputs of air pressure, volume airflow rate and supplied air temperature will be affected. These outputs are also affected by the inputs of atmospheric ambient heat transfer as well as by inputs of voltage applied on the motor of the chilled water pump. The prediction of system responses characteristics has been obtained by Whalley R. and Abdul-Ameer A. (2011) through employing numeric analysis methodology providing graphical time domain performance responses only.

However, the frequency domain representations are missing and were not addressed by authors in their research. Time domain in their research has been showed through system responses on graphs and not through time domain mathematical representation where the system is expressed by linear differential equations in respect to time. The major control techniques to be used in the study would be frequency domain equations-based techniques. Considering ( $s = j\omega$ ), the frequency domain equations are basically a rational transfer functions in Laplace "s" variable where these functions can be processed and analysed using the s-plane when designing a control system. Such process incorporates defining the location of the poles and zeroes that represent the roots of transfer functions denominator and numerator respectively, on the s-plane and assessing the stability of the closed loop system by making sure that all system poles are placed in the left hand side of the s-plane. This analytical process can't cope with time domain equations. Therefore, this study will process the time domain model responses converting them to frequency domain maintaining the dynamical characteristics of the system and obtaining a three inputs-three outputs multivariable transfer function matrix, which is the basis of analysing and regulating HVAC system performance.

## **Chapter Three**

### **Literature Review**

#### **HVAC Control Techniques**

According to the energy efficiency concept, the main aim of designing a control system for a HVAC system is to achieve low energy consumption without sacrificing the building occupants' thermal comfort and indoor air quality. Thermal processes of HVAC systems are characterized with time lag due to the big mass of some HVAC system substances, such as conditioned space, building envelope, and so on, so that such components take a significant time in storing, losing and transferring thermal energy. Pressure inside the indoor spaces as an output for the fan operation takes some time also to start raising to a nominal value. Therefore, controlling industrial processes with time delay can be a challenging task as such time delay creates phase shifts, where the phase shift in feedback control, usually causes limitations on the control bandwidth that in turn influences the stability of the closed loop system. Some control design algorithms cannot directly handle time delay processes, such as root locus, Linear Quadratic Gaussian (LQG) control, and pole placement so that time delay must be approximated (MathWorks, 2018). The dynamics and the setting points of the system are time variant and affected with many disturbances. Non-linearity of temperature in a HVAC system operation adds challenge to designing a control system so that compensation techniques must be incorporated. Changes in the external climatic conditions, as well as indoor inhabitants' behaviour, can act as uncertainties affecting the designing of the control system. The control strategy must be capable enough to tackle all these challenges.

Nonlinearity of a process can be handled by some techniques to convert it into a linear process so that the set point is maintained. However, if the nonlinearity of the process is weak around the operating condition point, the influence of the nonlinearity can be considered negligible and traditional feedback control can be employed so that the system performance can be satisfactory.

Hence a control technique that handles HVAC system models must cope with all these control tasks.

### **3.1 Classic Control Techniques**

Classic controllers have been employed for HVAC systems using simple control techniques. The classical ON-OFF procedure with thermistor feedback control is common in some residential buildings where the control system can be either OFF or ON. The system operation is OFF when temperature reaches the set point and ON when the indoor temperature is higher than the set point. Advances can be employed by associating the function of the HVAC system with the status of indoor spaces occupancy (Agarwal *et al.*, 2011). However, despite this intuitive control method being simple, it gives poor performance because of the steady state error and oscillation around the set point that occurs in most cases. Proportional, Integral and Derivative (PID) control is a more complicated classical control strategy and has been employed in the HVAC systems. It has provided good results when tuned for specific operating conditions. For example, Jin *et al.*, (2011) employed a PID controller for their mathematical model that was built based on the identification of specific parameters values for the nonlinearity features of the model. The authors managed to identify all the non-linearities of the system responses range and designed corresponding PID controlling parameters so that the system does not need PID calibration. Jetté, Zaheer-Uddin and Fazio (1998) used PI to control the fans of the HVAC dual duct, but the authors stressed that on real industrial applications,

the manual tuning consumes considerable time, and much care is required to achieve the right settings. PID auto tuning was also approached by many researchers and can be used in single input single output (SISO) systems as well as multiple input multiple output (MIMO) systems. In the case of SISO systems, a test phase can be implemented so that the input and output data of the process are collected. After completion of the test phase, data can be analysed to realize the process model for a range of operational values to identify suitable PID controller parameters. The system afterwards can be switched to auto tuner with the aid of an algorithm and data records to select the exact PID gains that match the online operating condition (Bi *et al.*, 2000). Lim, Rasmussen and Swaroop (2009) approached the problem in a similar way when they tuned a PID controller linked with a gain value identification process. They offered design tools that give important data to determine gain values that can achieve a trade-off between system robustness and performance. PID controller auto tune can also be employed for MIMO systems, however, due to the coupling effect between the inputs and outputs, the system has to be decoupled first then multiple PID controllers can be applied (Wang *et al.*, 1997).

PID controllers have dominated the process control problem for approximately 50 years (Wang *et al.*, 1997), but they are in some cases responsible for the inconsistency of process system performance. Meanwhile, tuning a PID controller can be difficult, expensive and time consuming (Bi *et al.*, 2000). A PID controller can be a good solution when it is confined to one specific condition, but with the variations of operating condition, it has to be tuned again and this becomes an exhausting process consuming extra efforts.

### **3.2 Advanced Control Techniques**

The current advanced communication and computing devices, as well as the advances achieved in data storage, led to more advanced control techniques for industrial processes. Advanced control techniques employed for HVAC systems were also addressed in the literature of HVAC

control. Gain Scheduling Control (GSC) is a control theory that can be employed where the procedure is to divide the system into several linear zones so that a specific self-tuned gain can be set for a PI or PID controller for each specific linear zone. The PI or PID controller can be applied for a specific linear zone associated with its operating condition so that self-tuning can be implemented based on the system state values (Afram and Janabi-Sharifi, 2014b). For example, (Tahersima *et al.*, 2010) used two different PI controllers which are tuned for HVAC hydronic-radiator at the states of high heat and low heat requirements. In Pal and Mudi (2008) the authors focused on controlling the pressure of supplied air in a HAVC system using a PI controller. The controller was tuned based on the gains that form the error between the measured pressure and the set point of the air supply. Rasmussen and Alleyne (2010) have used the same control concept by offering a study to control an air conditioning system based on MIMO representation. The control strategy employed in this regard is GSC to improve the efficiency of the system during the demands of changing the cooling capacity.

A feedback linearization is also a technique that was used for HVAC nonlinear system models. Instead of linearizing the nonlinear process near an operating point, the process can be subjected to a feedback linearization to transform it to an equivalent linearized process for the whole range of operating points (Miskovic and Vukic, 2009). Many researchers have used the Feedback Linearization Control methodology as employed by Thosar, Patra and Bhattacharyya (2008) and He and Asada (2003). They used a feedback linearization method to eliminate the nonlinearity in HVAC system dynamics and to generate a linear function enabling further control procedures. The researchers also employed a PI controller after achieving equivalent linear model to achieve the desired system performance. Semsar-Kazerooni, Yazdanpanah and Lucas (2008) also followed the same technique by linearizing the HVAC process first then applying a back-stepper controller to achieve the desired performance. The controller used in

their research was also able to reject the disturbance caused by external leaked heat and moisture

The study of Moradi, Saffar-Avval and Bakhtiari-Nejad (2011) focused on proposing a nonlinear control for a nonlinear air handling unit, modelled as a MIMO system. The inputs considered in the study were the positions of the valves controlling the cold water and airflow rates while the outputs were the indoor temperature and relative humidity. The researchers have employed comparisons between two different control techniques, these are Gain Scheduling Control and the Feedback Linearization Control in which the dynamic behaviour of one controller was better than the other. He and Asada (2003) also used Feedback Linearization Control in their study. They managed to transform the linearity of the multi-unit HVAC system to a linear system for the whole range of operating points and thereafter applied a simple PI control.

Robust Control is one of the control techniques that also has been used for controlling HVAC systems. The Robust Control technique is employed to assure the performance of the system under control regardless of the changes in the system dynamics. The Robust control technique is considered as static in comparison with the adaptive control technique, because it does not adapt to the system dynamic variations but assess the performance and the stability of the system for a bounded range of unknown variables. Anderson *et al.* (2008) followed a robust control technique for a HVAC system to examine some other advanced controllers. They found that a robust control system could provide potential performance improvement. Based on robust control, Al-Assadi *et al.* (2004) achieved improved system performance pertaining to multiple zones indoor temperature and achieved stability with the presence of uncertainties of the model and external disturbances.

Qin and Badgwell (2003) also studied Model Predictive Control (MPC) and defined it as a class of computer algorithms developed for controlling that predicting the plant future responses by computing a sequence of future manipulated variable adjustments. The technique is very popular since it does not need expert involvement during long time of operation period. Some design techniques that emanate from the MPC technique can be used for controlling industrial processes, such as Model Algorithmic Control, Dynamic Matrix Control, Internal Model Control and Inferential Control technique (García, Prett and Morari, 1989). MPC is one of the advanced control techniques that has been implemented to regulate HVAC system operations in the last few years. It employs the system model aiming to predict the future behaviour of the system and applying afterwards the proper control technique (Ulusoy, 2018). The MPC control technique employs an explicit HVAC model to forecast the future system states based on which a vector of controllers can be proposed within certain constrains and expected disturbances in order to optimise the control function cost and system performance (Afram and Janabi-Sharifi, 2014b). Aswani *et al.* (2012) have developed an MPC control technique to optimise the controlling cost of the transient and steady state responses of a HVAC system. The control technique was based on learning the amount of emitted heat by indoor occupancy during the day, month and year. The strategy used in this research is indeed a learning-based technique. Xi, Poo and Chou (2007) have employed a nonlinear MPC control to regulate the indoor temperature and relative humidity based on an optimization algorithm, which was used to generate the control signals online within the control constraints. The obtained results showed good control performance and low steady state errors.

Due to the nonlinearity and the different time lags and inertia, which are inherent characteristics of HVAC systems, it is a challenging task as mentioned in chapter two to develop an accurate mathematical model describing the real HVAC process over wide operating conditions.

Therefore, intelligent control techniques are promising alternative control solutions for HVAC system in comparison with the traditional control methods. When using fuzzy logic controllers as intelligent control technique which is depending on Knowledge Base (KB), no mathematical modelling is required to design the controller (Mirinejad *et al.*, 2012). In the KB procedure the “if-then” which is designed based on human expertise, or according to learning and self-organization methods, does not need the mathematical model of the system. Erez *et al.* (2003) used genetic algorithms in order to develop a fuzzy logic controller incorporating smart tuning to regulate a HVAC system. The authors used real experiments combined with simulations to validate the effectiveness of the proposed control technique.

### **3.3 Multivariable System Control**

An advanced HVAC system is classified as a synthesized system with many functional components and with more than one input and output variables. Various inputs interact on different levels with various outputs so that the HVAC system is highly recommended to be modelled as a multiple input multiple output system. However, as per Macfarlane (1970) multivariable system control is specified with some difficulties and restrictions. The main difficulty when the feedback control is applied arises from the internal interactions between the various feedback loops, which influence each other. Such interaction can influence the system stability margins in contrast to SISO systems.

The Inverse-Nyquist-Array technique is a multivariable control technique that combines the competency of the modern algebra with the analytical procedures of classical control theory. The main procedure of this control methodology is to reduce the interactions between the numbers of classical control loops, which is equal to the number of system outputs. Hawkins (1972) employed Inverse-Nyquist-Array on two examples of multivariable systems. The technique proposed in the study was to have diagonal matrix with decoupled internal

interaction in the system. He emphasized the fact that there is no guarantee to reach a system solution. One more British school multivariable control technique is Characteristic Locus proposed for the first time by Macfarlane (1970). He called the controller a “Commutative Controller” so that spectral analysis can be accomplished to establish a set of transfer functions that reflect the characteristics of the system. Spectral analysis can be formed based on extracting the eigen frame of the system transfer function represented by diagonal eigenvalue matrix which in turn characterizes the directions of system transfer function. Based on this procedure the system can be considered as decoupled so that traditional control techniques for a SISO system can be applied. A compensator can be chosen having similar direction of the system eigenvector. Layton (1970) criticized the approach claiming that it will generate irrational polynomials when eigenvalues are computed, which makes the mathematical process impractical. Consequently, Macfarlane came back in 1971 defending his technique and said that getting the detailed knowledge of the eigenvalues as a function of Laplace variable “ $s$ ” is not necessary, and just getting the eigenvalues represented graphically would be enough for the purpose of compensation. The controller would then be considered as an approximated “Commutative Controller”. The graphical representation of the eigenvalue indeed can replace the eigenvalues vector since it shares the same direction and frequency of the eigenvalue vector (Macfarlane and Belletrutti, 1973).

Based on the emergence of state space, which is a mathematical representation of the time domain system dynamics, the American Multivariable Control School established optimal control technique. It employs the concept of the optimization that relies on the values of the minimum or maximum value of a Performance Index governed by mathematical constraints. Including the optimization concept in the feedback of the proposed control technique is called the Optimal Control. Performance Index can be formed by several methods. Bryson (1996)

stated that the first research pertaining to the employment of feedback control optimization was presented in the 1940s, when the researchers at that time suggested minimizing the Performance Index containing the integral of a squared tracking error. Kalman (1960) suggested another idea by including the state feedback in the Performance Index for the purpose of control optimization. In order to calculate the matrix of the state feedback gains, he employed the Riccati Equation as an algorithm to accomplish the calculation of gain matrix for the state feedback. Later, his control technique employing the Performance Index based on the Riccati Equation was termed the Linear Quadratic Regulator problem.

### **3.4 Least Effort Multivariable Control Technique**

Based on optimization procedures, control effort can be minimized which can be attained by the Least Effort (LE) control technique. Consequently, the control effort in this context is understood to be the maximum amplitude of the control signals or the integral of a specific control function.

A control strategy based on minimizing the control energy has been proposed two decades earlier. It concentrated on minimizing the control energy that needed to get a well- behaved system especially with disturbance rejection condition. It determines what is best possible in terms of optimal energy consumption through writing Performance Index as a mathematical expression. In general, the content of the Performance Index can alter according to the objective of the minimization process. It can be formulated with steady state errors, rise time, cost of operation and amount of required efforts. Consequently, many Performance Indices can be written for different control schemes and control objectives. The minimization procedure in this study incorporates specifying a Performance Index (sometimes called cost function) with content of control signals aiming to minimize the energy consumption. The control signals in this study are voltages on the inlet and exit fans, voltage on the chilled water pump and ambient

heat transfer to ventilated volume which is temperature (equivalent to voltage) multiplied by inverse of thermal resistor (equivalent to electric resistor) according to Ohm law. The control inputs can be written in a form that includes the forward control gains, feedback control gains and system outputs (see section 4.5.3), where the control inputs are written as

$$\begin{aligned} & (|k_1 h_1| + |k_2 h_1| + \dots + |k_m h_1|) y_1(t) + (|k_1 h_2| + |k_2 h_2| + \dots + |k_m h_2|) y_2(t) + \dots + \\ & + (|k_1 h_m| + |k_2 h_m| + \dots + |k_m h_m|) y_m(t) \end{aligned}$$

where  $(k_1, k_2 \dots k_m)$  are the forward control gains,  $(h_1, h_2 \dots h_m)$  are the feedback control gains and  $(y_1, y_2 \dots y_m)$  are the system outputs. Detailed derivation is discussed in section 4.5.3

Squaring the control signals is a part of the calculation process that computes the energy spent by the control system. Applying the integration operation on the summation of the control inputs squared is indeed the optimization process execution. The optimization process will explore when the Performance Index Equation is minimum so that values of the forward and feedback gains at the minimum value of Performance Index Equation are corresponding to the minimum control energy to operate the HVAC plant and achieving in the same time well behaved system performance. It can be understood that the optimized control energy is the minimized energy to operate the plant so that without applying the optimization procedure the plant can dissipate higher control energy which is proportional to the cost of energy

The added value of optimizing the control efforts of a specific control technique can be recognised by comparing the control energy consumption by alternative control technique whose control energy is required to operate HVAC plant. It is highly recommended to research and to propose solutions of least control energy technique to contribute to the engineering efforts to achieve sustainable built environment.

The control strategy based on minimizing the control energy has emerged from the British Control School and called Least Effort (LE) control technique. It was proposed for the first time by Whalley R. and Ebrahimi M. (1999) to control multivariable systems. The authors worked with their colleagues employing this technique on many further industrial processes. They have obtained good results pertaining to decoupling the internal loops interaction of multivariable systems and improved the dynamics and the steady state responses with minimum control energy dissipation. Improved disturbance rejection was also achieved in their researches. Multivariable LE Control is a controller design method that uses the output feedback, proportional regulation and passive compensators so that the feedback structure is configured by inner and outer loops enabling improvements on transient, steady state and disturbance rejection associated with least control energy dissipation. The avoidance of employing active elements in the design procedure, such as integrators, is the major feature of this control methodology that enabled the researchers to accommodate many industrial applications, like automobile, military and aerospace systems. These industrial processes are characterized with limitations on the mass, inertia and space of power supply. The safe working span of the system components is also assured by the avoidance of integral controllers as its corrective actions is strictly increasing under sustained error conditions (Whalley R. and Ebrahimi M., 2006) . At the first stage, the design procedure aims to secure well-behaved system dynamics under the closed loop configuration. This design procedure is implemented through generating a specific polynomial function that forms the numerator of a transfer function whose denominator is the characteristic Equation of the system. This transfer function in turn is subjected thereafter to root locus design procedure to allocate the poles of the system at positions where the system has well behaved dynamics. Consequently, the coefficients of the generated polynomial will be selected to secure well behaved system dynamics and to be

used in the Performance Index to find a solution for the gain ratios. Once the gain ratios values are computed and selected to make the Performance Index function minimum, they can be used simultaneously to compute the values of the forward gains and along with the generated polynomial. They can be used to compute the feedback gains as well. At the end, the forward and feedback gains are calculated with good secured system dynamics and minimized control efforts alike.

Thereafter, minimum coupling at the steady state system outputs responses can be achieved by pre-compensation, whereas the disturbance recovery can be enhanced satisfactorily by the outer feedback loop gains calibration associated with minimum control energy dissipation.

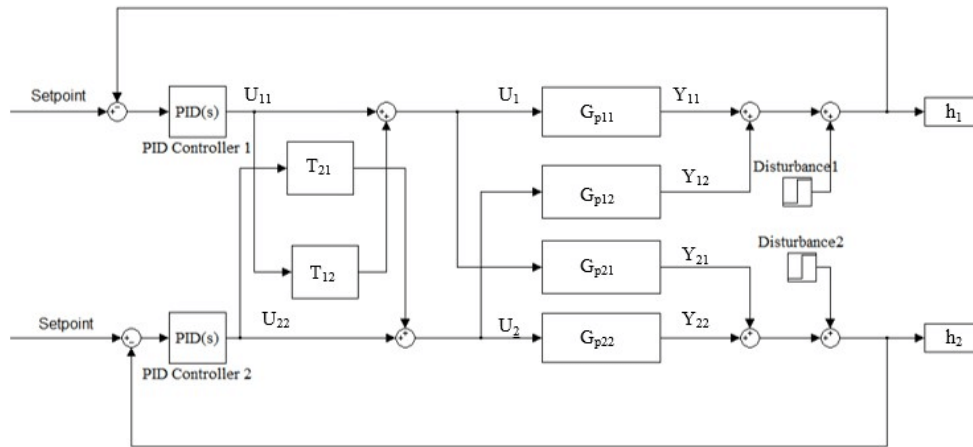
The LE control technique multivariable control has the same control concept of tradition multivariable control techniques, by employing decoupling compensators and close loop control elements to achieve accurate steady state values and to secure well behaved dynamics.

Figure 3.1 shows tradition multivariable control block diagram showing the close loop traditional PID control and decoupling compensators (Vhora, H. and Patel, J., 2016). LE control technique is using the same concept but with different control structure configuration.

The LE control technique utilizes an inner control loop employing forward and feedback control gains to secure the dynamics of the system responses and feedback outer loop to secure the accurate steady state responses as well as enhancing the disturbance rejection calibration.

Figure 4.10, in chapter four shows the block diagram of LE Controller showing the inner and outer loops configuration.

One more differentiator with the LE control technique is that it calculates the forward and the feedback control element gains based on the optimization process so the LE controller can attain a well-behaved system response but with least control effort dissipation.



**Figure 3.1.** Block diagram of tradition multivariable control technique (Vhora, H. and Patel, J., 2016, pg2)

A LE control strategy has been proposed by Whalley R. and Ebrahimi M. (2004) to control a gas turbine system modelled as a two inputs two outputs multivariable system. A transfer function matrix was obtained and root locus on frequency responses methodology was followed in the design of an inner loop where the regulation of the system dynamics occurs. An outer loop is used to secure steady state output accuracy with outer feedback loop for adjusting and enhancing the disturbance recovery with minimum control energy.

The control technique has been employed by Professor Whalley and his colleagues on many other applications. Whalley R. and Ebrahimi M. (2000) applied the control technique to regulate a mixing-tank liquid level. Whalley R. and Ebrahimi M. (2004) in another research study employed the same control technique on Automotive Gas Turbine application. The results in all the application have shown improved system dynamics, accurate steady state responses, minimum internal loops coupling and minimum control energy dissipation to recover the disturbances entering the system.

This project will employ the same concept by using the LE control technique on a HVAC system but modelled with more complexity by incorporation of HVAC system with three inputs

and three outputs. The proposed solution herein aims also to obtain improved system dynamics, accurate steady state responses, minimum internal loops coupling and minimum control energy dissipation to recover the disturbances affecting the system. However, to show the claimed improvements, an alternative multivariable control strategy will also be employed, enabling a comparison study.

## Chapter Four

### HVAC Mathematical Modelling and Control Techniques Approaches

#### 4.1 HVAC Hybrid Distributed-Lumped Parameter model

The readily derived HVAC Hybrid Distributed-Lumped Parameter model for Air Conditioning (AC) function developed by Whalley R. and Abdul-Ameer A. (2011) will be the basis of the mathematical model to be employed in this research. Bartlett, H., and Whalley, R. (1998) studied the lumped distributed parameter modelling technique in their research. They reviewed several lumped distributed parameter topologies; e.g. considering distributed element with final lumped termination such that (D-L) model. In some applications, there might be several distributed parameter modules between two lumped impedance modules such as (L-D-D...D-L). In HVAC model, the topology to be used is (L-D-L) which means lumped impedance module – distributed parameters module – lumped impedance module. Figure 4.1 shows a representation of transmission line which can be the basis to interpret the dispersed systems.

The transmission line element as per the Figure 4.1 is one of an infinite series of distributed elements comprising the dispersed system. For each distributed element in a dispersed system,

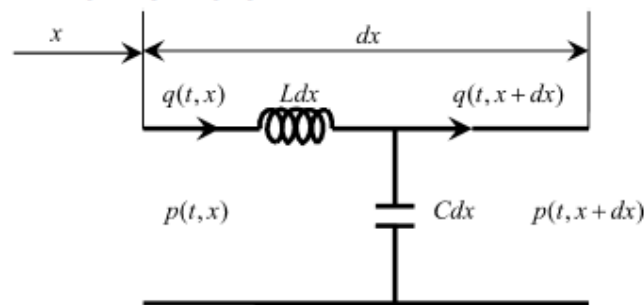


**Figure 4.1.** The transmission line as of distributed element, Whalley R. and Abdul-Ameer A. (2011)

it is assumed that it has an input such as pressure, force, voltage etc. as well as an output such as flow rate, deflection, current etc. (Whaley, R. 1988). So that an input disturbance which can be transmitted from a distributed element to the next adjacent one and at specific frequency is propagated, reflected and attenuated so that once a dispersed system is subjected to an input signal it sends waves through both adjacent distributed sections continuously until quiescence is achieved.

This phenomenon in the dispersed system creates time delay between the inlet and outlet outputs as well as between the inlet and outlet inputs which can affect the control stability band and creates challenges for some control techniques

In this research application, the conditioned volume or air shaft that needs to be ventilated, air conditioned and controlled as multivariable system has the length of ( $L$ ) and a diameter of ( $2r_1$ ). As per the distributed parameter modelling technique by Whalley R. and Abdul-Ameer A. (2011), each element in the infinite series with very small length of ( $dx$ ) is subjected to pressure inputs and pressure outputs  $p(t, x)$  and  $p(t, x + dx)$  respectively. The difference between the input and out pressures creates volume air flow rate  $q(t, dx)$  and  $q(t, x + dx)$ , respectively. Moreover, each element has an associated series inductance ( $L$ ) which is equivalent to the gas or air path inertia per unit length. A shunt capacitance ( $C$ ), equivalent to the gas/air stream compliance per unit length, is also considered, where:

$$L = \frac{1}{\pi r_1^2}, \text{ The gas/air stream inductance per unit length, so the gas/air inductance is}$$

proportional to the inverse air shaft radius squared

$C = \frac{V}{RT\gamma}$ , The gas stream capacitance per unit length and  $V = \pi r_1^2 l_1$ , where  $(l_1)$  is the air shaft length and  $(r_1)$  is the air shaft radius,  $(\gamma)$  is the amount of gas/air,  $(R)$  is the gas characteristics constant and  $(T)$  is the gas temperature.

At the end, Whalley R. and Abdul-Ameer A. (2011) followed specific mathematical steps and operations employing trigonometry branch of mathematics to derive in details the air shaft distributed parameter model for the length  $(l_1)$  and diameter of  $(2r_1)$  and with implementing the Laplace transformation with zero initial conditions, a hybrid distributed parameter model can be expressed in the following general matrix equation, relating the pressure  $(p_1)$  and air flow rate  $(q_1)$  at the inlet with the pressure  $(p_2)$  and air flow rate  $(q_2)$  at the outlet of the dispersed system

$$\begin{bmatrix} p_1 \\ 0 \end{bmatrix} = \begin{bmatrix} \zeta w(s) & -\zeta (w^2(s)-1)^{1/2} \\ \zeta (w^2(s)-1)^{1/2} & -\zeta w(s) - f(p_2) \end{bmatrix} \begin{bmatrix} q_1(s) \\ q_2(s) \end{bmatrix},$$

where:

$$w(s) = \frac{e^{2l_1\Gamma(s)} + 1}{e^{2l_1\Gamma(s)} - 1}, \text{ delay form}$$

$$\zeta = \sqrt{L/C}$$

$$\Gamma(s) = s\sqrt{LC}$$

$$L = \frac{1}{\pi r_1^2}$$

$$C = \frac{\pi r_1^2}{\gamma RT}$$

According to the basic equations governing the pressure and airflow around the system as in Figure 2.3 including forcing the air inside the ventilated volume, the extraction equations of air from the ventilated volume and the equations governing the air circulated in the ducts and mixing the circulated air with the fresh air, the hybrid lumped distributed parameter air shaft transfer function model as per Figure 2.3 can be expressed as

$$G_{hyb}(s) = \frac{\begin{bmatrix} \zeta_1 w_1(s) + \gamma_2(s) & \zeta_1 (w_1^2(s) - 1)^{1/2} \\ \zeta_1 (w_1^2(s) - 1)^{1/2} & \zeta_1 w_1(s) + \gamma_1(s) \end{bmatrix} \begin{bmatrix} K_1 & 0 \\ 0 & K_2 \end{bmatrix}}{\Delta(s)(\tau s + 1)}, \quad (4.1)$$

where

$$\gamma_1(s) = \frac{(0.01m_1s + f_1)}{a_2}$$

$$\gamma_2(s) = \frac{(m_2s + f_2)}{a_2}$$

$$\zeta_1 = \sqrt{L_1 / C_1}$$

$$w_1(s) = \frac{e^{2t_1\Gamma_1(s)} + 1}{e^{2t_1\Gamma_1(s)} - 1}, \text{ this term represents the time delay in the model}$$

$$L_1 = \frac{1}{\pi r_1^2}$$

$$C_1 = \frac{\pi r_1^2}{\gamma RT}$$

$$\Gamma_1(s) = s\sqrt{L_1 C_1}, \text{ ventilated volume propagation function}$$

$$g_{11}(s) = \zeta_1 w_1(s) + \gamma_2(s)$$

$$g_{12}(s) = \zeta_1 (w_1^2(s) - 1)^{1/2}$$

$$g_{21}(s) = \zeta_1 (w_1^2(s) - 1)^{1/2}$$

$$g_{22}(s) = \zeta_1 w_1(s) + \gamma_1(s)$$

$$\Delta(s) = \zeta_1 (\gamma_1(s) + \gamma_2(s)) w_1(s) + \gamma_1(s)\gamma_2(s) + \zeta_1^2$$

$L_1$  Ventilated volume air stream inductance per unit length

$C_1$  Ventilated volume air stream capacitance per unit length

$m_1$  Mass of air in the ventilated volume

$m_2$  Mass of air in recirculating ducting

$f_1$  Friction at the entrance of ventilated volume

$f_2$  Friction at the entrance of recirculating ducting

$K_1$  Inlet fan gain

$K_2$  Exhaust fan gain

$\tau$  Inlet and exhaust fan time constant

$\Gamma_1(s)$  Ventilated volume propagation function

$R$  Characteristic gas constant  $J / kg \text{ } ^\circ C$

The final complete HVAC system model is an integration of the mathematical hybrid distributed-lumped parameter model, as in Equation 4.1, with the mathematical equations governing the following temperature variations in the lumped modelling form that are clearly derived and developed by Whalley R. and Abdul-Ameer A. (2011) in the final Air Conditioning multivariable mathematical system model, these equations are pertaining to:

- i. Air stream temperature variations caused by the changes in the air pressure and airflow at the inlet of the ventilated volume.
- ii. Air stream temperature variations caused by the air conditioning and recirculation effect.
- iii. Air stream temperature variations caused by the changes in the air pressure and airflow at the outlet from the ventilated volume.
- iv. The model has also considered the typical losses related to steady state frictional, dynamic impedance, circulation network and ducting.

The authors have used MATLAB and SIMULATION software to obtain the model time domain responses of the open loop structure. The employment and integration of such model can be performed by undertaking the open loop HVAC system time domain responses obtained by the authors in their research and converting them to frequency domain responses. Enabling 3-inputs 3-outputs multivariable HVAC model. The three time domain outputs responses selected for this study as shown in Figures 4.3, 4.4 and 4.5 are the volume airflow, the  $q_1(t)$  air pressure  $P_1(t)$  and air temperature  $T_1(t)$  at the inlet of the ventilated volume while the inputs of the system to be considered are the voltages at both the inlet and exist fans  $v_1(t)$  and  $v_2(t)$  applied simultaneously, the voltage at the chilled water pump  $v_{wp}(t)$  and the atmospheric ambient heat transfer  $Q(t)$ .

It is worth noting that the Air Conditioning system model operation in the open loop representation has been scaled and calibrated by Whalley R. and Abdul-Ameer A. (2011). This means that at zero value changes at the inputs of the system during the system operation, the Air Conditioning system keeps working and providing the same mentioned steady state values, thus zero output changes. The parameters are also selected by the authors to provide specific

transient and steady state values for indoor volume airflow rate, air pressure and air stream temperature. In order to assess the performance of the system in the open loop situation, a step input change has been applied on the inputs of the system. Using numeric integration software, the system output responses have been obtained and portrayed as time domain responses in Figures 4.3, 4.4 and 4.5 at 1% step changes in the voltages of inlet and exit fan motors  $v_1(t)$  and  $v_2(t)$ , 1% step change in voltage applied on the chilled water pump  $v_{wp}(t)$  and 1% step change in the atmospheric ambient heat transfer  $Q(t)$  respectively (Whalley R. and Abdul-Ameer A., 2011). The application of step change on one of the inputs and in a successive manner as mentioned above, is meant to see the reaction to this reference input change on the three system outputs away from the other inputs, and that's why they must remain zero. The system reaction performance must be analysed in terms of system output coupling and the influence of this reference input change on the dynamics of the other system output responses. Heavy coupling can be witnessed in the output system responses as per Figures 4.3, 4.4 and 4.5. Interpretation of the system outputs are reviewed adequately in section 4.3

The authors have provided the system responses as time domain only as per Figures 4.3, 4.4 and 4.5 where the Laplace transformed transfer function matrix was not approached in their research. However, these time domain simulation results of the hybrid model show all system dynamical characteristics which are essential for maintaining integrity and accuracy of system mathematical model when transferring it from time domain to frequency domain.

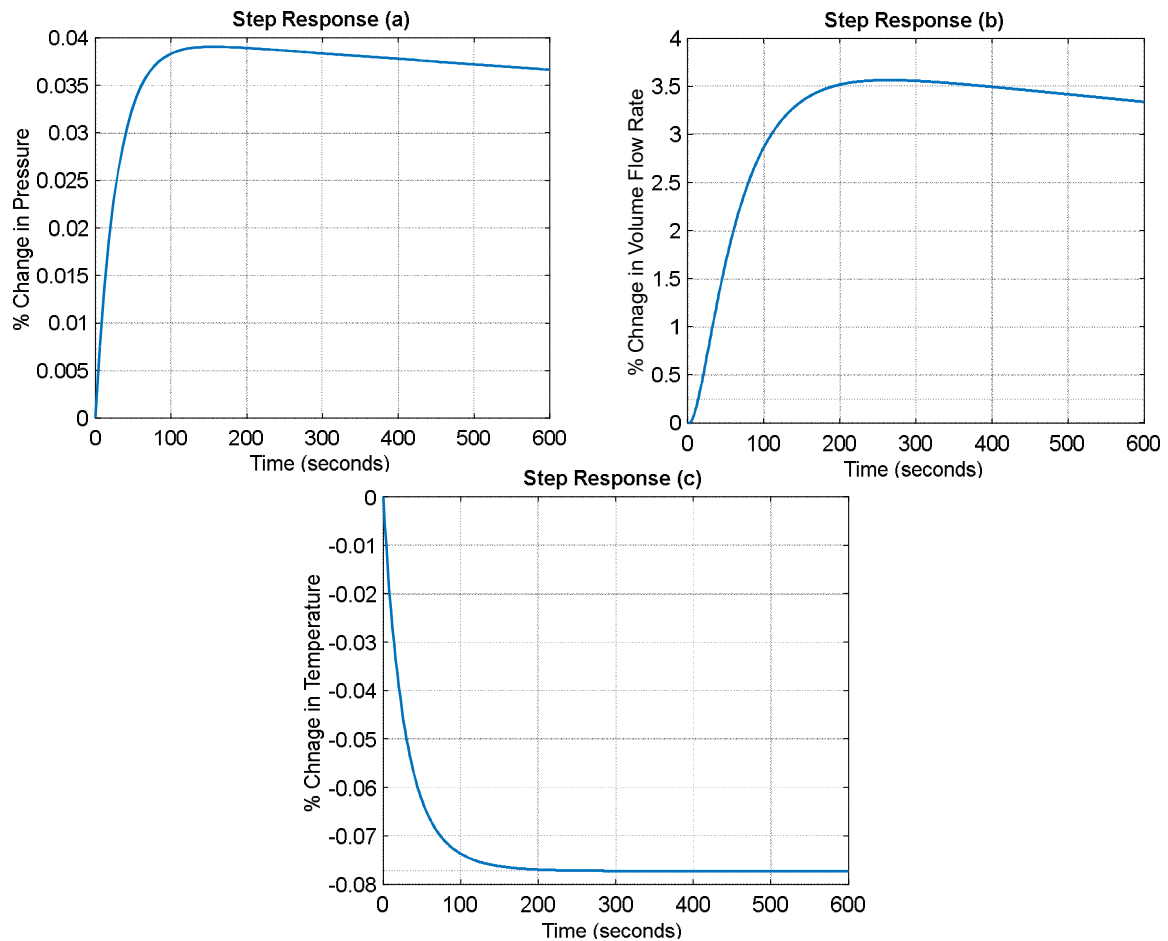


**Figure 4.3. a:** Time domain pressure response. **b:** Time domain volume air flow response. **c:** Time domain temperature response when 1% step change in the  $v_1(t)$  and  $v_2(t)$  voltages is applied at the inlet and exit fan motors

This study will extend their work and compute the transfer function matrix in Laplace representation based on the time domain model responses so that it will be the basis for developing the Air Conditioning multivariable, closed loop feedback control strategy.

#### **4.2 Deriving the Air Conditioning System Transfer Function Matrix**

The system model in the frequency domain is essential to enable controller design and analysis, hence identifying the transfer function matrix in the frequency domain is the basis of designing a control strategy for the Air Conditioning system in this study. The major control techniques to be used in the study would be the equations of frequency domain-based techniques. The frequency domain equations are basically a rational transfer functions in Laplace "s" variable where these functions can be processed and analysed using the s-plane when designing a control system. Such process incorporates defining the location of the poles of the transfer function on the s-plane and assessing the stability of the closed loop system by making sure that all system poles are parking in the left-hand side of the s-plane. This analytical process can't cope with time domain equations. Therefore, this study will process the time domain model responses converting them to frequency domain and obtaining a three inputs-three outputs multivariable transfer function matrix, which is the basis of analysing and regulating HVAC system performance.

Hence there are some methods that can be applied to obtain the system frequency domain representation from the time domain. These methods are as follows:

### 4.2.1 Fast Fourier Transform (FFT)

The FFT is a mathematical operation that converts the signal from its time or space pattern into frequency domain. It handles the time domain signal by observing and measuring when the signal is passing cycles so that amplitude, rotation speed and offset of each different cycle are defined and computed. Based on this computation procedure, the set of amplitudes and angles against specific frequencies can be identified so that the model of the system in the frequency domain can be obtained. However, looking at the responses in Figures 4.3, 4.4 and 4.5 it can be noticed clearly that the output signals do not adequately pass clear cycles and none of the

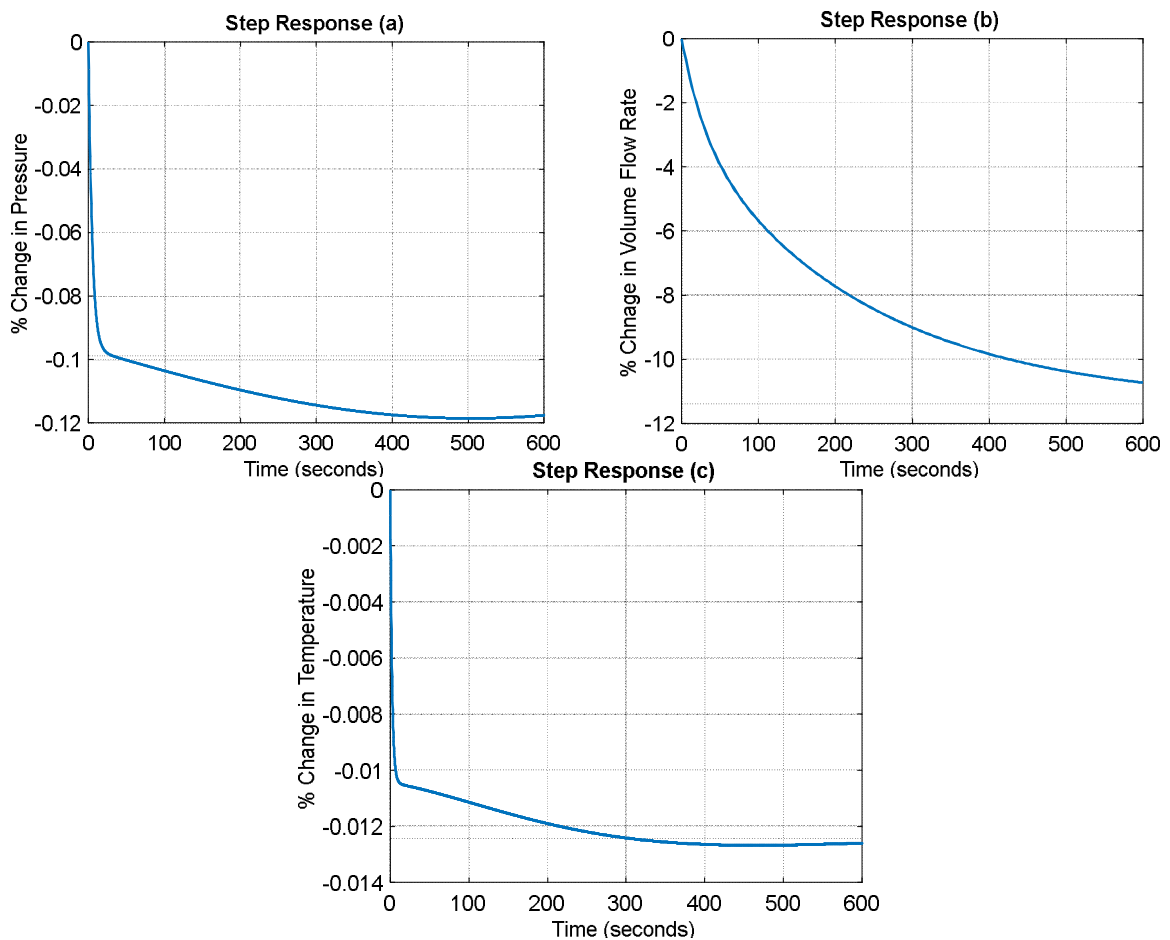


**Figure 4.4, a:** Time domain pressure response. **b:** Time domain volume air flow response. **c:** Time domain temperature response when 1% step change in the voltage  $v_{wp}(t)$  is applied at chilled water pump

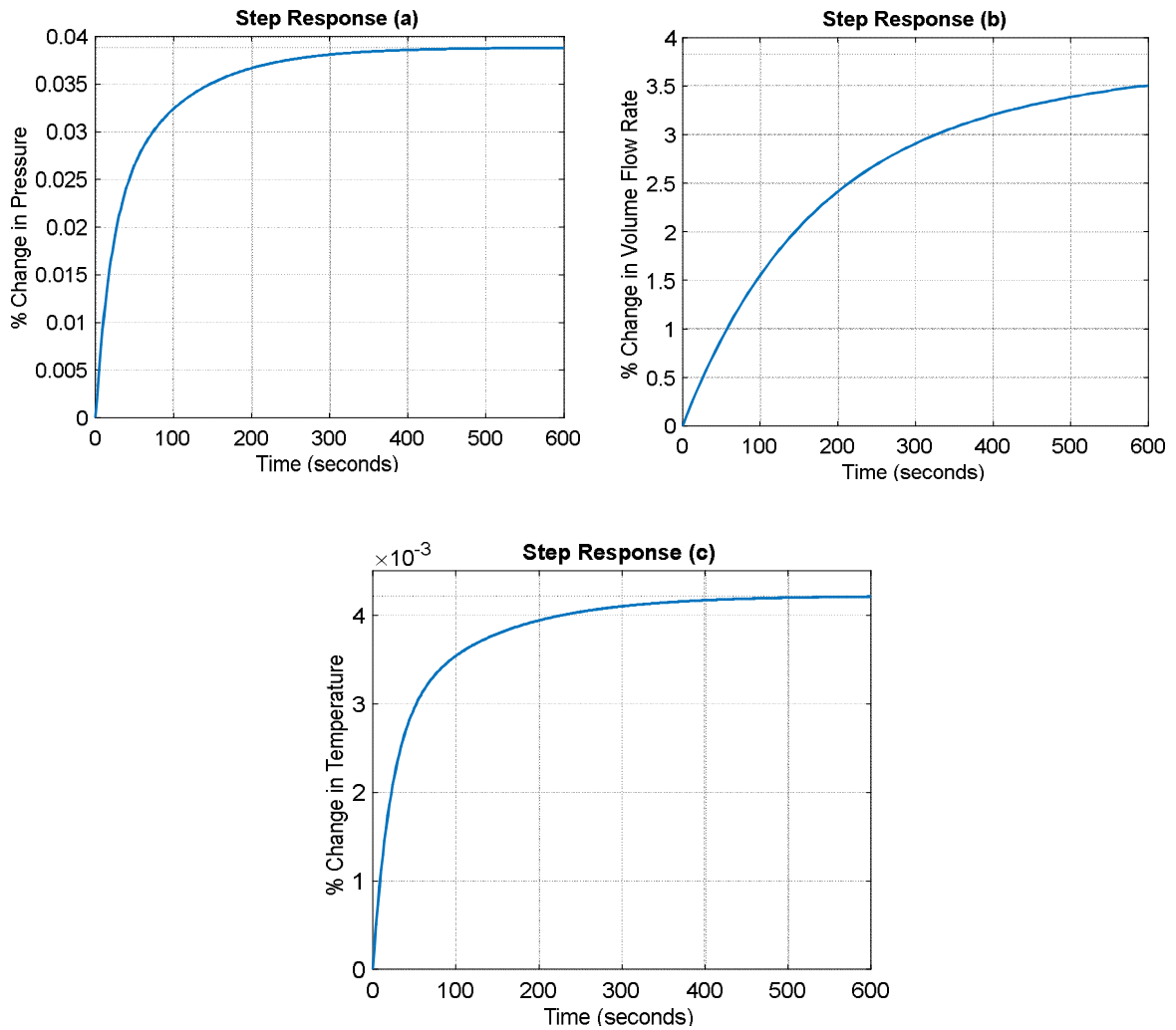


**Figure 4.5, a:** Time domain pressure response. **b:** Time domain volume air flow response. **c:** Time domain temperature response when 1% step change in the ambient heat transfer  $Q(t)$  is applied.

signals in these Figures are repeated in a clear cycle. Therefore, using FFT is not the most efficient technique to obtain the system representation in the frequency domain for this study.

#### 4.2.2 System Identification Toolbox

This is a software toolbox provided by the numerical computation software MATLAB enabling system engineers and process control designers to construct mathematical models of dynamic systems from measured input-output data. Using the System Identification Toolbox (SIT) by

MATLAB in this study will aim to employ the time-domain data as illustrated in Figures 4.3, 4.4 and 4.5, in order to extract the continuous time transfer function in Laplace transformation representation. The procedure in SIT will first require identifying the input-output data through x-y coordinates of each time domain system response illustrated in Figures 4.3, 4.4 and 4.5 so that the dynamic characteristics of each system response is introduced to MATLAB. The time domain system responses coordinates have been identified through simple process, the x-coordinate of a point is the value that tells how far from the origin the point is on the horizontal, or x-axis while y-coordinate of a point is the value that tells how far from the origin the point is on the vertical, or y-axis. To find the(x-y) coordinate of a point on the time response graph, a straight line has been drawn from the point directly to the x-axis and another straight line from the point directly to the y-axis has been also drawn. The pair of numbers where both lines hit both axes are the coordinate of the point on time response graph

The table below shows x-y coordinates of the time domain volume air flow rate response as in Figures 4.3 b when 1% step change in the  $v_1(t)$  and  $v_2(t)$  voltages is applied at the inlet and exit fan motors:

x	0	25	50	75	100	125	150	175	...	500	525	550	575	600
y	0	0.68	1.68	2.37	2.87	3.17	3.33	3.47	...	3.42	3.4	3.38	3.36	3.34

Similar tables of the remaining time domain responses have been identified and fed to the SIT application. The tool has managed to generate nine transfer function elements representing the open loop multivariable Air Conditioning system transfer function matrix. The transfer function elements have been identified based on the introduced dynamic characteristics of the time domain responses so the transfer function matrix in frequency domain can be written as:

$$G(s) = \begin{bmatrix} \frac{0.001402 s - 2.04e-07}{s^2 + 0.03509 s + 3.44e-09} & \frac{-0.02075 s^2 - 2.227e-05 s - 2.162e-07}{s^3 + 0.2141 s^2 + 8.726e-05 s + 2.189e-06} & \frac{0.001252 s + 2.159e-05}{s^2 + 0.06249 s + 0.0005558} \\ \frac{-0.007734 s^2 + 0.004677 s + 7.761e-08}{s^3 + 0.08749 s^2 + 0.001259 s + 3.132e-07} & \frac{-0.1314 s - 0.001673}{s^2 + 0.0385 s + 0.000147} & \frac{0.02071 s + 6.281e-05}{s^2 + 0.009175 s + 1.64e-05} \\ \frac{-0.002809 s - 8.36e-05}{s^2 + 0.06943 s + 0.001082} & \frac{-0.004665 s^2 - 4.227e-05 s - 3.085e-07}{s^3 + 0.4551 s^2 + 0.003889 s + 2.48e-05} & \frac{0.000137 s + 1.657e-06}{s^2 + 0.05461 s + 0.0003927} \end{bmatrix},$$

so that the input- output relationship of HVAC open loop multivariable system in the matrix form becomes:

$$\begin{bmatrix} P_1(s) \\ q_1(s) \\ T_1(s) \end{bmatrix} = \begin{bmatrix} g_{11}(s) & g_{12}(s) & g_{13}(s) \\ g_{21}(s) & g_{22}(s) & g_{23}(s) \\ g_{31}(s) & g_{32}(s) & g_{33}(s) \end{bmatrix} \begin{bmatrix} v_{fans}(s) \\ v_{wp}(s) \\ Q(s) \end{bmatrix}, \quad (4.2)$$

where the input – output individual Equations can be written as:

$$P_1(s) = g_{11}(s)v_{fans}(s) + g_{12}(s)v_{wp}(s) + g_{13}(s)Q(s),$$

$$q_1(s) = g_{21}(s)v_{fans}(s) + g_{22}(s)v_{wp}(s) + g_{23}(s)Q(s),$$

$$T_1(s) = g_{31}(s)v_{fans}(s) + g_{32}(s)v_{wp}(s) + g_{33}(s)Q(s).$$

Consequently, based on these Equations, the block diagram as in Figure 4.6 comprising a three-inputs, three outputs open loop Air Conditioning multivariable system can be built:

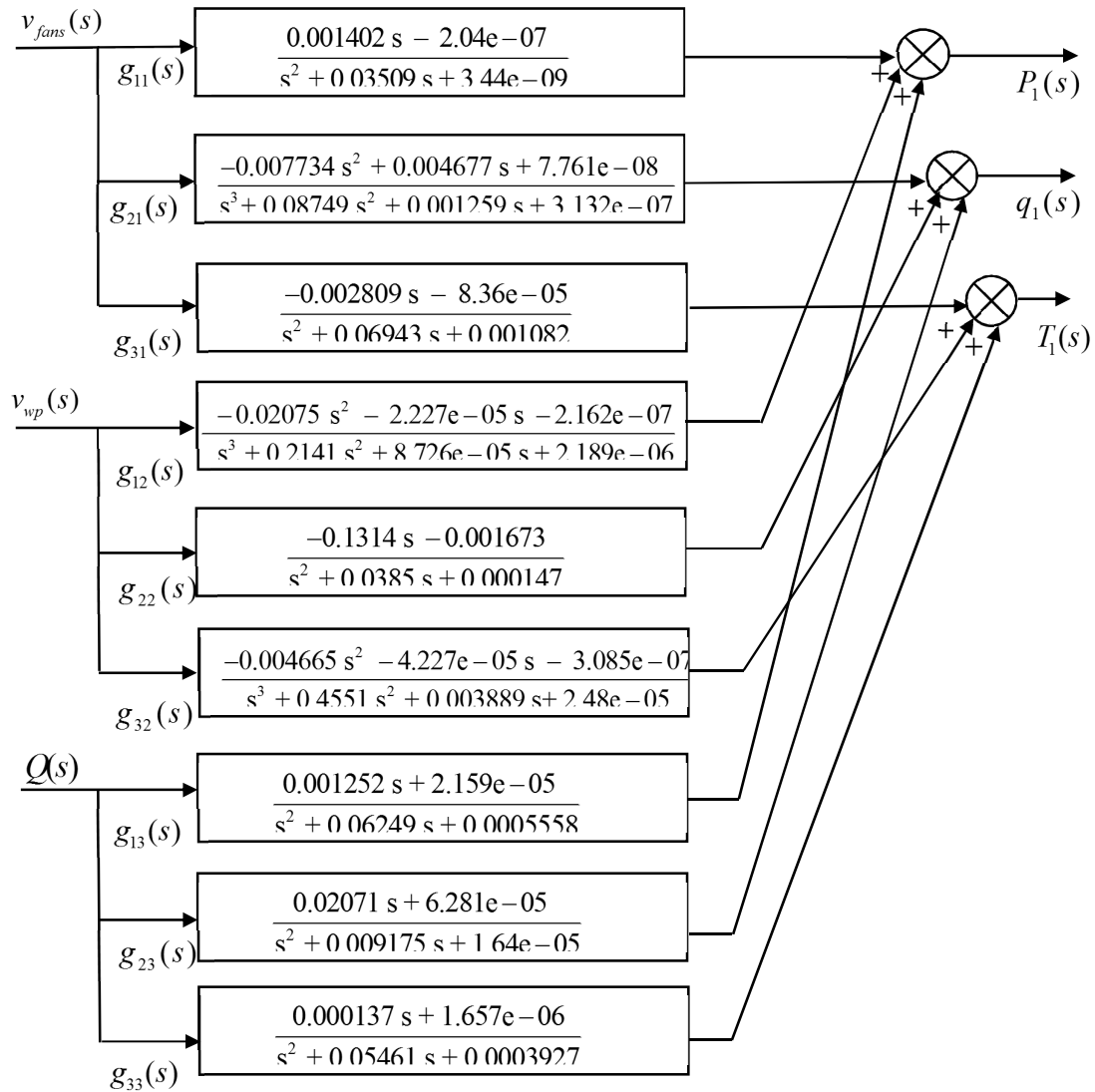


**Figure 4.6,** Open loop Air Conditioning complete block diagram in transfer function form

### 4.3 Air Conditioning Multivariable Open Loop Responses

An open loop transfer function matrix has been derived through the previous section. The open loop transfer function responses as per the block diagram in Figure 4.6 can be plotted through the MATLAB and SIMULATION software. Figure 4.7, 4.8 and 4.9 show the open loop responses of both time domain responses overlapping with the converted frequency domain

responses; they are overlapping and fit to estimation of more than 98%. Figure 4.7 shows the open loop output responses when 1% step change only is applied at the voltages of the fan motors at the inlet and exit of the ventilated volume

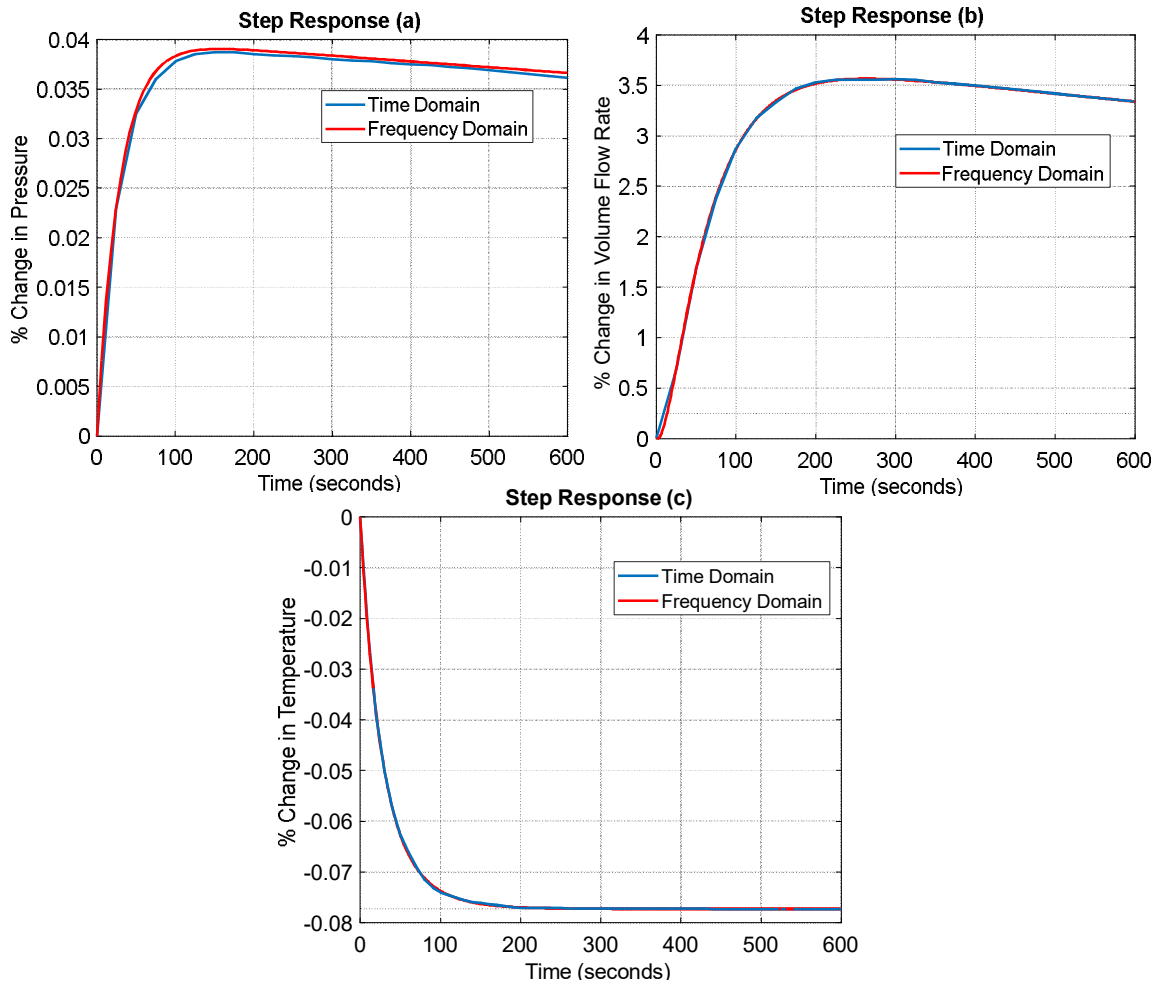


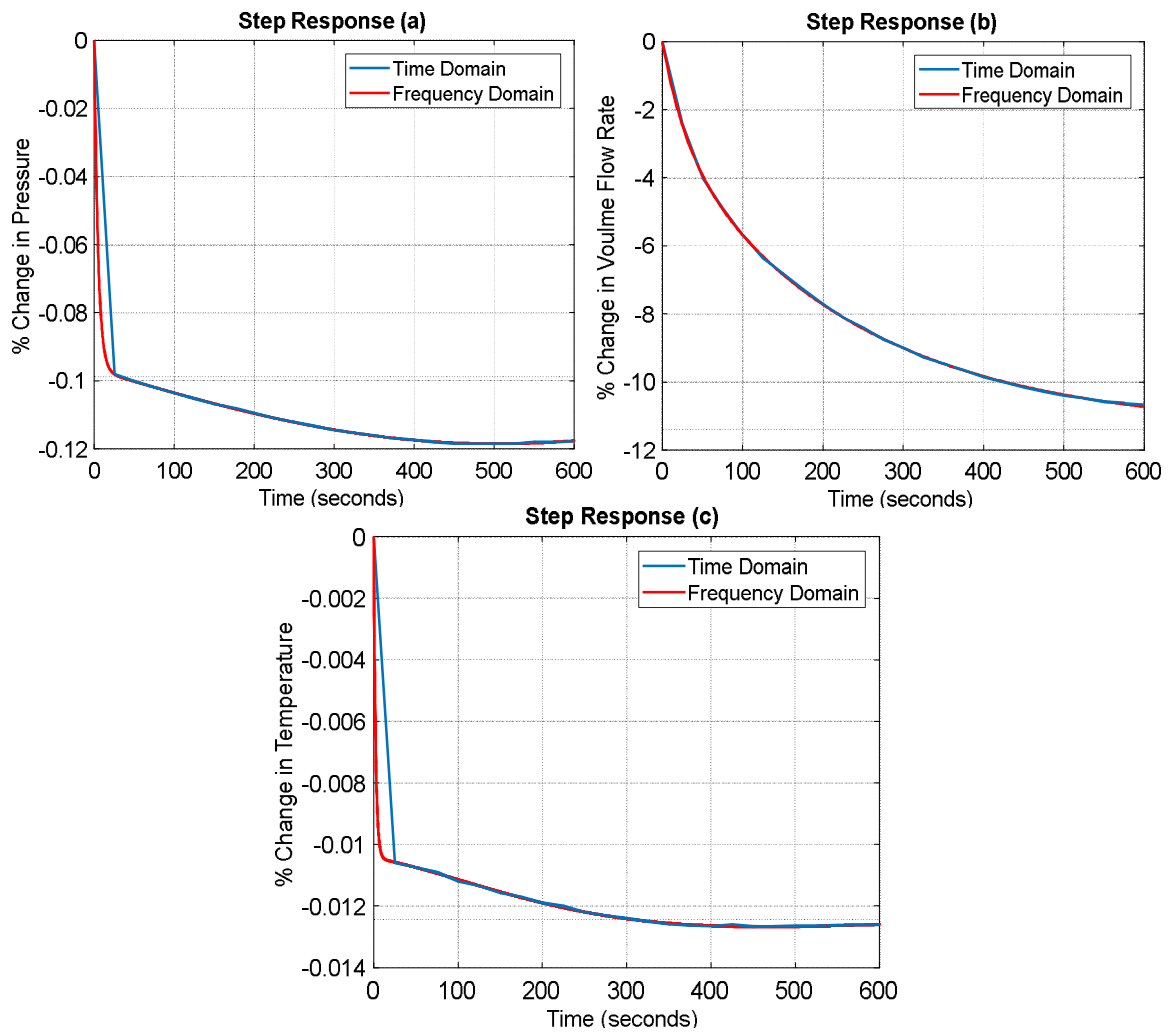
**Figure 4.7, a:** Time and frequency domain pressure responses. **b:** Time and frequency domain volume airflow rate responses. **c:** Time and frequency domain air temperature responses when 1% step change in the voltages  $v_1(t)$  and  $v_2(t)$  applied on the inlet and exit fan motors

Input of 1% step change in  $v_1(t)$  and  $v_2(t)$  simultaneously with 0% change at all other inputs causes the air pressure at the inlet of the ventilated volume to raise exponentially from the

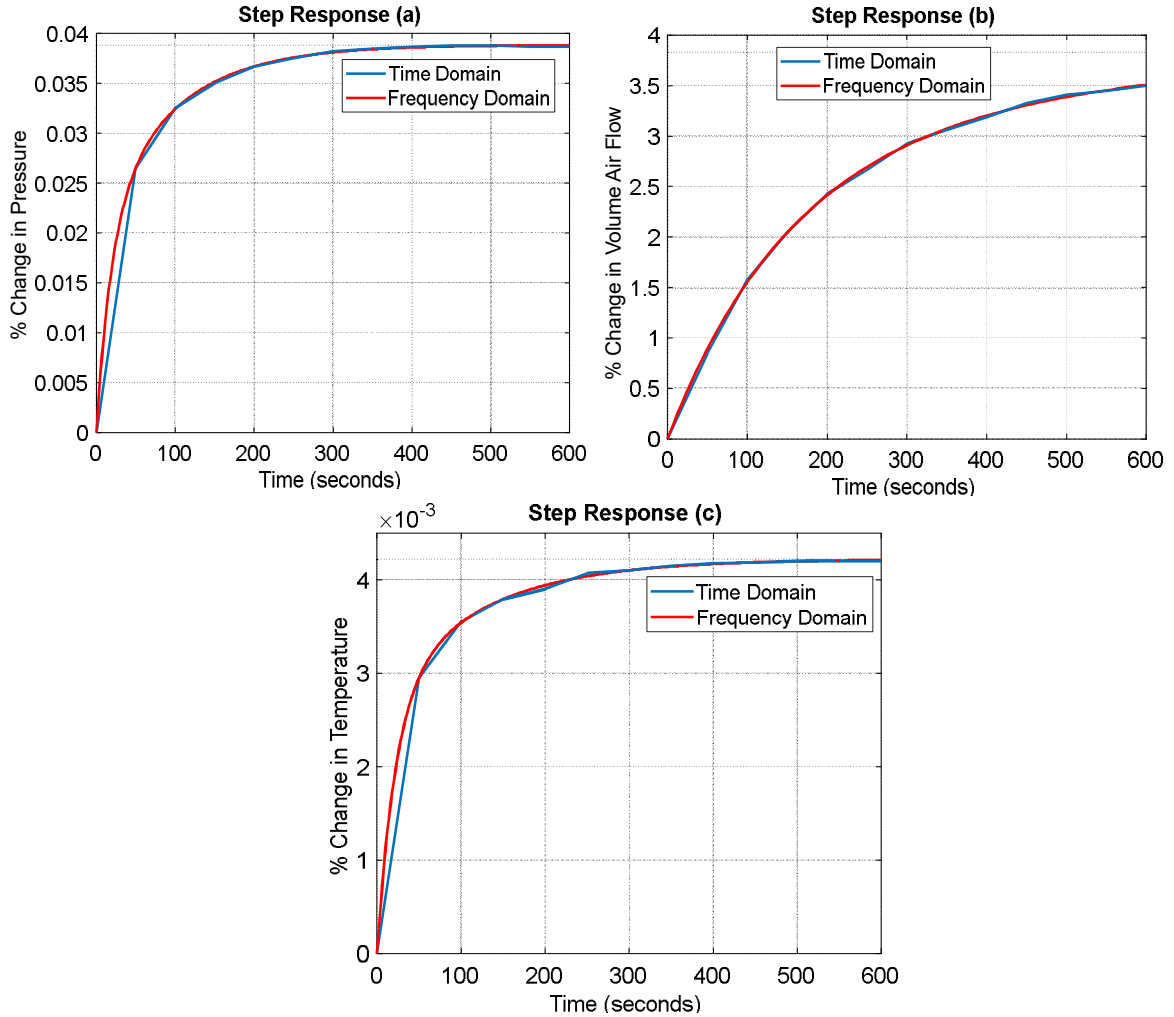
original steady state value to a new one before it goes to new steady state value. Consequently, the volume airflow rate is raising from the original steady state value as well corresponding with the pressure rise reaching a new steady state value. The air temperature value at the inlet of the ventilated volume will be decreased to a new lower steady state value caused by an increase in the air pressure creating an increase in air velocity that carries more cooled air exchanged with chilled water.

Figure 4.8 shows the open loop response when the input of a 1% step change is applied at the voltage of the chilled water pump  $v_{wp}(t)$  while the change on the other inputs remain zero. A 1% step change at the voltage of the chilled water pump  $v_{wp}(t)$  will cause a rapid reduction in the temperature  $T_1(t)$  of the inlet of the ventilated volume, such temperature reduction will make the molecules of the air to move more slowly causing a drop in the air pressure. The reduction in the air pressure  $P_1(t)$  will cause a slow reduction in the air flow rate  $q_1(t)$  as well, commensurate with the lower temperature and transient, volumetric air compression effects.

Figure 4.9 shows the open loop responses when 1% change in the in atmospheric ambient heat transfer  $Q(t)$  to the ventilated volume is initiated. When an input of 1% step change in the atmospheric ambient heat transfer 0% change with occurs, and to the ventilated volume  $Q(t)$  at all other inputs, a corresponding increase in the temperature at the inlet of the ventilated volume will be encountered. Raising the temperature will cause ascent in the air pressure  $P_1(t)$  as well increasing accordingly and slowly the airflow rate.  $q_1(t)$



**Figure 4.8, a:** Time and frequency domain pressure responses. **b:** Time and frequency domain volume airflow rate responses. **c:** Time and frequency domain air temperature responses when 1% step change in the voltage  $v_{wp}(t)$  is applied in the chilled water pump



**Figure 4.9, a:** Time and frequency domain pressure responses. **b:** Time and frequency domain volume airflow rate responses. **c:** Time and frequency domain air temperature responses when 1% step change in the ambient heat transfer  $Q(t)$  is initiated

#### 4.4 Control Objectives

Referring to the open loop system responses in Figures 4.7, 4.8 and 4.9, it can be noticed that significant coupling exists between the output responses so that any step change at any of the system inputs causes corresponding variations in all system outputs. Moreover, the steady state error is obvious. However, the system is stable and well-behaved with no oscillation around the steady state value.

As a result, reducing the coupling between the outputs should be one of the control objectives so that when any of the inputs is altered, the effect on the other system outputs will be as small as possible. An acceptable low coupling percentage between the outputs is also one of the control objectives and must be investigated and confirmed. Meanwhile, the system in the closed feedback control must show stability and to behave satisfactorily. Moreover, HVAC systems are exposed to many sources of disturbances. Therefore, the closed feedback control must be able to reject such disturbances with the least time and energy dissipation.

#### **4.5 LE Control Theory**

LE theory as presented by Whalley and Ebrahimi (2006) will be the main control procedure to be employed in this study. LE Control is a method that employs output feedback, passive compensators and proportional gains for multivariable process industries. The controller structure incorporates two major loops, the inner loop where the dynamics and transient responses of the system are configured, and the outer loop where improving the system steady state error and disturbance rejection is achieved.

##### **4.5.1 Closed Loop Plan**

Closed loop plan is a set of procedures and mathematical operations to configure the transient and the steady state system performance taking into consideration optimising the control energy and improving the disturbance rejection. Figure 4.10 illustrates the LE controller including the inner loop where the forward and feedback gains are incorporated and the outer loop where the pre-compensators and the outer feedback gains are also incorporated. HVAC plant transfer function in Figure 4.6 is also integrated in the LE control system block diagram in Figure 4.10.

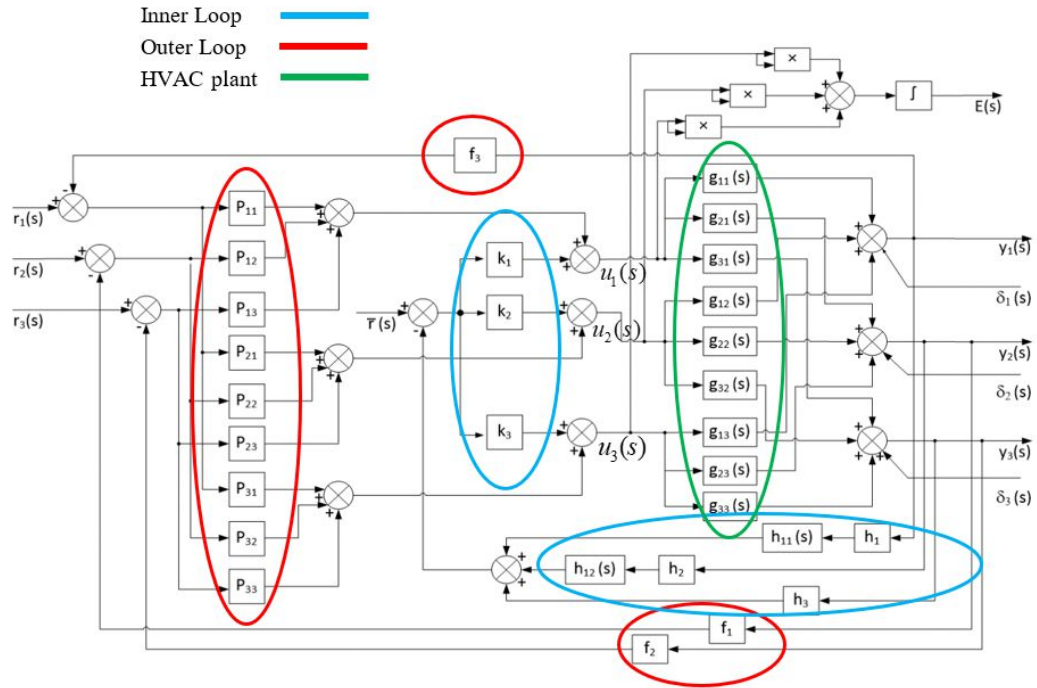


**Figure 4.10.** Block diagram of LE Controller showing the HVAC model, inner loop and outer loop

As per the block diagram in figure 4.10 the output vector Equation can be expressed as follows:

$$y(s) = G(s)u(s) + \delta(s), \quad (4.3)$$

where the control law for  $(m)$  independent inputs, outputs and disturbances, the system Equation becomes:

$$u(s) = k(s)(\bar{r}(s) - h(s)y(s)) + P(r(s) - Fy(s)), \quad (4.4)$$

where  $F = \text{Diag}(f_1, f_2, \dots, f_m)$ ,  $0 < f_j < 1$ ,  $1 \leq j \leq m$ .

Considering  $\bar{r}(s) = 0$ , the Equation of the closed loop system can be written as:

$$y(s) = (I_m + G(s)(k(s) \times h(s) + PF))^{-1} \times (G(s)Pr(s) + \delta(s)), \quad (4.5)$$

where

$\|G(s)(k(s) \times h(s) + PF)\|_\infty$  is finite on the D contour for the values of  $s$ .

Selecting the steady state matrix  $S_s$  with specific element values so that:

$$y(0) = S_s r(0),$$

then referring to Equation (4.5) considering  $\delta(s)$  zero

$$P = (G(0)^{-1} + k(0) \gg h(0)) S_s (I - F S_s)^{-1}. \quad (4.6)$$

For zero steady state error and a completely decoupled system, the steady state matrix will be  $S_s = I_m$ , however to achieve practical system performance, low steady state interaction should be incorporated so that the values of the off-diagonal elements of the matrix have to be very small while the diagonal elements values remain unity. This situation will require:

$$|s_{ij}| \ll 1 \quad , \quad 1 \leq i \quad , \quad j \leq m, \quad i \neq j$$

Subsequently obtaining a specified steady state, closed loop non-interaction responses and substituting ( $P$ ) matrix of Equation (4.6) in Equation (4.5) yields:

$$y(s) = \{I_m + G(s)[k(s) \gg h(s) + (G(0)^{-1} + k(s) \gg h(s))(I_m - F)^{-1} F]\}^{-1} \times \\ \times \{G(s) Pr(s) + \delta(s)\}. \quad (4.7)$$

Dealing with low frequencies which is the nature of most industrial processes:

$$G(s) \approx G(0) \quad \text{and} \quad G(s)G(0)^{-1} \approx I_m$$

so that Equation (4.7) approaches

$$y(s) \approx \{[I_m + G(s)k \gg h(s)][I_m + (I_m - F)^{-1} F]\}^{-1} \times \{G(s) Pr(s) + \delta(s)\}. \quad (4.8)$$

The elements of  $F$  values should be:

$$f_1 = f_2 = \dots = f_m = f \quad , \quad 0 < f < 1,$$

so that Equation (4.8) can be simplified to:

$$y(s) \approx (1 - f)[I_m + G(s)k(s) \gg h(s)]^{-1} \times [G(s) Pr(s) + \delta(s)] \dots \quad (4.9)$$

Since

$$G(s)P = G(s)[G(0)^{-1} + k(0) \gg h(0)][I_m - F]^{-1} \quad ,$$

so that at low frequencies it becomes:

$$G(s)P = G(s)[G(0)^{-1} + k(0) \gg h(0)][I_m - F]^{-1} . \quad (4.10)$$

Based on Equation (4.10), Equation (4.7) on approaching steady state conditions becomes:

$$y(s) = I_m r(s) + S(s)\delta(s) , \quad (4.11)$$

where in Equation (4.11)

$$S(s) = (1 - f)(I_m + G(s)k(s) \gg h(s))^{-1} , \quad 0 < f < 1 , \quad (4.12)$$

is low frequency sensitivity matrix.

Following reference input changes, steady state, non-interaction responses can be achieved as per Equation (4.11). Furthermore, with increasing the value of ( $f$ ) which should be less than unity, the rejection of steady state disturbance will increase with a condition that stability is maintained.

Referring to Equation (4.5) which represents a conventional multivariable control structure consisting of feedback path compensators  $H(s)$  matrix and forward path  $K(s)$  matrix, these matrices can be easily computed by following the closed loop Equation:

$$y(s) = (I_m + G(s)K(s)H(s))^{-1}[G(s)K(s)r(s) + \delta(s)] . \quad (4.13)$$

Comparing Equation (4.5) with (4.13)

$$K(s) = P , \quad (4.14)$$

$K(s)H(s) = k(s) \gg h(s) + PF$  , so that:

$$H(s) = P^{-1}k(s) \gg h(s) + F . \quad (4.15)$$

The compensators of  $K(s)$  and  $H(s)$  in Equation (4.14) and (4.15) are constant and full rank ( $m \times m$ ) matrices, respectively. The feedback matrix  $H(s)$  is stable, proper, ( $m \times m$ ) minimum phases realization which could be configured based on passive compensators. Based on such theory, the procedure to design the controller is to adjust the inner loop  $k(s)$  and  $h(s)$  vectors

aiming to achieve well behaved system dynamics. The pre- compensators ( $P$ ) afterwards will be configured to provide acceptable steady state output coupling. The outer loop of feedback ( $f$ ) gain will be acting as a final specific design value to provide final requested dynamic and disturbance rejection characteristics.

#### 4.5.2 Inner Loop Analysis

It essential to assume that  $G(s)$  which is represented in Figure 4.6 block diagram and expressed in Equation (4.3) has to be a matrix of ( $m \times m$ ) linear, regular, proper, or strictly proper realization and can accept a factorization process such that:

$$G(s) = L(s) \frac{A(s)}{d(s)} R(s) \Gamma(s), \quad (4.16)$$

where  $L(s), A(s), R(s), \Gamma(s)$  and elements of  $\frac{A(s)}{d(s)} \in H_\infty$ ,  $s \in \mathbb{C}$

$L(s)$  is a matrix containing left (row) factors,  $R(s)$  matrix contains the right (column) factors while  $\Gamma(s)$  matrix contains the transformed actuator finite time delays of  $G(s)$  so that these matrices are:

$$L(s) = \text{Diag} (\lambda_j(s) / p_j(s)),$$

$$R(s) = \text{Diag} (\rho_j(s) / q_j(s)),$$

$$L(s) = \text{Diag} (e^{-sT_j}), \quad 1 \leq j \leq m$$

$A(s)$  in Equation (4.16) is a non-singular matrix of rational function such that determinant of matrix  $A(s) \neq 0$  containing elements such as:

$$a_{ij}(s) = a_{ij}s^{m-1} + b_{ij}s^{m-2} + \dots + \gamma_{ij}, \quad i, j \leq m. \quad (4.17)$$

As the input-output disturbance relationship is explained as per following Equation:

$$y(s) = G(s)u(s) + \delta(s), \quad (4.18)$$

and the control of inner loop law is

$$u(s) = k(s)[\bar{r}(s) - h(s)y(s)], \quad (4.19)$$

Equation (4.18) after substituting (4.19) in it becomes:

$$y(s) = (I_m + G(s)k(s) \gg h(s))^{-1} (G(s)k(s)\bar{r}(s) + \delta(s)). \quad (4.20)$$

The finite time delays in  $\Gamma(s)$  may be ordered with  $T_i \geq T_j, 1 \leq j \leq m, i \neq j$  so that the forward path gain vector can be arranged as:

$$k(s) = \left[ k_1(s)e^{-s(T_1-T_j)} \quad k_2(s)e^{-s(T_1-T_2)} \quad \dots \quad k_j(s) \quad \dots \quad k_m(s)e^{-s(T_1-T_m)} \right]^T. \quad (4.21)$$

Since:

$$h(s) = (h_1(s), h_2(s), \dots, h_m(s)), \quad (4.22)$$

with the condition that

$$k_j(s) = k_j \varphi_j(s) \quad \text{and} \quad h_j(s) = h_j \chi_j(s) \quad 1 \leq j \leq m,$$

where  $\varphi_j(s)$  and  $\chi_j(s)$  are proper or strictly proper, stable, realizable, minimum phase functions, then they can be selected in such a manner Equation (4.20) yields to be:

$$y(s) = \left( I_m + e^{-sT_1} n(s)L(s) \frac{A(s)}{d(s)} k(s) \gg h(s) \right)^{-1} \times \left( n(s)L(s) \frac{A(s)}{d(s)} k e^{-sT_1} r(s) + \delta(s) \right), \quad (4.23)$$

$$\text{where } k = [k_1 \quad k_2 \quad \dots \quad k_m]^T, \quad (4.24)$$

$$\text{and } h = [h_1 \quad h_2 \quad \dots \quad h_m], \quad (4.25)$$

where  $d(s) = s^\kappa + a_1 s^{\kappa-1} + \dots + a_0$  and  $\deg(n(s)a_{ij}(s)) < \kappa \quad 1 \leq i, j \leq m$ .

In Equation (4.23) the determinant can be expressed as

$$\det \left( I_m + e^{-sT_i} n(s) L(s) \frac{A(s)}{d(s)} k(s) \right) = 1 + e^{-sT_i} n(s) < h \frac{A(s)}{d(s)} k >. \quad (4.26)$$

Based on Equation (4.26) the inner product can be written as

$$< hA(s)k > = \begin{bmatrix} 1 & s & \cdots & s^{m-1} \end{bmatrix} \times \begin{bmatrix} \gamma_{11} & \gamma_{12} & \cdots & \gamma_{mm} \\ \vdots & \vdots & \vdots & \vdots \\ b_{11} & b_{12} & \cdots & b_{mm} \\ a_{11} & a_{12} & \cdots & a_{mm} \end{bmatrix} \begin{bmatrix} k_1 h_1 \\ k_2 h_1 \\ \vdots \\ k_m h_m \end{bmatrix}, \quad (4.27)$$

where  $a_{ij}$  is coefficient of term  $a_{ij}s^0$  of  $A_{ij}(s)$  polynomial,  $b_{ij}$  is coefficient of term  $b_{ij}s^1$  of  $A_{ij}(s)$  polynomial, and  $\gamma_{ij}s^{m-1}$  of  $A_{ij}(s)$  polynomial.

From Equation (4.27), the gain ratios can be expressed with the assumption as follows:

$$k_2 = nk_1, \quad k_3 = n_2 k_1, \quad \cdots, \quad k_m = n_{m-1} k_1, \quad (4.28)$$

and

$$< hA(s)k > = b(s), \quad (4.30)$$

so that Equation (4.30) infers that:

$$k_1 [Q]h = [b_{m-1} \quad b_{m-2} \quad \cdots \quad b_0]^T, \quad (4.31)$$

where

$$Q = \begin{bmatrix} \gamma_{11} + \gamma_{12}n_1 + \dots + \gamma_{1m}n_{m-1} & \dots & \gamma_{21} + \gamma_{22}n_1 + \dots + \gamma_{2m}n_{m-1} & \dots & \gamma_{m1} + \gamma_{m2}n_1 + \dots + \gamma_{mm}n_{m-1} \\ \vdots & \dots & \vdots & \dots & \vdots \\ b_{11} + b_{12}n_1 + \dots + b_{1m}n_{m-1} & \dots & b_{21} + b_{22}n_1 + \dots + b_{2m}n_{m-1} & \dots & b_{m1} + b_{m2}n_1 + \dots + b_{mm}n_{m-1} \\ a_{11} + a_{12}n_1 + \dots + a_{1m}n_{m-1} & \dots & a_{21} + a_{22}n_1 + \dots + a_{2m}n_{m-1} & \dots & a_{m1} + a_{m2}n_1 + \dots + a_{mm}n_{m-1} \end{bmatrix}, \quad (4.32)$$

$b_j$ , where  $0 \leq j \leq m-1$ , are the coefficients of  $b(s)$  in Equation (4.30).

Providing the matrix  $[Q]$  is invertible then there will be a unique solution for  $(h_1, h_2, \dots, h_m)$

After selecting the coefficients of  $b(s)$  and computing the values of the gain ratios  $(n_1, n_2, \dots, n_{m-1})$ , the closed loop dynamics exerted by Equation (4.23) can be completely defined. From the solution of Equation (4.31), the values vector  $(h)$  can be computed based on arbitrary value for  $(k_1)$ .

### 4.5.3 Optimization of the Gains

From the previous section, the closed loop system design employing the transfer function matrix  $G(s)$  and output measurements has been obtained. However, such a process can be optimized with adequate freedom to do so due to the arbitrary of selecting the gain ratios  $(n_1, n_2, \dots, n_{m-1})$ .

The detection of the absolute minimum control efforts applied to suppress the disturbance entering the system operation under the closed-loop conditions and generating specific polynomial would give a useful benchmarking. The generated polynomial will affect the migration pattern of the system closed loop poles in such a manner the minimized control effort exerted to suppress the disturbances and the desired system dynamics could be achieved simultaneously. The Equation of the controller for ( $m$ ) inputs and ( $m$ ) outputs is given by Equation (4.4). The control inputs are equal to:

$$\begin{aligned} & (|k_1 h_1| + |k_2 h_1| + \dots + |k_m h_1|) y_1(t) + (|k_1 h_2| + |k_2 h_2| + \dots + |k_m h_2|) y_2(t) + \dots + \\ & + (|k_1 h_m| + |k_2 h_m| + \dots + |k_m h_m|) y_m(t) \end{aligned}$$

To calculate the control energy at a time ( $t$ ), the input signals need to be squared, so that the cost of the control energy under these conditions are proportional to

$$E(t) = \int_{t=0}^{t=T_f} \left( \sum_{i=1}^m k_i^2 \sum_{j=1}^m h_j^2 y_j^2(t) \right) dt, \quad (4.33)$$

so that for arbitrary changes in the transformed output vector  $y(t)$ , following arbitrary disturbance changes

$$J = \sum_{i=1}^m k_i^2 \sum_{j=1}^m h_j^2, \quad (4.34)$$

would minimize the required control energy which is given by Equation (4.33). Now if the relationships of the gain ratios  $k_2 = n k_1$ ,  $k_3 = n_2 k_1$ ,  $\dots$ ,  $k_m = n_{m-1} k_1$  are employed in the derivation, then Equation (4.34) can be expressed as:

$$J = (k_1)^2 (1 + n_1^2 + n_2^2 + \dots + n_{m-1}^2) \times (h_1^2 + h_2^2 + \dots + h_m^2). \quad (4.35)$$

From Equation (4.31) the vector ( $h$ ) can be written as:

$$h = k_1^{-1} Q^{-1} b, \quad (4.36)$$

so that substituting Equation (4.36) in Equation (4.35) yields:

$$J = (1 + n_1^2 + n_2^2 + \dots + n_{m-1}^2) b^T (Q^{-1})^T Q^{-1} b. \quad (4.37)$$

In this study  $m = 3$  so that the Performance Index ( $J$ ) equation becomes:

$$J = (1 + n_1^2 + n_2^2) b^T (Q^{-1})^T Q^{-1} b.$$

With  $m = 3$ , Equation (4.37) is a multivariable Equation with  $(n_1)$  and  $(n_2)$  variables. Finding the values of  $(n_1)$  and  $(n_2)$  that leads to obtain a minimum value for the Equation ( $J$ ) would be the optimised values for the forward and feedback gains associated with minimized control energy, Mathematically, to find the minimum value of Equation (4.37), the following conditions have to be fulfilled

$$\left\{ \begin{array}{l} \frac{\partial J}{\partial n_1} = 0, \quad \frac{\partial J}{\partial n_2} = 0. \\ \frac{\partial^2 J}{\partial n_1^2} \frac{\partial^2 J}{\partial n_2^2} - \left( \frac{\partial^2 J}{\partial n_1 \partial n_2} \right)^2 > 0, \quad \text{if} \quad \frac{\partial^2 J}{\partial n_1^2} > 0 \end{array} \right. \quad (4.38)$$

The partial differential equation in respect to  $(n_1)$  and the partial differential equation in respect to  $(n_2)$  have to be zero. Graphically it means that plane of  $(n_1)$  and  $(n_2)$  has to be zero when this plane touches extremum points of Equation ( $J$ ). However, to make sure that the plane touches the minimum value of Equation ( $J$ ) the second test

$$\frac{\partial^2 J}{\partial n_1^2} \frac{\partial^2 J}{\partial n_2^2} - \left( \frac{\partial^2 J}{\partial n_1 \partial n_2} \right)^2 > 0, \quad \text{if} \quad \frac{\partial^2 J}{\partial n_1^2} > 0 \quad \text{must be fulfilled:}$$

For systems with  $(m > 3)$  a numerical optimization routine can be used to identify the values of  $n_1, n_2, \dots, n_{m-1}$  that minimize the Performance Index ( $J$ ) (Whalley and Ebrahimi, 2006).

#### 4.5.4 Disturbance Rejection Calibrator for LE control technique

Configuring the inner loop has been investigated in the last section. Such configuration allowed certain system dynamics associated with least control efforts. But the employment of the inner loop and an absolute minimum effort controller through achieving poles placement will not perform specified steady state disturbance recovery conditions. However, it can affect the transient disturbance suppression. The outer loop with the feedback gain ( $f$ ) would determine the steady state disturbance offset conditions. This can be attained by increasing the value of ( $f$ ) between zero and unity commensurate with Equation (4.11). It has to be noticed that while calibrating the disturbance rejection by increasing the value of ( $f$ ), this might perturb the behaviour of the system's transient, such perturb has to be recognized and compensated when designing the inner loop aiming to achieve modest improved dynamics.

#### 4.5.5 Stability of the System with LE Control

The stability of the system must be examined, including both inner and outer loops. Using the root locus technique, the inner loop can be designed. This will provide a wide margin to design the loop with enough stability. Stability of the inner loop will lead to outer loop conditional stability. The stability condition heavily relies on the denominator of input-output relationship for the complete, closed-loop system as per Equation (4.7). The determinant of the matrix in Equation (4.7) can be expressed as follows:

$$\det \left( I_m + G(s)k(s) \gg h(s) \left( \frac{F}{(I_m - F)} \right) + \frac{G(s)G(0)^{-1}F}{(I_m - F)} \right), \quad (4.39)$$

where the outer loop feedback gain matrix ( $F$ ) is given by:

$$F = \text{Diag} (f_1, f_2, \dots, f_j), \quad 0 < f_j < 1, \quad 1 \leq j \leq m.$$

The determinant in the above expression shows that the values of diagonal elements of  $(F)$  matrix have to vary between  $0 < f < 1$  and must not reach unity value. Although increasing the value of  $(f)$  will improve the disturbance rejection as per Equation (4.11), assigning  $(f = 1)$  will make the expression  $(1 - f)$  going to zero so that the determinant of the matrix in Equation (4.7) will go to infinity and cause the system to be unstable. Such a scenario must be avoided. The performance of the (LE) control technique must be verified and compared with alternative control technique that able to deal with system model characterized with time delay between the system inputs and outputs which is the major characteristic of hybrid lumped distributed parameter models. Some control design algorithms cannot directly handle time delayed system responses, such as root locus, Linear Quadratic Gaussian (LQG) control, and pole placement. Optimal control as a multivariable control technique has been assessed to control Hybrid lumped distributed parameter model but found unworkable technique. Many other techniques might fit for the same model and after trying to employ Direct Nyquist Array (DNA) control technique, it is found capable to deal with time delay system application and considered as a proper alternative candidate control technique to verify the (LE) control technique performance.

#### **4.6 Direct Nyquist Array (DNA)**

The Direct Nyquist Array (DNA) procedure is a multivariable control technique where the problem of the multivariable feedback control design is reduced to a set of single closed loops control design (Arkun, Manousiouthakis and Putz, 2007). The procedure is based on reducing the interactions between system outputs by decoupling such outputs so that a closed loop control technique can be applied on each loop independently.

Figure 4.11 shows typical multivariable closed loop control where  $G(s)$  is the plant transfer matrix,  $K(s)$  is the decoupling compensators matrix and  $C(s)$  is the diagonal transfer function controllers. All matrices have the same  $(m \times m)$  dimensions.

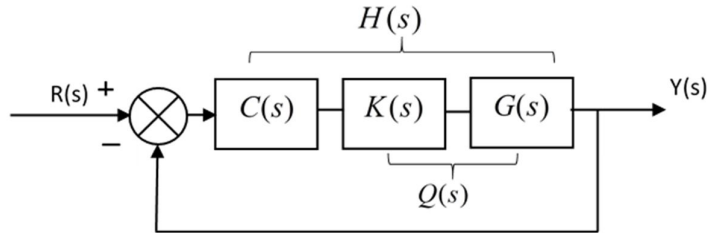


**Figure 4.11.** HVAC multivariable closed loop control with (DNA) controller

#### 4.6.1 System Decoupling

The decoupling procedure incorporates a process of designing a matrix of compensators  $K(s)$  so that when it is multiplied by the plant transfer function  $G(s)$  the resultant is a diagonal dominant matrix. Afterwards, a closed loop control technique can be applied on each loop independently. Mathematically, diagonal dominant means that the modulus of any diagonal element is greater than the summation of the moduli of the off-diagonal elements for a row or a column. Let  $Q(s)$  ( $m \times m$ ) be a complex elements matrix, then  $Q(s)$  can be said row dominant when:

$$\left| q_{ii}(s) \right| - \sum_{\substack{j=1 \\ i \neq j}}^m \left| q_{ij}(s) \right| > 0, \quad (4.40)$$

for all  $i = 1, 2, \dots, m$  and  $q_{ii}(s)$  is a diagonal element. But  $Q(s)$  can be said Column dominant when:

$$\left| q_{ii}(s) \right| - \sum_{\substack{j=1 \\ i \neq j}}^m \left| q_{ji}(s) \right| > 0, \quad (4.41)$$

for all  $i = 1, 2, \dots, m$ .

Mixture of row and column dominance is not applicable for a matrix to be diagonal dominance, so either definition will be enough (Leininger, 1975). Diagonal dominance matrix can be also investigated graphically. A row in a matrix is graphically dominant when the union of circles centred by  $q_{ii}(s)$  with radius:

$$r_i = \sum_{\substack{j=1 \\ i \neq j}}^m |q_{ij}(s)|, \quad (4.42)$$

at an extended certain range of frequencies will exclude the origin of the complex plane.

Similarly, a column in a matrix is graphically dominant when the union of circles centred by

$$q_{ii}(s) \text{ with radius } r_i = \sum_{\substack{j=1 \\ i \neq j}}^m |q_{ji}(s)|, \quad (4.43)$$

at an extended certain range of frequencies will also exclude the origin of the complex plane.

A graphic example is shown in Figure 4.12.

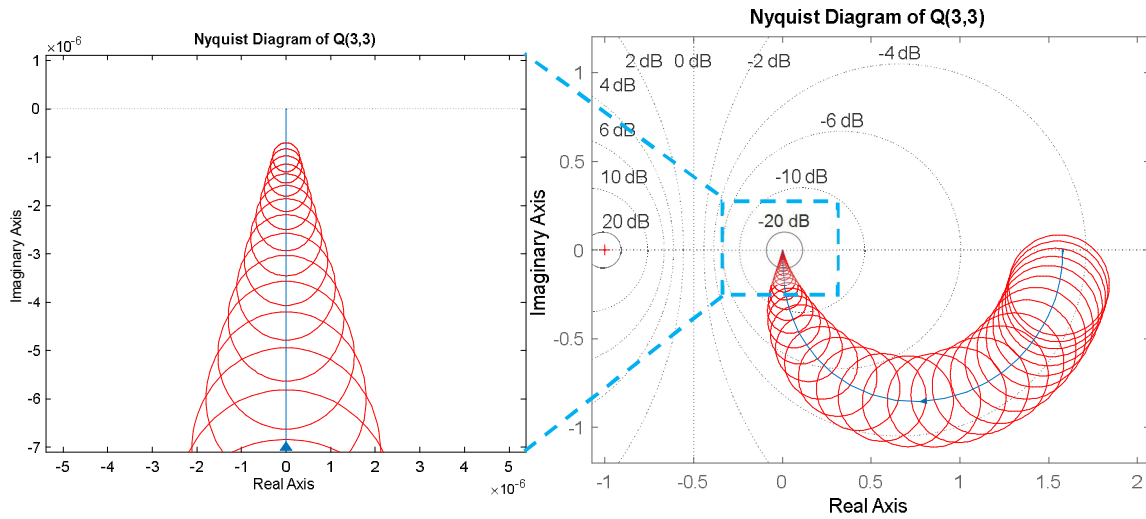


**Figure 4.12.** Graphical Example of diagonal dominance for a row or a column of square matrix

Once the system is decoupled with a small remained interaction, diagonal multi-loop controllers can be designed to shape the Gershgorin bands which aims to examine graphically the stability of each control loop system.

#### 4.6.2 Direct Nyquist Array Stability Theorem

Closed loop stability can be examined by forming the Gershgorin bands for the open loop transfer function:

$$H(s) = C(s)K(s)G(s), \quad (4.44)$$

where  $C(s)$  is the controller matrix such as PID controllers.

To guarantee the system stability under the closed loop structure, the Gershgorin bands centred about the diagonal elements must not enclose the  $(-1 + j0)$  point in the complex plane and encircle the same point a number of times fulfilling Nyquist stability theorem for multivariable processes. Nyquist stability criterion for multivariable systems is explained below. Let the Gershgorin bands centred about the diagonal elements  $h_{ii}(s)$  of open loop transfer function  $H(s)$ , where  $i = 1, 2, \dots, m$  with radii equal to the summation of the off-diagonal elements for

$h_{ii}(s)$  row or column, exclude the point  $(-1 + j0)$  in the complex plane and encircle the same point with a number of times equal to  $(N_i)$ . The closed loop system is stable if and only if:

$$\sum_{i=1}^m N_i = p_0 , \quad (4.45)$$

where  $(p_0)$  is number of the open loop transfer function  $H(s)$  poles located in the right hand side of s-plane (Pan *et al.*, 2012).

## Chapter Five

### HVAC System Model Simulation Results and Discussions

Based on reviewing the LE and Direct Nyquist Array control techniques for multivariable control in Chapter four, this chapter will review the application of both techniques and the analysis of the results.

MATLAB and SIMULATION software is the main research methodology and tool to be employed in the study. MATLAB is a software engineering package with abbreviation of two terms, Matrix Laboratory. MATLAB is a dedicated environment of programming that includes its own programming language and libraries with many Toolboxes. It is very powerful as large number of users are using MATLAB in system engineering and control system design. The application of control techniques will be basically employing MATLAB and SIMULATION software due to its high capability in dealing with big data where large data is very important in solving complex design challenges (Matlabtips.com. 2015). Whalley R. and Abdul-Ameer A. (2011) have used MATLAB and SIMULATION software as the main software to demonstrate the system responses for their developed HVAC system model, many others such as Bartlett, H. and Whalley, R. (1998) mentioned that among other software MATLAB can be also a powerful software tool to build hybrid lumped distributed parameter models.

It is very important to mention that the HVAC system responses in both control techniques that to be investigated ahead were subjected to reference unity change inputs multiplied with a time constant of 250 seconds, such as  $\frac{1}{250s+1}$ . This arrangement will improve the system responses

by reducing the overshoots and oscillations

## 5.1 LE Controller

The HVAC ( $3 \times 3$ ) transfer function matrix has been derived in the last section and can be recalled as follows:

$$G(s) = \begin{bmatrix} \frac{0.001402 s - 2.04e-07}{s^2 + 0.03509 s + 3.44e-09} & \frac{-0.02075 s^2 - 2.227e-05 s - 2.162e-07}{s^3 + 0.2141 s^2 + 8.726e-05 s + 2.189e-06} & \frac{0.001252 s + 2.159e-05}{s^2 + 0.06249 s + 0.0005558} \\ \frac{-0.007734 s^2 + 0.004677 s + 7.761e-08}{s^3 + 0.08749 s^2 + 0.001259 s + 3.132e-07} & \frac{-0.1314 s - 0.001673}{s^2 + 0.0385 s + 0.000147} & \frac{0.02071 s + 6.281e-05}{s^2 + 0.009175 s + 1.64e-05} \\ \frac{-0.002809 s - 8.36e-05}{s^2 + 0.06943 s + 0.001082} & \frac{-0.004665 s^2 - 4.227e-05 s - 3.085e-07}{s^3 + 0.4551 s^2 + 0.003889 s + 2.48e-05} & \frac{0.000137 s + 1.657e-06}{s^2 + 0.05461 s + 0.0003927} \end{bmatrix}, \quad (5.1)$$

### 5.1.1 Model Reduction Process

The order degree of some transfer function elements in the matrix expressed in Equation (5.1) are with the third order. As per the LE technique design requirement, the order of the transfer function elements must be  $(\leq m - 1)$  in order to comply with Equation (4.27). Based on  $(m = 3)$ , the order of the transfer function elements must be equal to the second order or below. Such a situation requires that higher order transfer function elements to be reduced in order to simplify the control analysis and design. One more reason for reducing the order of the transfer function elements is that multivariable control strategies incorporate a long and complicated mathematical and algebraic operation. Therefore, the higher orders of transfer function elements make such operations more complicated. Consequently, a reduced transfer functions order would be easier to realise and manipulate. The reduction must consider keeping the original model's major dynamics and characteristics, which are crucial for the process industry application. There are many methods that can be used to reduce the model order; the one to be used in this study is the Pole-Zero simplification which eliminates the similar or near pole-zero pairs.

As an outcome of applying the Pole-Zero simplification procedure, the reduction has been implemented on all  $G(s)$  elements so that the final reduced order transfer function matrix becomes:

$$G_{red}(s) = \begin{bmatrix} \frac{0.001319}{s + 0.03509} & \frac{-0.02386}{3.5s + 0.2137} & \frac{0.002003}{2.8s + 0.05175} \\ \frac{-0.007193s + 0.004349}{s^2 + 0.08724s + 0.001237} & \frac{-0.06996}{s + 0.006335} & \frac{0.02223}{s + 0.006335} \\ \frac{-0.003539}{1.4s + 0.04581} & \frac{-0.005388}{7s + 0.4465} & \frac{0.0001918}{2.228s + 0.04609} \end{bmatrix}. \quad (5.2)$$

All reduced order transfer functions elements as in Equation (5.2) are with either first or second order which can cope with the procedure of designing LE control technique. Figures 5.1 (a), (b), (c), (d), (e), (f), (g), (h) and (i) illustrate the model reduction results for  $G(s)$  elements in which the reduced models are approximated to lower transfer function order and their responses are superimposed with the original higher order transfer functions element responses. Figures 5.1 (a), (b), (c), (e), (g), (h) and (i) show approximately 95% - 99% fit between the original and reduces order transfer function elements while Figures 5.1 (d) and (f) show less fit with approximately 90% only. Figures 5.1 (e), (h) are critically damped in both original and reduced order transfer functions responses whereas Figures 5.1 (a), (b), (c), (d), (f), (g) and (i) are over damped for both original and reduced order transfer functions. However in all cases, the reduced order transfer functions responses are maintaining the major transient and steady state characteristics of original transfer functions responses so that with such reduction the procedure of designing Least Efforts Control Technique can be started and proceeded with no major changes in the transfer function elements.

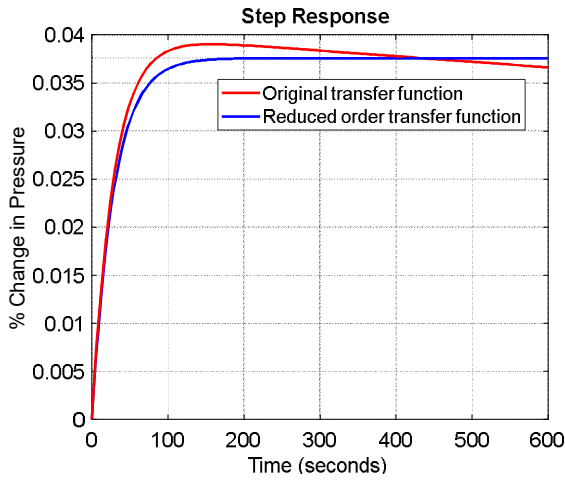


**Figure 5.1 a.** Original transfer function versus reduced order transfer function for  $g_{11}(s)$

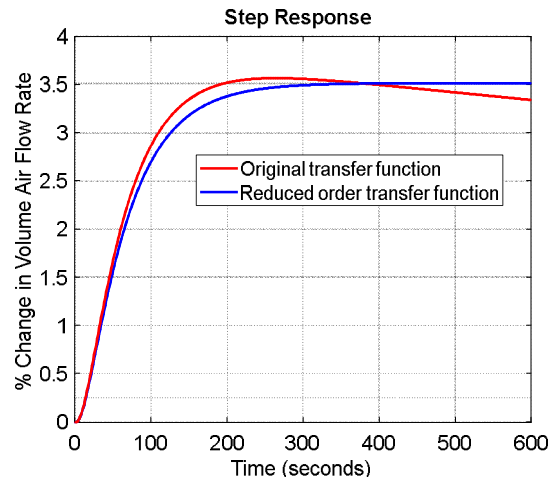


**Figure 5.1 b.** Original transfer function versus reduced order transfer function for  $g_{21}(s)$

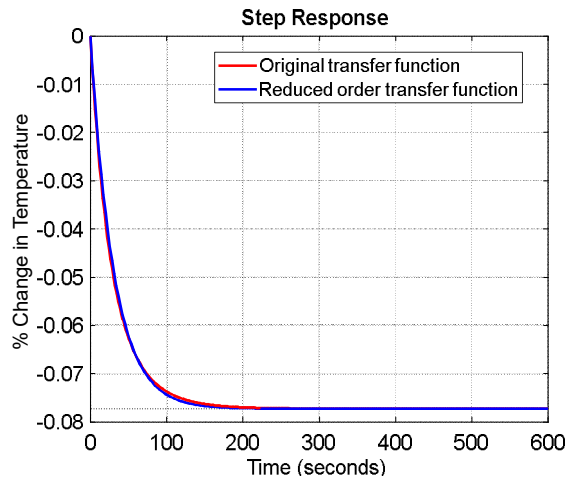


**Figure 5.1 c.** Original transfer function versus reduced order transfer function  $g_{31}(s)$

### 5.1.2 Inner Loop Configuration

The open loop system Equation is expressed by:

$$y(s) = G(s)u(s) + \delta(s), \quad (5.3)$$

where  $y(s) = [P_1(s) \ q_1(s) \ T_1(s)]^T$  are the Laplace transformed output signals of air pressure, air volume flow rate and air temperature at the inlet of the ventilated volume respectively.

Furthermore,  $u(s) = [v_{fans}(s) \ v_{wp}(s) \ Q(s)]^T$  are the Laplace transformed input signals for the voltage on the inlet fan, voltage on the chilled water pump and the atmospheric ambient heat transfer to the ventilated volume respectively, and  $\delta(s) = [\delta_1(s) \ \delta_2(s) \ \delta_3(s)]^T$  is the vector of Laplace transformed disturbance signals.

The system reduced order transfer function matrix in the zero-pole-gain form  $G_{red}(s)$  will be termed as  $G(s)$  to match the same symbol included the following Equations ahead:

$$G(s) = \begin{bmatrix} \frac{0.001319}{s + 0.03509} & \frac{-0.02386}{3.5s + 0.2137} & \frac{0.002003}{2.8s + 0.05175} \\ \frac{-0.007193s + 0.004349}{s^2 + 0.08724s + 0.001237} & \frac{-0.06996}{s + 0.006335} & \frac{0.02223}{s + 0.006335} \\ \frac{-0.003539}{1.4s + 0.04581} & \frac{-0.005388}{7s + 0.4465} & \frac{0.0001918}{2.228s + 0.04609} \end{bmatrix}. \quad (5.4)$$

In order to regulate and improve the performance of the HVAC system model with better disturbance rejection associated with least control effort, the inner loop first, have to be configured with suitable compensators, therefore the system provided by Equation (5.4) can be factorised and arranged as follows:

$$G(s) = L(s)A(s), \quad (5.5)$$

so that the Equation arrangement as per the Equation (4.16) can be performed by following terms:

$$L(s) = \begin{bmatrix} \frac{1}{(s+0.06106)(s+0.03509)(s+0.01848)} & 0 & 0 \\ 0 & \frac{1}{(s+0.06942)(s+0.01782)(s+0.006335)} & 0 \\ 0 & 0 & \frac{1}{(s+0.06379)(s+0.03272)(s+0.02069)} \end{bmatrix}$$

where

$$R(s) = I, \Gamma(s) = I$$

and  $A(s)$  is a matrix of polynomials with  $(\leq m-1)$  order so it can be selected to be as:

$$A(s) = \begin{bmatrix} 0.001319 (s+0.06106)(s+0.01848) & -0.0068179 (s+0.03509)(s+0.01848) & 0.00071543 (s+0.06106)(s+0.03509) \\ -0.007193 (s-0.6046)(s+0.006335) & -0.069964 (s+0.06942)(s+0.01782) & 0.022232 (s+0.06942)(s+0.01782) \\ -0.0025281 (s+0.06379)(s+0.02069) & -0.00076972 (s+0.03272)(s+0.02069) & 8.6086e-05 (s+0.06379)(s+0.03272) \end{bmatrix}$$

$A(s)$  elements must be a matrix of second order polynomials based on factorizing the matrix  $G(s)$ . The polynomial terms of  $A(s)$  elements are selected from the numerators of the  $G(s)$  elements in Equation (5.4).  $L(s)$  matrix is selected afterwards in such a manner when  $A(s)$  is multiplied with  $L(s)$ , the multiplication product will be the original  $G(s)$  as per Equation (5.4).

Aiming to secure the transient responses of the system, the inner loop feedback and forward gains can be designed in the following procedure:

The control law of the inner loop, considering zero disturbance can be expressed as follows:

$$y(s) = [I + G(s)k(s)h(s)]^{-1} (G(s)k(s)\bar{r}(s)), \quad (5.8)$$

so that the characteristic Equation of the system would be:

$$\det[I_m + (G(s)k \gg h(s))] = 1 + \langle h(s)G(s)k(s) \rangle = 0. \quad (5.9)$$

Substituting Equation (5.5) in Equation (5.9) yields:

$$\det[I_m + (G(s)k \gg h(s))] = 1 + \langle h(s)[L(s)A(s)]k(s) \rangle. \quad (5.10)$$

$h(s)$  can be configured and selected as:

$$h(s) = [h_1(s) \ h_2(s) \ h_3(s)], \quad (5.11)$$

where

$$h_1(s) = \frac{(s+0.06106)(s+0.03509)(s+0.01848)}{(s+0.06379)(s+0.03272)(s+0.02069)} \times h_1.$$

$$h_2(s) = \frac{(s+0.06942)(s+0.01782)(s+0.006335)}{(s+0.06379)(s+0.02069)(s+0.003272)} \times h_2.$$

$$h_3(s) = h_3,$$

And  $k(s)$  vector is configured to be:

$$k(s) = [k_1 \ k_2 \ k_3]^T. \quad (5.12)$$

The elements of the vectors and (5.12) (5.11) are selected as per equations  $k(s)$  and  $h(s)$  respectively so that when they are substituted along with matrix  $L(s)$  in Equation (5.10), the common closed loop Characteristic Equation can be obtained as follows so that it can be handled easily when it is subjected to Root Locus design procedure:

$$1 + \frac{[h_1 \ h_2 \ h_3]A(s)[k_1 \ k_2 \ k_3]^T}{(s+0.06379)(s+0.03272)(s+0.02069)} = 0. \quad (5.13)$$

It is obvious that the numerator of the term  $\frac{[h_1 \ h_2 \ h_3]A(s)[k_1 \ k_2 \ k_3]^T}{(s+0.06379)(s+0.03272)(s+0.02069)}$  is a second order polynomial so that Equation (5.13) comprises third order rational transfer function which is easy to handle when it is subjected to Root Locus design procedure for a multivariable system model.

Root Locus design technique will be used in order to select zeroes and a gain that can improve the transient responses of the system, which can be foreseen faster than the open loop responses. Comparing Equation (5.13) with Equation (4.30) yields:

$$\left\langle \frac{hA(s)k}{d(s)} \right\rangle = \frac{b(s)}{d(s)}, \quad (5.14)$$

where

$$d(s) = (s+0.06379) (s+0.03272) (s+0.02069). \quad (5.15)$$

The Characteristic Equation of the system becomes:

$$-1 = \frac{b(s)}{(s+0.06379) (s+0.03272) (s+0.02069)}. \quad (5.16)$$

### 5.1.3 Root Locus Design

Optimum solution can be obtained when specific selection for  $b(s)$  is identified by using the designing method of Root locus plot for Equation (5.16). In this regard, the following zeros ( $s = -0.03272$ ) and ( $s = -0.02069$ ) configuring  $b(s)$  polynomial are selected to be equal to the two poles in Equation (5.16), which are the slowest poles in the Equation, so they can cancel each other. This means that the closer are poles to the imaginary axis, the slower system response would be attained, and hence cancellation of the two slow poles will speed up the system response in the closed loop arrangement. Therefore, the two poles in the denominator which can be responsible for slow system response are eliminated and cancelled by the selected two zeros in the numerator of the characteristics Equation (5.16). Consequently, the open loop transfer function becomes:

$$\frac{b(s)}{d(s)} = \frac{b_0 (s+0.03272) (s+0.02069)}{(s+0.06379) (s+0.03272) (s+0.02069)}. \quad (5.17)$$

With this selection, the pole ( $s = -0.06379$ ) will be remained, and shifting this pole leftward

will speed up the response of the system depending on the selection of ( $b_0$ ) gain value.

Figure 5.2 shows the Root Locus plot where the two poles are overlapping with the two zeros and cancelling each other, while the third pole is going leftward and can stop at a location depending on the gain value ( $b_0$ )

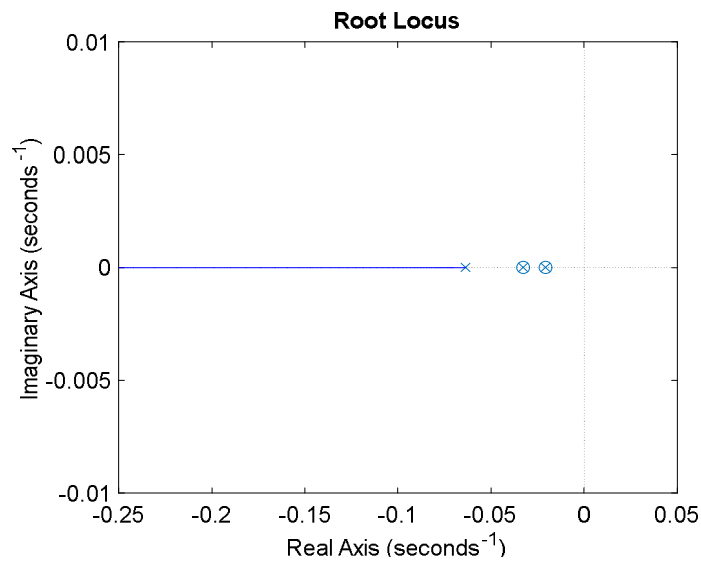


**Figure 5.2**, Root locus plot showing two poles overlapping with the two zeros while the third pole is going leftward to infinity

The gain in the root locus plot is selected to be  $b_0 = 0.23$  in order to achieve an improved system performance response, so that the responses will be faster as shown later. The polynomial  $b(s)$  would then become:

$$b(s) = 0.23 \times (s+0.03272) (s+0.02069), \quad (5.18)$$

so that ( $b$ ) coefficients' vector of the polynomial in equation (5.18) becomes:

$$b = [0.0002 \ 0.0123 \ 0.2300]. \quad (5.19)$$

Consequently, the closed loop pole destination would be ( $s = -0.294$ ) associated with the gain value of  $b_0 = 0.23$ . With this pole's location, the dynamics of the system responses will improve as shown later also by getting more speed. But before demonstrating such improvement, the values of forward and feedback gains  $k_1, k_2, k_3, h_1, h_2$  and  $h_3$  must be computed by the optimization procedure outlined in chapter four. The calculated optimized values of these gains will achieve least control effort for disturbance regulation purposes.

#### 5.1.4 Performance Index

As  $m = 3$ , and based on Equation (4.37) the Performance Index becomes:

$$J = (1 + n_1^2 + n_2^2) b^T (Q^{-1})^T Q^{-1} b, \quad (5.20)$$

and the  $(3 \times 3)$   $Q$  matrix as per equation (4.32) can be formulated as:

$$Q = \begin{bmatrix} 2.75 \times 10^{-5} - 8.65 \times 10^{-5} n_1 + 2.75 \times 10^{-5} n_2 & 1.48 \times 10^{-6} - 4.422 \times 10^{-6} n_1 + 1.533 \times 10^{-6} n_2 & -3.336 \times 10^{-6} - 5.21 \times 10^{-7} n_1 + 1.797 \times 10^{-7} n_2 \\ 0.004303 - 0.006104 n_1 + 0.001939 n_2 & 0.0001049 - 0.0003652 n_1 + 6.879 \times 10^{-5} n_2 & -0.0002136 - 4.111 \times 10^{-5} n_1 + 8.308 \times 10^{-6} n_2 \\ -0.007193 - 0.06996 n_1 + 0.02223 n_2 & 0.001319 - 0.006818 n_1 + 0.0007154 n_2 & -0.002528 - 0.0007697 n_1 + 8.609 \times 10^{-5} n_2 \end{bmatrix}. \quad (5.21)$$

Substituting both Equations (5.21) and (5.19) in Equation (5.20), the Performance Index  $J(n_1, n_2)$  in Equation (8.1) in the appendix can be formulated which represents a multivariable Equation with  $(n_1)$  and  $(n_2)$  variables. Dedicated MATLAB script file (8.4) in the appendix has been developed to derive Equation  $J(n_1, n_2)$  in the appendix. Equation (8.1) is too complicated to be traditionally solved. Moreover, the optimization procedure of the Performance Index incorporates partially differentiating Equation (8.1) several times, as per the mathematical conditions in (5.22) which create more complicated mathematical operation.

$$\begin{cases} \frac{\partial J}{\partial n_1} = 0, & \frac{\partial J}{\partial n_2} = 0 \\ \frac{\partial^2 J}{\partial n_1^2} \times \frac{\partial^2 J}{\partial n_2^2} - \left( \frac{\partial^2 J}{\partial n_1 \partial n_2} \right)^2 > 0, & \text{if } \frac{\partial^2 J}{\partial n_1^2} > 0. \end{cases} \quad (5.22)$$

Therefore, advanced Engineering software mainly MATLAB will be employed to conduct these operations. Equations in (5.22) can be graphically recognized by showing a flat tangent plane that touches the 3D graph of  $J(n_1, n_2)$  function at the absolute minimum value. At this point, the flat tangent plane slope in both  $(n_1)$  and  $(n_2)$  directions is zero. Figure 5.3 illustrates the graphical representation of an example multivariable function where the slope of the tangent plane in the two variable directions is equal to zero.

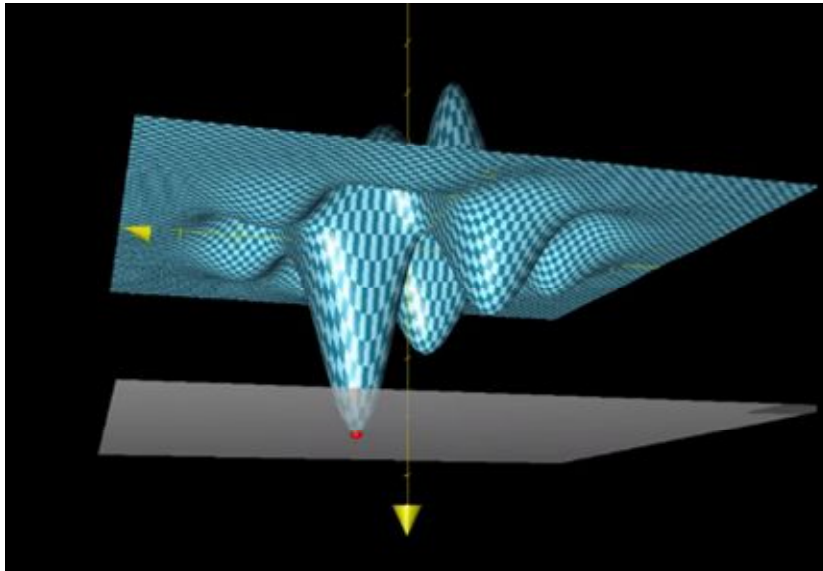


**Figure 5.3**, Graphical representation of multivariable function with minimum function value shown with corresponding zero plane slope in both variables direction (Sanderson, 2016)

Consequently, the task at the current stage is to calculate the values of  $(n_1)$  and  $(n_2)$  that make  $J(n_1, n_2)$  absolute minimum similar to Figure 5.3. Such procedure will require first to find a pair of roots values that satisfy the set of following partial differential Equations simultaneously:

$$\frac{\partial J}{\partial n_1} = 0, \quad \frac{\partial J}{\partial n_2} = 0. \quad (5.23)$$

Nevertheless, the obtained solution for Equations in (5.23) is a list of  $(n_1)$  and  $(n_2)$  pairs representing the roots that satisfy Equations (5.23) simultaneously, but cannot give an indication of which pair of roots exactly makes the function value local maximum or minimum. This is because in either case the slope of the flat tangent plane is equal to zero. Therefore, the combination of second partial derivatives and second mixed partial derivatives is an important test expressed in Equation (5.24) below to decide whether the pair of roots values make the function local minimum only:

$$\frac{\partial^2 J}{\partial n_1^2} \frac{\partial^2 J}{\partial n_2^2} - \left( \frac{\partial^2 J}{\partial n_1 \partial n_2} \right)^2 > 0, \quad \text{if } \frac{\partial^2 J}{\partial n_1^2} > 0. \quad (5.24)$$

Equation (8.2) in the appendix represents  $\partial J / \partial n_1$  which is the partial differential Equation of the Performance Index in Equation (8.1) in respect to  $(n_1)$ . On the other hand, the partial derivative  $\partial J / \partial n_2$  in respect to  $(n_2)$  is given by Equation (8.3) in the appendix.

A simultaneous solution for Equation (8.2) and Equation (8.3) in the appendix will be required to find the roots of these sets of Equations. One pair only would be the roots that make the Performance Index  $J(n_1, n_2)$  as global minimum so that the condition of optimization is fulfilled.

### 5.1.5 Multivariable Performance Index Equation Solution

Newton Raphson is a root calculation algorithm for a function employing numeric analysis procedure. It can be also used for solving system of nonlinear pairs of equations  $f_1(x, y) = 0$  and  $f_2(x, y) = 0$ . The formula of the procedure is expressed in the following equation for each iteration:

$$\begin{bmatrix} x_1 \\ y_1 \end{bmatrix} = \begin{bmatrix} x_0 \\ y_0 \end{bmatrix} - [J(x_0, y_0)]^{-1} \begin{pmatrix} f_1(x_0, y_0) \\ f_2(x_0, y_0) \end{pmatrix}. \quad (5.25)$$

Where  $(x_0)$  and  $(y_0)$  are initial suggested values for the first iteration

$[J(x, y)]$ : is Jacobean matrix and can be expressed as:

$$[J(x, y)] = \begin{pmatrix} \frac{\partial f_1}{\partial x} & \frac{\partial f_1}{\partial y} \\ \frac{\partial f_2}{\partial x} & \frac{\partial f_2}{\partial y} \end{pmatrix}. \quad (5.26)$$

In the first iteration the suggested initial values  $(x_0)$  and  $(y_0)$  have to be substituted in the inverse of Jacobean matrix and in  $f_1(x, y)$  and  $f_2(x, y)$  functions alike so that equation (5.25) can be an equation of known terms and then the values of  $(x_1)$  and  $(y_1)$  can be easily calculated.

Once  $(x_1)$  and  $(y_1)$  are calculated and defined, they can be considered as initial values for the second iteration and the same process can be repeated for further iterations. The difference between an iteration and its next one is called an error and once an acceptable error value is reached, the process by then is converging and the final values of  $(x_i)$  and  $(y_i)$  represent indeed

the pair of roots that satisfy equations  $f_1(x, y) = 0$  and  $f_2(x, y) = 0$  simultaneously, where  $(i)$  is the number of iterations.

Newton Raphson algorithm has been developed as MATLAB script file and showed in appendix (8.8). Using many different suggested initial values and carrying out the Newton Raphson operation for 200 iteration for each operation, some simultaneous solutions of equations (8.2) and (8.3) in the appendix have been defined. The list below shows the roots that satisfy simultaneously both equations.

Group (I) of roots satisfy the set of Equations (8.2) and (8.3) for minimum values by fulfilling the condition in equation (5.24), while Group (II) of roots satisfy the same set for maximum values since they are not fulfilling the condition in equation (5.24)

**Group (I):**

$$[n_1 = -7.4987, n_2 = -32.8401], J(n_1, n_2) = 2998.63$$

$$[n_1 = -3.4610, n_2 = 0.9163], J(n_1, n_2) = 755.33$$

$$[n_1 = 3.2175, n_2 = 1.0644], J(n_1, n_2) = 601.8$$

**Group (II):**

$$[n_1 = -0.3030, n_2 = -5.9440], J(n_1, n_2) = 57808$$

$$[n_1 = 3.6339, n_2 = -1.7779], J(n_1, n_2) = 1054.1$$

$$[n_1 = -0.3, n_2 = -5.944], J(n_1, n_2) = 57808$$

$$[n_1 = 2.7, n_2 = -8.86], J(n_1, n_2) = 3297160$$

It is worth mentioning that 200 iterations are used as at this value, the error of  $10^{-6}$  is guaranteed and reached which gives the result acceptable accuracy.

However, although this technique has given solution for the pair of equations (8.2) and (8.3) in the appendix based on suggesting random initial values of  $(x_i)$  and  $(y_i)$  but it is not a complete solution as there is no clue what other  $(x_i)$  and  $(y_i)$  to be suggested and where to stop on the suggestion process. Moreover, this technique is providing real roots only and cannot calculate the complex pair of roots which might be a solution also for the pair of Equations. Therefore, Newton Raphson algorithm is discarded, and MATLAB software is used to get the complete solution for Equations (8.2) and (8.3) in the appendix.

MATLAB software has been used to find a complete simultaneous solution for Equation (8.2) and Equation (8.3) and to execute the mathematical operations in Equation (5.24). Script file (8.4) as shown in the appendix has been developed and run to find the list of the roots that satisfy Equation (8.2) and Equation (8.3) simultaneously. After running the script file, 64 pairs of roots have been resulted from the solution, the pairs are listed and shown in the appendix (8.5)

The list in the appendix includes many complex values which are not realistic solution, therefore real roots will be considered only for finding the extremum values of  $J(n_1, n_2)$  where the plane slope is zero in both directions. The following pairs list shows the real remaining roots after excluding the complex ones:

$n_1$	$n_2$
-1.71e+62	128.3006638
3.217531148	1.064370365
655360	6.253705797
4.31e+93	502.834547
8.81e+57	102.2124131
8.37e+52	84.65391354
-3.461022444	0.916254542
3.633893826	-1.77785253
Inf	-3.00e+29
1.01e+62	-121.5049929
0	-5.944045915

-4.38e+34	-32.84011291
-34359738377	-8.86542806
Inf	4.75e+28
4.813641995	-2.349099765
Inf	2.89e+34
-1.71e+62	128.3006638

It is worth mentioning herein that there is no clue which pairs are making  $J(n_1, n_2)$  local minimum or maximum. Therefore the second test as stated in the set of Equations (5.24) is important to identify the pairs that make  $J(n_1, n_2)$  only local minimum. MATLAB script file (8.6) in the appendix is developed and executed to apply the second test as stated in the set of Equations (5.24) which identified the pair that makes  $J(n_1, n_2)$  only local minimum:

$n_1$	$n_2$	$J(n_1, n_2)$
3.217	1.064	982.44

At this pair,  $J(n_1, n_2)$  is global minimum when  $n_1 = 3.2175$  and  $n_2 = 1.0644$  because  $J(n_1, n_2)$  has the minimum value of (982.44) at this pair of roots.

Selecting  $k_1 = 1$  arbitrarily, and based on equation (4.28) considering the identified values of ( $n_1$ ) and ( $n_2$ ), the forward gains vector can be computed so it becomes:

$$\begin{bmatrix} k_1 \\ k_2 \\ k_3 \end{bmatrix} = \begin{bmatrix} 1 \\ 3.2175 \\ 1.0644 \end{bmatrix} . \quad (5.27)$$

The feedback gains can now also be calculated through the following procedure:

Substituting the values  $n_1 = 3.2175$  and  $n_2 = 1.0644$  in Equation (5.21),  $Q$  matrix becomes:

$$Q = \begin{bmatrix} -0.0000111 & -0.000222 & -0.0000048 \\ -0.000997 & -0.01327 & -0.00033698 \\ -0.019856 & -0.20864 & -0.004913 \end{bmatrix}. \quad (5.28)$$

By substituting Equation (5.28) and Equation (5.18) in Equation (4.31), the feedback gains vector can be computed through following procedure:

$$k_1 \begin{bmatrix} -0.0000111 & -0.000222 & -0.0000048 \\ -0.000997 & -0.01327 & -0.00033698 \\ -0.019856 & -0.20864 & -0.004913 \end{bmatrix} \begin{bmatrix} h_1 \\ h_2 \\ h_3 \end{bmatrix} = \begin{bmatrix} 0.0002 \\ 0.0123 \\ 0.2300 \end{bmatrix}, \quad (5.29)$$

so that

$$\Rightarrow \begin{bmatrix} h_1 \\ h_2 \\ h_3 \end{bmatrix} = \begin{bmatrix} -0.000222 & -0.0000111 & -0.0000048 \\ -0.01327 & -0.000997 & -0.00033698 \\ -0.20864 & -0.019856 & -0.004913 \end{bmatrix}^{-1} \begin{bmatrix} 0.0002 \\ 0.0123 \\ 0.2300 \end{bmatrix}$$

Consequently, the feedback gains vector can be defined as:

$$\begin{bmatrix} h_1 \\ h_2 \\ h_3 \end{bmatrix} = \begin{bmatrix} -8.8559 \\ -0.2493 \\ -0.4461 \end{bmatrix}. \quad (5.30)$$

The feedback and the forward path of the inner loop parameters are by now fully defined in Equations (5.27) and (5.30) completing the inner closed loop design.

Figure (5.4) shows the system responses of the inner loop for a unit step reference input change on  $\bar{r}(t)$  in comparison with HVAC open loop responses. The system produced quicker pressure, air flow rate and the temperature responses than the responses of the open loop system which are superimposed and shown in the figure and based on the definition of the Rise Time which is the time required for system response to reach 95% of its steady state value. The speed in the responses based on the Rise Time definition can be obviously recognised when looking at the responses in Figure (5.4).

Nevertheless, based on the inner loop configuration, the outer loop control can be designed to secure accurate steady state output values as well as least output coupling which must be confined to a level that secures system stability.

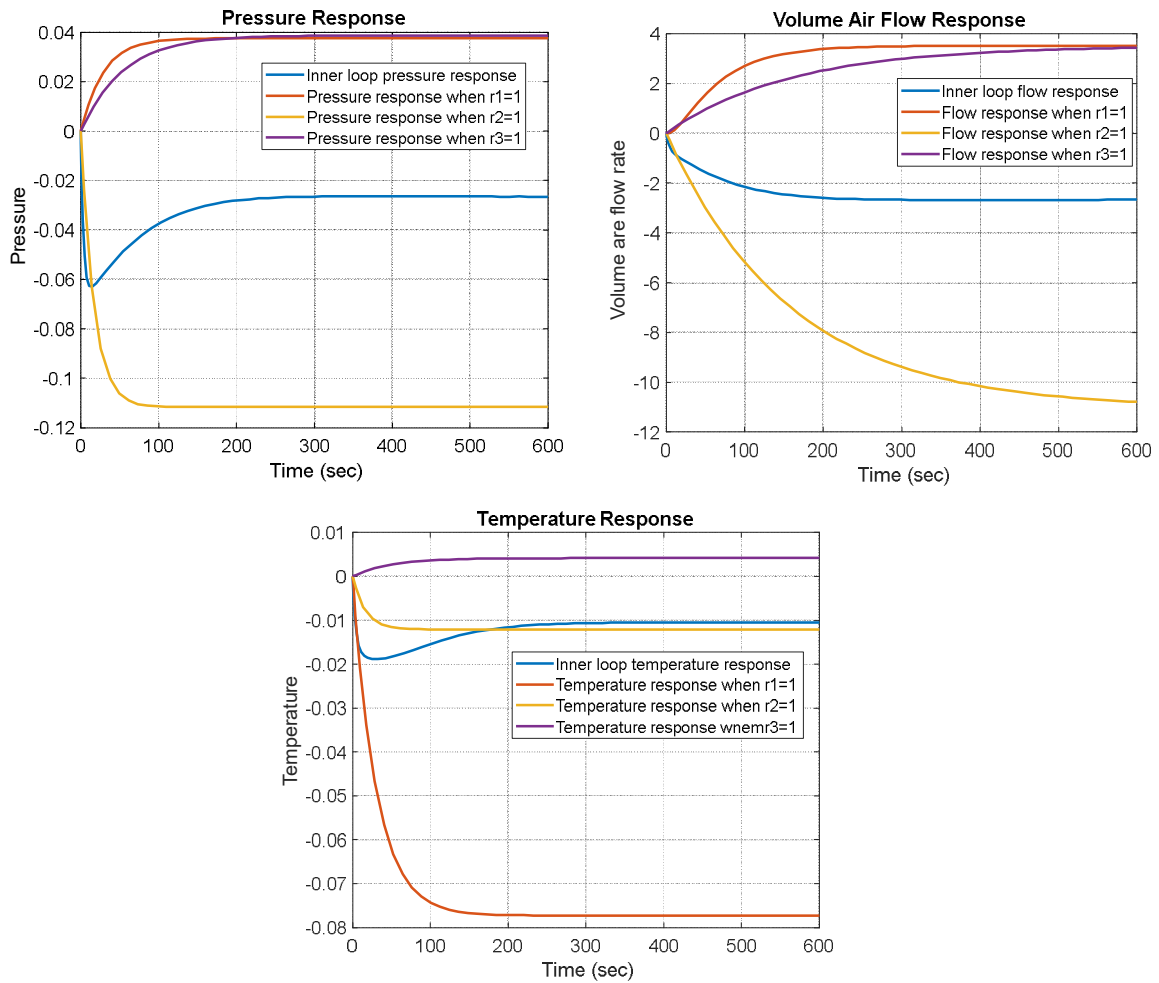


**Figure (5.4).** Inner loop system responses in comparison with the open loop responses

### Outer Loop Design

Based on the closed loop in Equation (4.13), which represents the conventional multivariable regulator structure,  $K(s)$  in the Equation equals to  $(P)$ , which is the matrix of forward pre-compensators that have to be computed by Equation (4.6) to obtain specified steady state output coupling. Once  $(P)$  matrix is calculated and the feedback gains matrix  $(F)$  is selected, the feedback compensators  $H(s)$  in Equation (4.13) can automatically be defined.  $(S_s)$  in Equation (4.6) is the matrix that can be defined based on zero steady state error requirement

and system outputs couplings of 5 percent. This coupling percentage is selected to be the value that guarantees the system stability. Accordingly, ( $S_s$ ) can be formulated as follows:

$$S_s = \begin{bmatrix} 1 & 0.05 & 0.05 \\ 0.05 & 1 & 0.05 \\ 0.05 & 0.05 & 1 \end{bmatrix}. \quad (5.31)$$

To define ( $F$ ) matrix in Equation (4.6), the study will assume three different feedback outer loop gains,  $f_1 = 0.1$ ,  $f_2 = 0.5$  and  $f_3 = 0.8$  to demonstrate the impact of increasing ( $f$ ) value on the disturbance rejection. ( $f$ ) must not be equal to unity, as such value will make the system unstable as per the stability criteria explained in chapter four. Consequently, the diagonal ( $F$ ) matrices can be selected as:

$$F_1 = \begin{bmatrix} 0.1 & 0 & 0 \\ 0 & 0.1 & 0 \\ 0 & 0 & 0.1 \end{bmatrix}, F_2 = \begin{bmatrix} 0.5 & 0 & 0 \\ 0 & 0.5 & 0 \\ 0 & 0 & 0.5 \end{bmatrix}, F_3 = \begin{bmatrix} 0.8 & 0 & 0 \\ 0 & 0.8 & 0 \\ 0 & 0 & 0.8 \end{bmatrix}. \quad (5.32)$$

Next, calculating ( $P$ ) matrices corresponding to ( $F$ ) matrices is based on calculating the matrices of  $G(0)$ ,  $k(0)$  and  $h(0)$  which are calculated as:

$$G(0) = \begin{bmatrix} 0.037 & -0.111 & 0.038 \\ 3.515 & -11.043 & 3.509 \\ -0.077 & -0.012 & 0.004 \end{bmatrix}, h(0) = [-8.85 \quad -0.25 \quad -0.446], k(0) = \begin{bmatrix} 1 \\ 3.217 \\ 1.064 \end{bmatrix}. \quad (5.33)$$

Based on Equations (5.31), (5.32) and (5.33), ( $P$ ) matrices are calculated and their values are:

$$P_1 = \begin{bmatrix} -9.27 & -1.54 & -14.65 \\ 78.88 & 2.13 & 1.08 \\ 337 & 15.43 & 26.24 \end{bmatrix}_{f_1=0.1}, P_2 = \begin{bmatrix} -18.14 & -4.81 & -27.41 \\ 143 & 10.62 & 8.81 \\ 612.88 & 58.68 & 78 \end{bmatrix}_{f_1=0.5}, P_3 = \begin{bmatrix} -66 & -36.75 & -27.42 \\ 397.2 & 107.78 & 103.84 \\ 1731 & 518.78 & 561 \end{bmatrix}_{f_1=0.8} \quad (5.34)$$

By calculating ( $P$ ) matrices the specific values of ( $f$ ) and certain output coupling percentages, the feedback configuration of the system can be represented in the closed loop system block diagram shown in Figure 5.5.

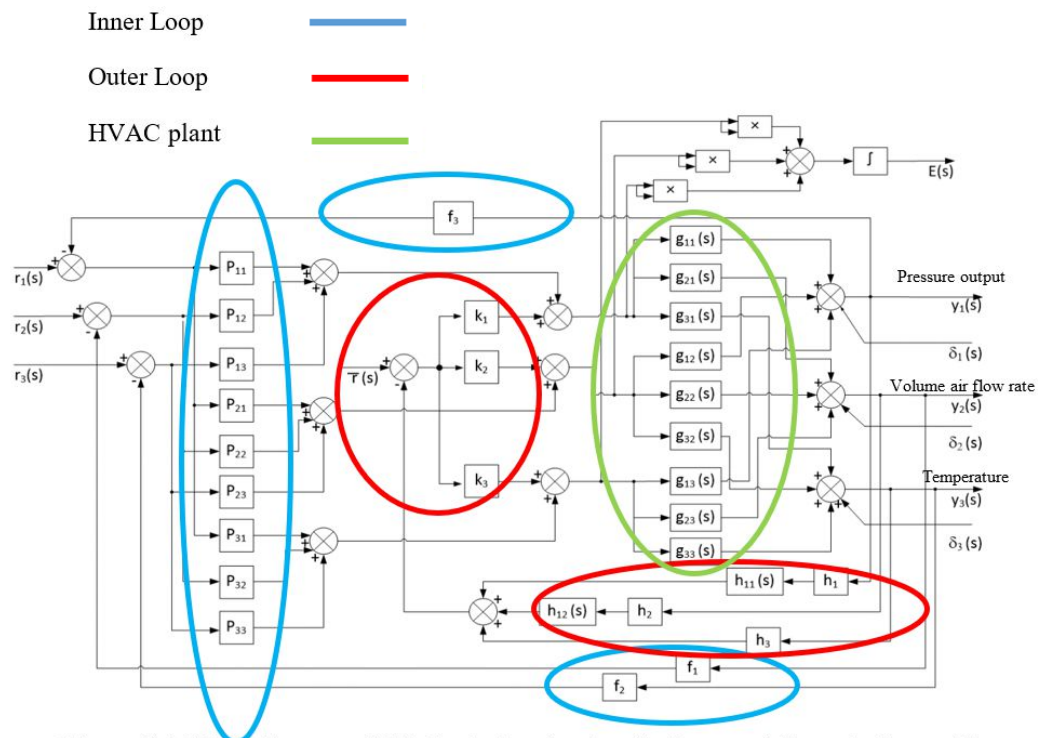


**Figure 5.5.** Block diagram of LE Controller showing the inner and the outer loop with forward and feedback gains

### 5.1.6 System Performance Analysis under the LE Controller

In order to analyse the performance of the system controlled by LE control technique under closed loop configuration, the time of 1800 seconds (half an hour) is selected as simulation time to compare and demonstrate all the system responses under all scenarios. It is a uniform time to analyse the performance of selected control techniques enabling clear comparison. The Simulation of the block diagram representation in Figure 5.5 is configured and run through SIMULATION and MATLAB software so that the system output responses following the unity step input change on  $r_1(t)$  at different values of  $f = 0.1$ ,  $0.5$  and  $0.8$  while other outputs remain zero changes are illustrated in Figures 5.6. ( $f$ ) values are selected to have a range of  $0 < f < 1$  in order to decide on the trade-off between system stability and amount of disturbance rejection as mentioned before in section 4.5.5. Whalley, R. and Ebrahimi, M. (2006) has

selected the values of  $(f = 0.1)$ ,  $(f = 0.5)$ ,  $(f = 0.8)$  in their research so that the same range will be used in this study as well.

Meanwhile, applying a unity step input change on  $r_2(t)$  and then on  $r_3(t)$  while the change on the other inputs remain zero will lead to have system responses as per Figures (5.7) and (5.8) respectively.

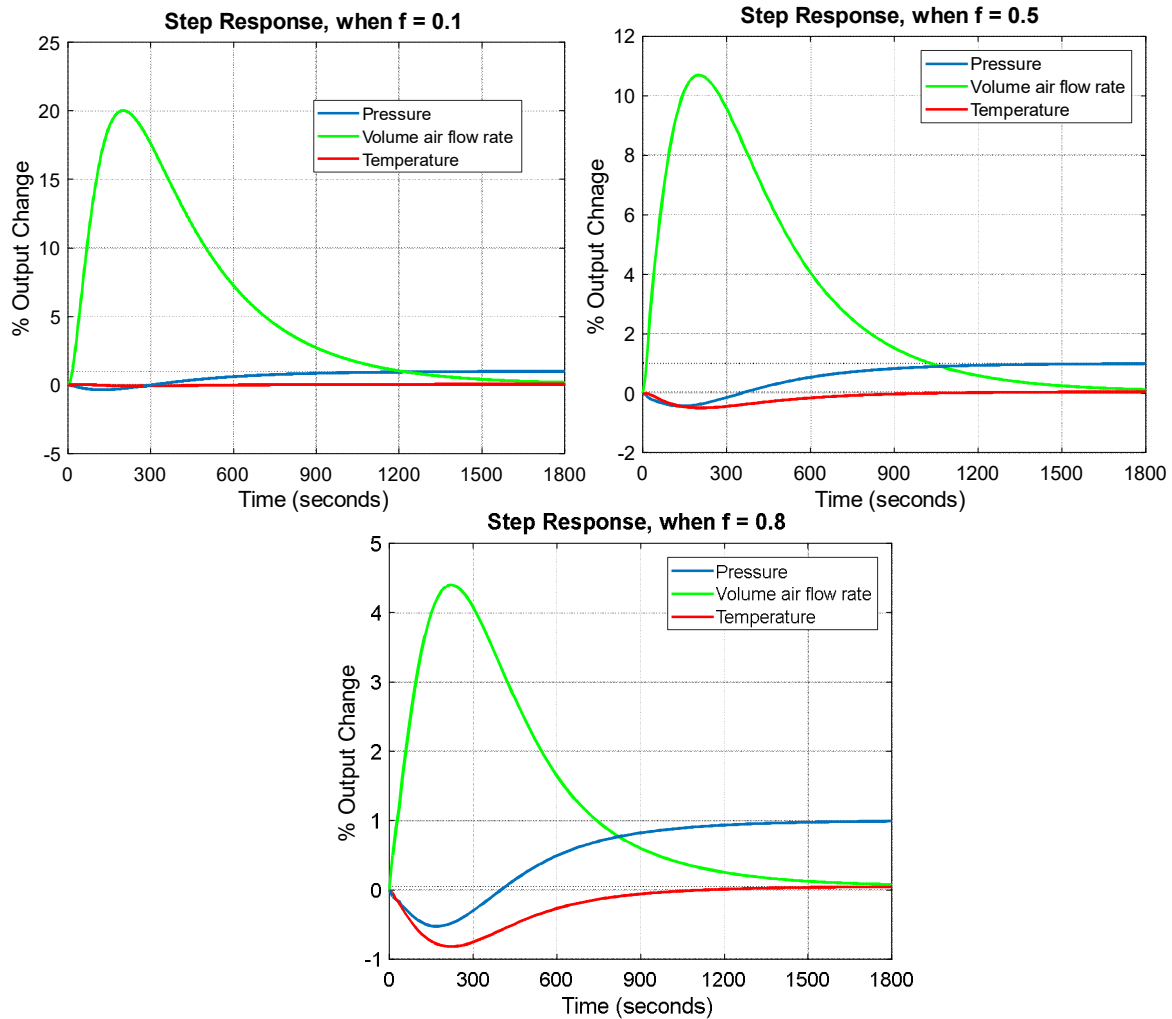


**Figure 5.6.** System output responses following unity step input change on  $r_1(t)$  at different values of  $f = 0.1$  ,  $0.5$  and  $0.8$

Referring to the output system responses in Figure 5.6, they are stable with zero steady state error. The outputs responses are significantly decoupled with unity value for air pressure ( $P$ ) and value of 0.05 for the volume air flow rate ( $q$ ) as well as air temperature ( $T$ ) responses at the inlet of the ventilated volume, as specified in the steady state matrix. The system shows improved performance by increasing the value of ( $f$ ). It shows large overshoot for the air volume flow rate ( $q$ ) when  $f = 0.1$  and becomes less when  $f = 0.5$  but with least overshoot

when  $f = 0.8$ . The responses of the volume air flow rate ( $P$ ) and air temperature ( $T$ ) are achieved with non-minimum phase, which means that the transfer functions for both outputs have one zero at least in the left hand side of the s-plane. The non-minimum phase situation will cause the system to go in the opposite direction for some time before it changes the direction and goes to the desired direction achieving the desired output response. Such situation will add some delay on the system responses which can be clearly observed in the the responses of the volume air flow rate ( $P$ ) and air temperature ( $T$ ) in Figure (5.6)

In Figure 5.7 where the unity step input change is applied at  $r_2(t)$ , while other inputs remain zero. The output system responses are decoupled also according to the steady state matrix with zero steady state error. The system shows 20% overshoot in the air volume flow rate response before it goes to its unity steady state value. The overshoot in the air volume flow rate response is decreased and completely gone by increasing the value of ( $f$ ). The responses of pressure ( $P$ ) and Temperature ( $T$ ) are decoupled with steady state value of 0.05 as well

Similarly, in Figure 5.8 where unity step input change is applied at  $r_3(t)$  while other inputs remain zero. The responses are decoupled with 0.05 values as specified in the steady state matrix. Zero steady state error values are attained, and the best-behaved responses are achieved when  $f = 0.8$ . Minimum phase system response is encountered in the pressure ( $P$ ) response and oscillation response is found with the volume air flow rate response which decreases by increasing the value of ( $f$ ).

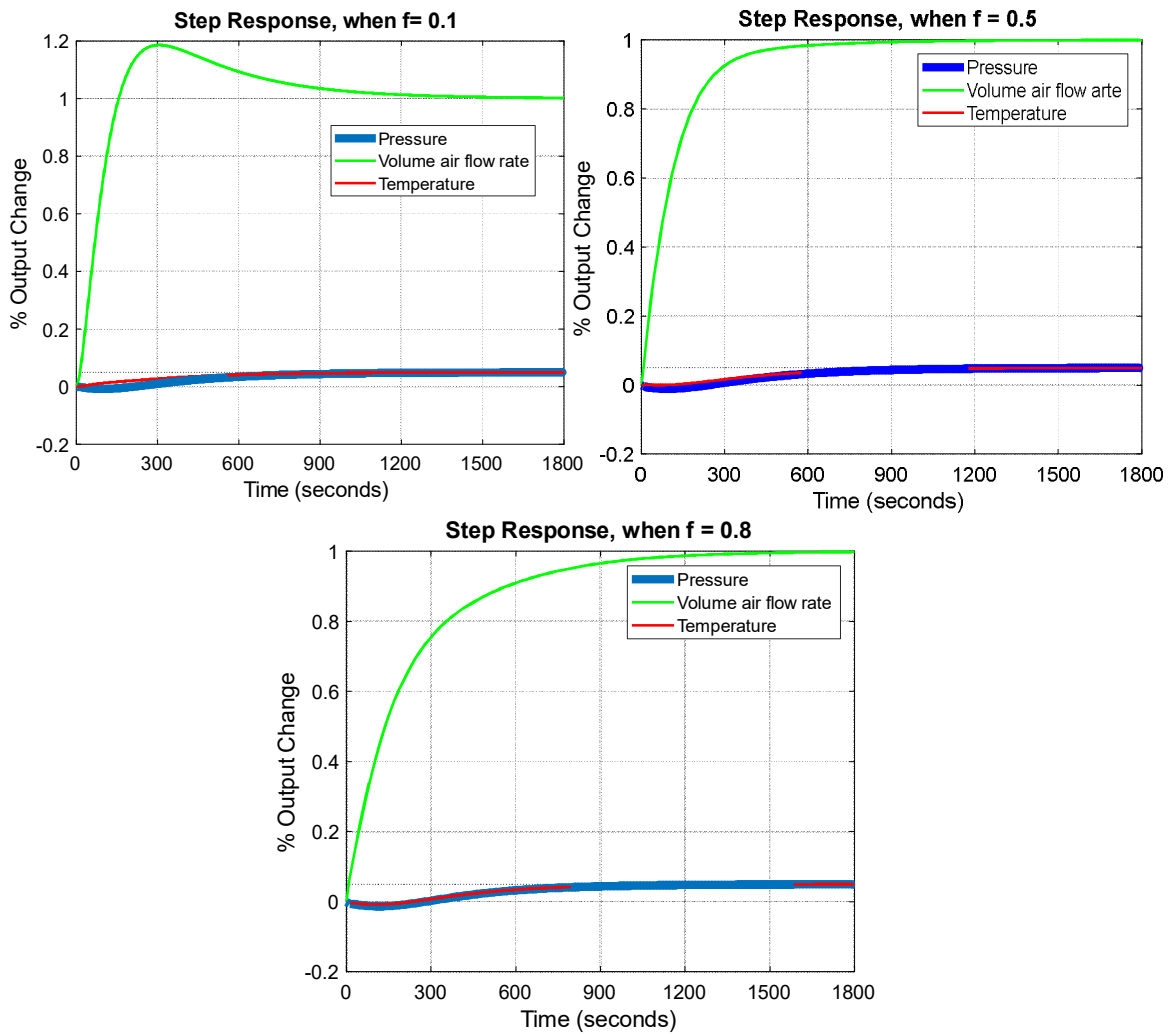


**Figure 5.7.** System output responses following unity step input change on  $r_2(t)$  at different values of  $f = 0.1$  ,  $0.5$  and  $0.8$

The overshoots in the volume air flow rates showed in the last Figures must be avoided as such overshoots can create annoying air noise in the HVAC system operation. This can be attained by the proper selection of the outer feedback gain ( $f$ ).

The selection of the outer feedback gain ( $f$ ) value has also to be investigated in the section of disturbances rejection analysis. Combining the results of the closed loop system responses will determine the best trade-off value of the outer feedback gain ( $f$ ) that can be used to attain well-behaved system responses associated with the best case for rejecting the disturbance.

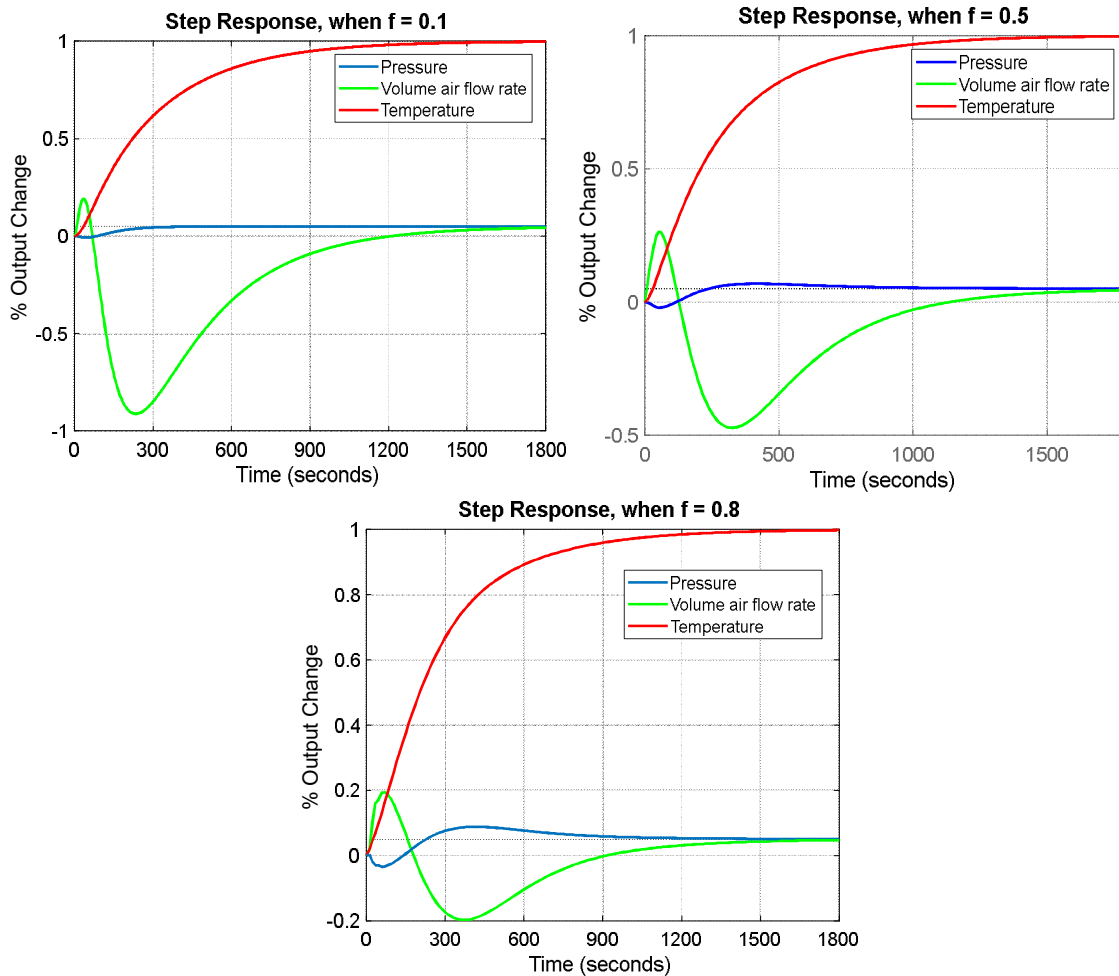


**Figure 5.8.** System output responses following unity step input change on  $r_3(t)$  at different values of  $f = 0.1$ ,  $0.5$  and  $0.8$

### 5.1.7 Disturbance Rejection Analysis Under LE Controller.

In the previous section, the system performance under the LE Controller was investigated and analysed. System disturbance operations is one important aspect to be investigated also and analysed, especially with HVAC system operations which have been characterized with a high probability to be disturbed by many sources. The disturbance can take place when unexpected thermal gains are loaded in the indoor space. This can be, for example, excess inhabitants entering the ventilated volume or more objects, such as additional furniture that are added

inside the ventilated volume. Other sources of disturbances can be unexpected opening of the doors or windows or any other opening that can expose the ventilated volume to the external environment, which has different pressure and temperature. Therefore, the HVAC system controller must show capability of rejecting such disturbances exerted on system output responses within an adequate time and by the least control effort.

In order to analyse the impact of the disturbance on the system responses it will be considered that there are no changes at the system inputs so that  $r_1(t) = r_2(t) = r_3(t) = 0$ . Meanwhile the analysis of system performance under the disturbance impact will test first the unity disturbance  $\delta_1(t)$  applied on the first output while other disturbance  $\delta_2(t)$  and  $\delta_3(t)$  signals remain equal to zero. This arrangement is simulated, and system responses are obtained and illustrated in Figure 5.9.

Figures 5.9 shows the output responses when disturbance signal  $\delta_1(t)$  at different values of  $f = 0.1$ ,  $0.5$  and  $0.8$  is applied at the inlet of the ventilated volume. The controller has managed to reduce the impact of the disturbance for the volume air flow rate, but to a value which still considered as high and significant deviation from the zero reference inputs values. The volume air flow rate has been impacted significantly with the disturbance change at the pressure output, but the impact is reduced by increasing the value of ( $f$ ). At  $f = 0.8$ , the impact is reduced to a value of  $-4.75$  which is still away from the reference inputs value. Best disturbance rejection for the temperature output is attained when  $f = 0.1$  and worsening by increasing the value of ( $f$ ) while the disturbance is not recovered for the Pressure response regardless of the value of ( $f$ ).

The performance is quite perfect, when signal  $\delta_2(t)$  is applied on the pressure at the inlet of the ventilated volume. This case is illustrated in Figure 5.10. The impact of the disturbance

signal  $\delta_2(t)$  is completely recovered throughout the whole values of ( $f$ ) with zero change at the inlet of the ventilated volume for the pressure and temperature responses. The volume air flow rate response is recovering to better amounts by increasing value of ( $f$ ) and the best recovery value for the volume air flow rate is 0.1 corresponding to  $f = 0.8$  which is rather acceptable.

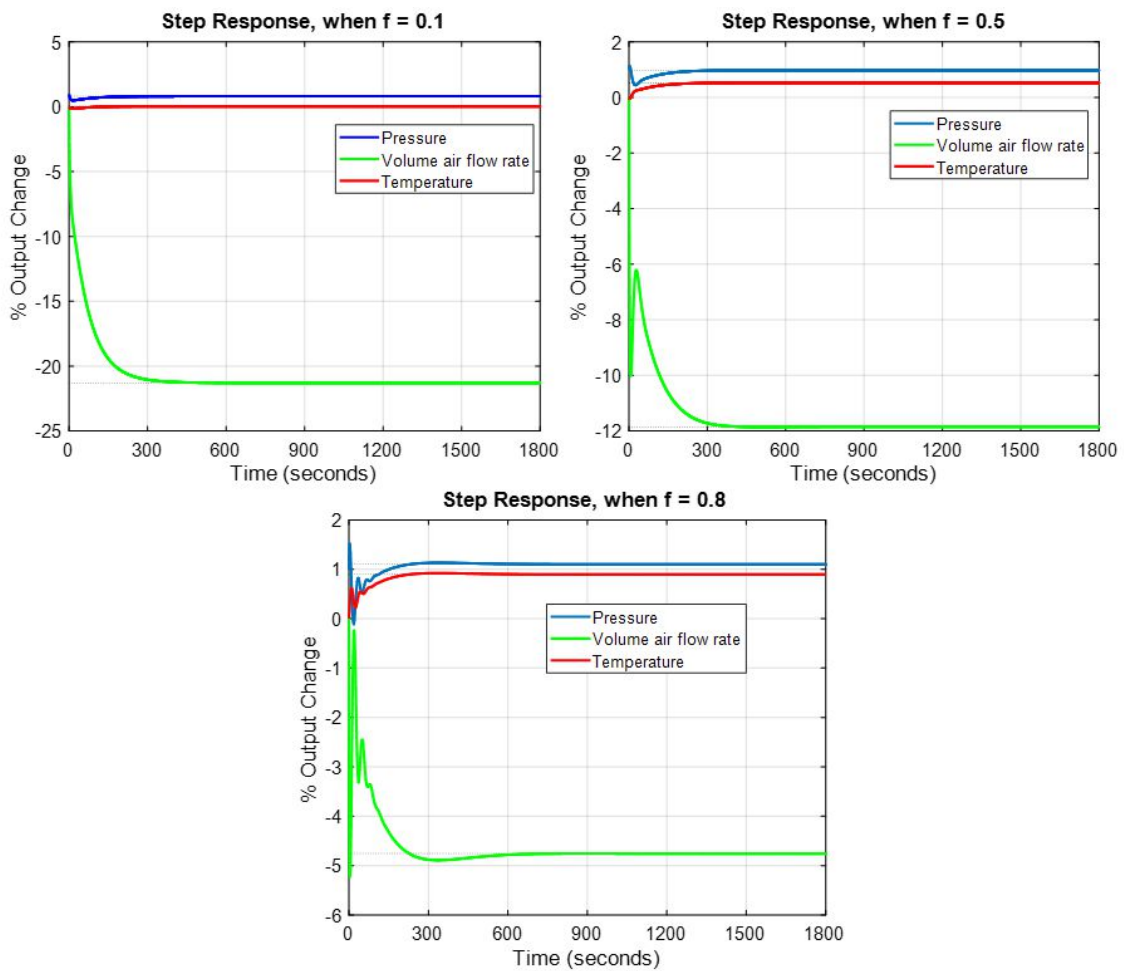


**Figure 5.9.** System output responses following unity disturbance step input change on  $\delta_1(t)$  at different values of  $f = 0.1$  , 0.5 and 0.8

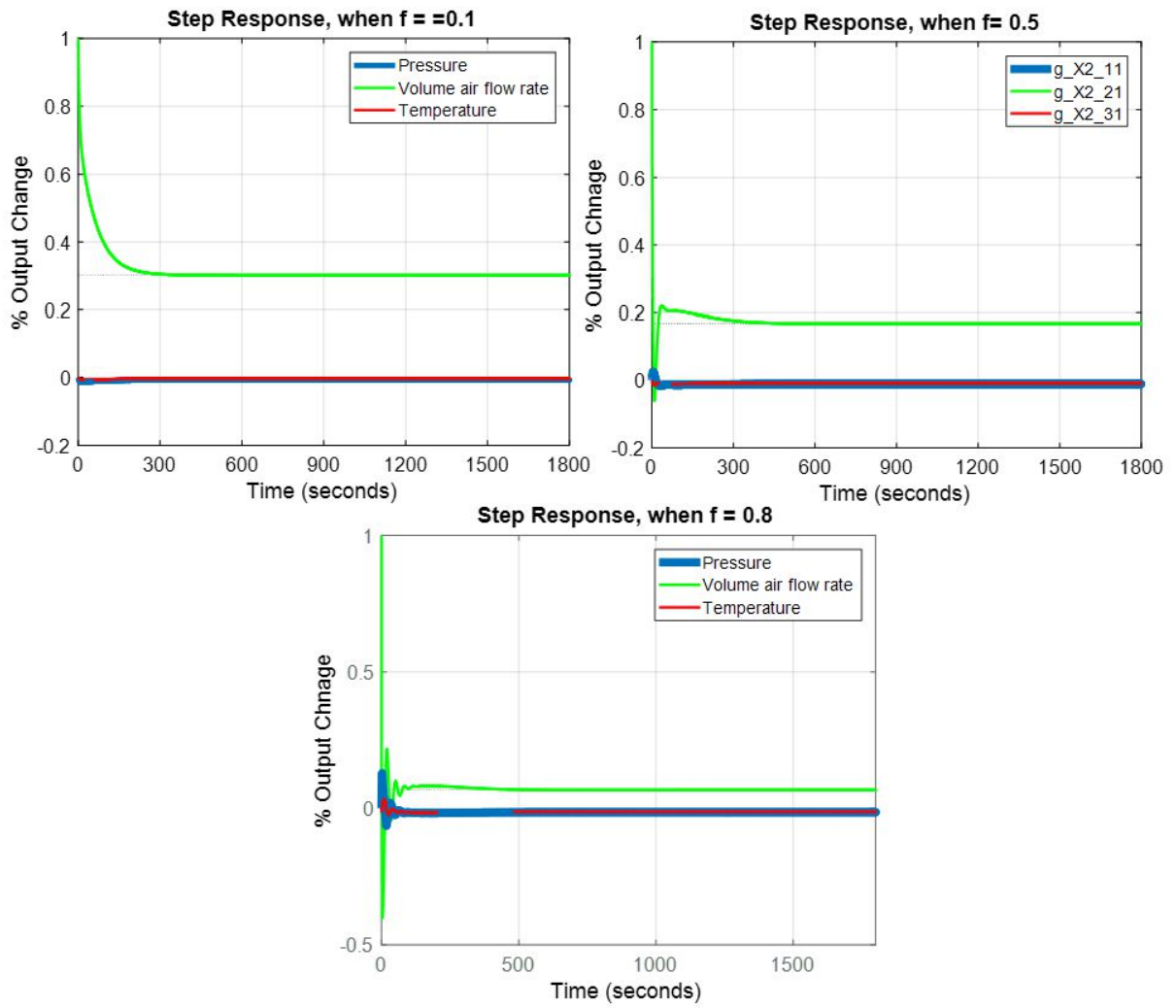


**Figure 5.10.** System output responses following unity disturbance step input change on  $\delta_2(t)$  at different values of  $f = 0.1$ ,  $0.5$  and  $0.8$

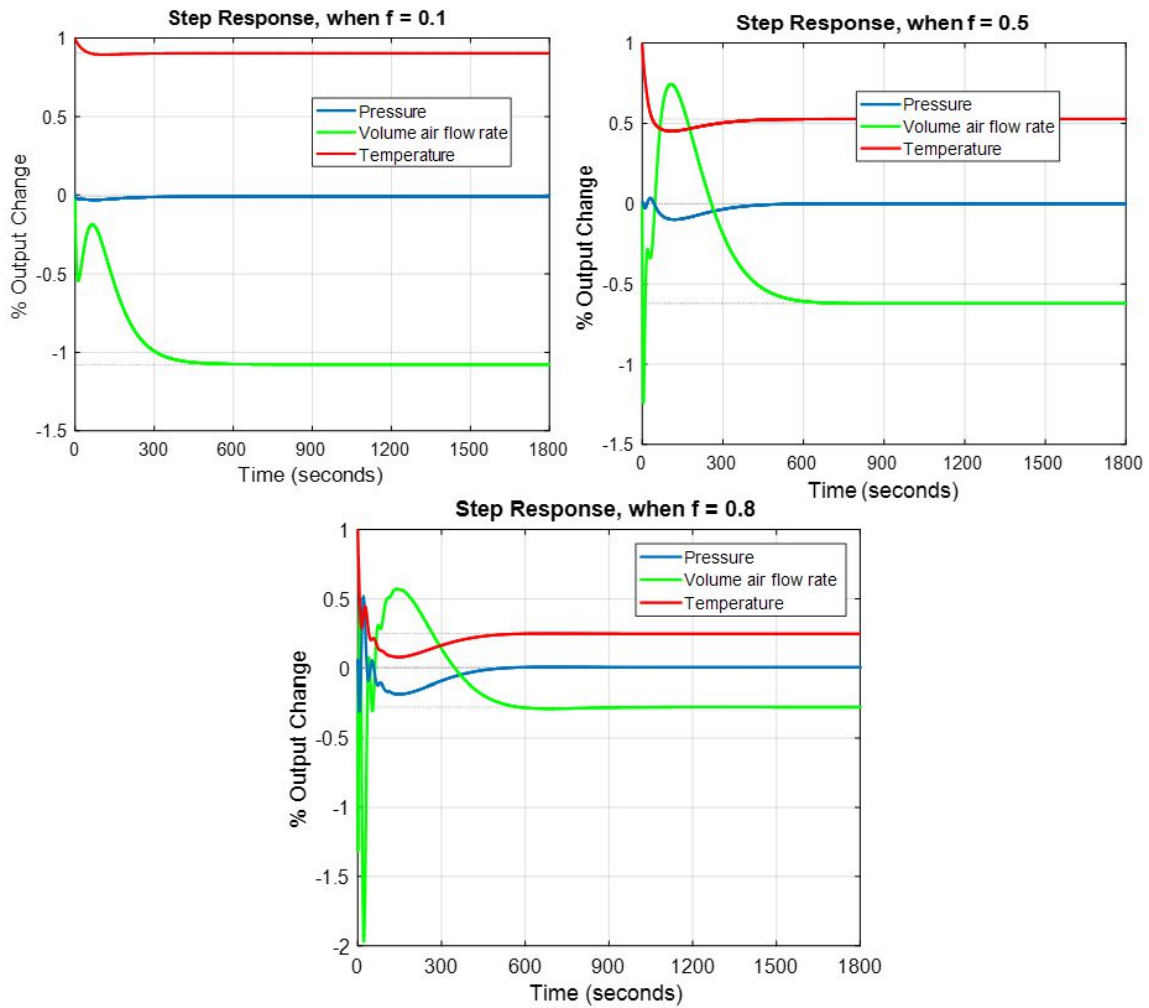


**Figure 5.11.** System output responses following unity disturbance step input change on  $\delta_3(t)$  at different values of  $f = 0.1$  ,  $0.5$  and  $0.8$

In Figure 5.11, the controller has also managed to recover the impact of the disturbance  $\delta_3(t)$  signal applied at the temperature of the inlet of the ventilated volume. The disturbance caused by  $\delta_3(t)$  signal is suppressed with several levels according to ( $f$ ) values, where the best suppression level is attained when  $f = 0.8$ . At  $f = 0.8$ , the change in the pressure response is zero while for the temperature and volume air flow rate is 0.25 and  $-0.27$  respectively which are also rather acceptable.

## 5.2 Direct Nyquist Array

The Direct Nyquist Array (DNA) multivariable control methodology as presented by many researchers can be considered as an extension from single input-single output control to multivariable control design (Leininger, 1977). Generally, the DNA control design consists of two major stages, the first one is to design a pre-compensator matrix to decouple the plant multivariable transfer function converting it to diagonal dominance matrix employing Gershgorin circles theorem to verify the diagonal dominance of the matrix, where the second stage is to apply multi-loop controllers to figure the Gershgorin circles bands also aiming to examine the stability of the system (Pan *et al.*, 2012).

The reduced order open loop Air Conditioning multivariable transfer function can be recalled as:

$$G(s) = \begin{bmatrix} \frac{0.001319}{s + 0.03509} & \frac{-0.02386}{3.5s + 0.2137} & \frac{0.002003}{2.8s + 0.05175} \\ \frac{-0.007193s + 0.004349}{s^2 + 0.08724s + 0.001237} & \frac{-0.06996}{s + 0.006335} & \frac{0.02223}{s + 0.006335} \\ \frac{-0.003539}{1.4s + 0.04581} & \frac{-0.005388}{7s + 0.4465} & \frac{0.0001918}{2.228s + 0.04609} \end{bmatrix}. \quad (5.35)$$

The procedure of control design is to figure out a compensators matrix  $K(s)$  so that when it is multiplied with  $G(s)$ , the resultant matrix:

$$Q(s) = G(s)K(s), \quad (5.36)$$

is row or column diagonal dominance as per the inequality conditions expressed in Equations (4.40) and (4.41) in chapter four.

### 5.2.1 Decoupling compensators

Decoupling the plant transfer function is not a simple procedure at all. Trial and error approach is the traditional process to identify the compensators matrix that decouple the plant transfer function  $G(s)$  with no guarantee on a specific time required to reach acceptable results. Based on this challenge, a dedicated MATLAB script file (8.7) in the appendix has been developed to identify the proper compensators that can decouple the plant transfer function  $G(s)$  based on trial and error approach. The process in the script file is developed to generate random compensators' coefficients establishing the compensators matrix so that when multiplied with the plant transfer function matrix  $G(s)$ , the resultant  $Q(s)$  is tested for row dominance. The test can be achieved by developing a loop in the MATLAB script file (8.7). The loop is set for  $(10^6)$  cycles and can stop only when the row dominance is achieved. More coefficients to be randomly generated increasing the order of the compensators' transfer functions once the "for loop" is completely run for  $(10^6)$  cycles without positive result. MATLAB script file (8.7) shows generating compensators' transfer functions with 11<sup>th</sup> order.

After several attempts employing MATLAB script file (8.7) which took a long time, the compensators matrix  $K(s)$  that able to decouple the plant transfer function  $G(s)$  is identified as follows:

$$K(s) = \begin{bmatrix} K_{11}(s) & K_{12}(s) & K_{13}(s) \\ K_{21}(s) & K_{22}(s) & K_{23}(s) \\ K_{31}(s) & K_{32}(s) & K_{33}(s) \end{bmatrix} \quad (5.37)$$

where:

$$K_{11}(s) = \frac{3.4737(s-57.15)(s+1.367)(s+0.2)(s+0.106)(s+0.07)(s+0.035)(s+0.0327)(s+0.03)(s+0.01782)}{(s+2.5)(s+2)(s+1.15)(s+1.1)(s+0.03496)(s+0.02151)(s+0.01702)(s^2+0.1335s+0.004464)}$$

$$K_{21}(s) = \frac{-217.01(s+3.5)(s+0.067)(s+0.06379)(s+0.06)(s+0.035)(s+0.023)(s^2+0.03386s+0.00003)(s^2+3.328s+2.9)}{(s+2.5)(s+2)(s+1.15)(s+1.1)(s+0.03496)(s+0.02151)(s+0.01702)(s+0.000248)(s^2+0.1335s+0.004464)}$$

$$K_{31}(s) = \frac{-676.7(s+3.656)(s+0.077)(s+0.035)(s+0.02)(s+0.01848)(s+0.018)(s^2+0.116s+0.003474)(s^2+3.233s+2.751)}{(s+2.5)(s+2)(s+1.15)(s+1.1)(s+0.03496)(s+0.02151)(s+0.01702)(s+0.000248)(s^2+0.1335s+0.004464)}$$

$$K_{12}(s) = \frac{-70.7(s+4.931)(s+2.634)(s+1.5)(s+1.2)(s+1.05)(s+0.07)(s+0.064)(s+0.035)(s+0.032)(s+0.0216)(s+0.0178)}{(s+4)(s+3)(s+2.5)(s+2)(s+1.15)(s+1.1)(s+0.03496)(s+0.02151)(s+0.01702)(s^2+0.1335s+0.004464)}$$

$$K_{22}(s) = \frac{38.8(s+6.7)(s+1.28)(s+0.86)(s+0.064)(s+0.06)(s+0.054)(s+0.034)(s+0.021)(s^2+0.036s+0.0004082)(s^2+6.464s+10.56)}{(s+4)(s+3)(s+2.5)(s+2)(s+1.15)(s+1.1)(s+0.03496)(s+0.02151)(s+0.01702)(s+0.000248)(s^2+0.1335s+0.004464)}$$

$$K_{32}(s) = \frac{-100(s+7)(s+1.36)(s+0.46)(s+0.064)(s+0.035)(s+0.02)(s+0.02)(s+0.018)(s^2+0.092s+0.00774)(s^2+6.274s+10)}{(s+4)(s+3)(s+2.5)(s+2)(s+1.15)(s+1.1)(s+0.03496)(s+0.02151)(s+0.01702)(s+0.000248)(s^2+0.1335s+0.004464)}$$

$$K_{13}(s) = \frac{-366.38(s+3.889)(s+3.173)(s+1.977)(s+0.07)(s+0.0638)(s+0.035)(s+0.03271)(s+0.02)(s+0.018)}{(s+4)(s+3)(s+1.15)(s+1.1)(s+0.03496)(s+0.02151)(s+0.01702)(s^2+0.1335s+0.004464)}$$

$$K_{23}(s) = \frac{-166.71(s+4.482)(s+0.06379)(s+0.06106)(s+0.03889)(s+0.03283)(s+0.0207)(s-0.02298)(s^2+4.12s+4.449)}{(s+4)(s+3)(s+1.15)(s+1.1)(s+0.03496)(s+0.02151)(s+0.01702)(s^2+0.1335s+0.004464)}$$

$$K_{33}(s) = \frac{-633.71(s+4.394)(s-0.1131)(s+0.0638)(s+0.03367)(s+0.03222)(s+0.02069)(s+0.01848)(s^2+4.328s+4.805)}{(s+4)(s+3)(s+1.15)(s+1.1)(s+0.03496)(s+0.02151)(s+0.01702)(s^2+0.1335s+0.004464)}$$

are the elements of  $K(s)$  matrix in which each element includes a multiplication of multiple compensators with first or second order.

### 5.2.2 Gershgorin Circles

A Nyquist array can be now obtained by plotting the Nyquist contour of the diagonal element  $q_{ii}(s)$  of  $Q(s)$  matrix which is a connection of points representing the centres of the Gershgorin circles at each point of frequency in the complex plane. The range of frequencies considered in this study varies from  $(0.1)$  to  $(10^6)$  rad/sec. This range can cover the working

frequencies that industrial processes work within. The Gershgorin band is then established by the circles centred by  $q_{ii}(j\omega)$  and the radii of either

$$\sum_{\substack{j=1 \\ j \neq i}}^3 |q_{ij}(j\omega)| \text{ for a column} \quad \text{or} \quad \sum_{\substack{j=1 \\ j \neq i}}^3 |q_{ji}(j\omega)| \text{ for a row at the range of } (0.1) \text{ to } (10^6) \text{ rad/sec}$$

frequencies.

If the Gershgorin bands of the diagonal elements do not encircle the origin of the complex plane, then  $Q(s)$  matrix is said to be a diagonal dominant matrix. The level of dominance and level of cross interaction between the system responses can be confirmed by the width of the band so that more diagonal dominance matches narrower Gershgorin band and more cross decoupling between the system outputs. Meanwhile, wider Gershgorin band corresponds to less diagonal dominance and then reflected on less cross-decoupling effect between the system outputs.

Multiplying plant transfer function matrix  $G(s)$  with the identified decoupling pre-compensators matrix  $K(s)$  and simplifying the multiplication product based on cancelling all pole/zero pair, yield to formulate  $Q(s)$  matrix as follows:

$$Q(s) = \begin{bmatrix} g_{11}(s) & g_{12}(s) & g_{13}(s) \\ g_{21}(s) & g_{22}(s) & g_{23}(s) \\ g_{31}(s) & g_{32}(s) & g_{33}(s) \end{bmatrix} \begin{bmatrix} K_{11}(s) & K_{12}(s) & K_{13}(s) \\ K_{21}(s) & K_{22}(s) & K_{23}(s) \\ K_{31}(s) & K_{32}(s) & K_{33}(s) \end{bmatrix},$$

so the product of the multiplication would be:

$$Q(s) = \begin{bmatrix} \frac{s+2}{s^2+2.25s+1.265} & \frac{0.1s+1}{s^2+4.5s+5} & \frac{0.2s+1}{s^2+7s+12} \\ \frac{0.1s+1.1}{s^2+4.5s+5} & \frac{s^2+4.434s+5}{s^3+4.75s^2+7s+3.163} & \frac{0.2s^2+0.975s-0.117}{s^3+7s^2+12s+0.07603} \\ \frac{0.1s+1}{s^2+4.5s+5} & \frac{0.2s+1}{s^2+7s+12} & \frac{s+2}{s^2+2.25s+1.264} \end{bmatrix}. \quad (5.38)$$

$Q(s)$  is quite diagonal dominant matrix for any row or column, the diagonal dominance of the matrix can be demonstrated graphically by drawing Gershgorin circles for each diagonal element  $q_{ii}(s)$  at all frequency values of the range from (0.1) to  $(10^6)$  rad/sec. The DNA controller design and analysis will be based on the row dominance arrangement. Figure 5.12 a shows the Gershgorin band and Nyquist diagram for  $Q(s)$  matrix element  $q_{11}(s)$ , while Figures 5.12 b and 5.12 c show the same results for  $q_{22}(s)$  and  $q_{33}(s)$  respectively

As per Figures 5.12 a, b and c,  $Q(s)$  is graphically quite diagonal dominant matrix as the Gershgorin circles of each row do not encircle the origin of the complex plane so that all the rows of the matrix are diagonal dominant.

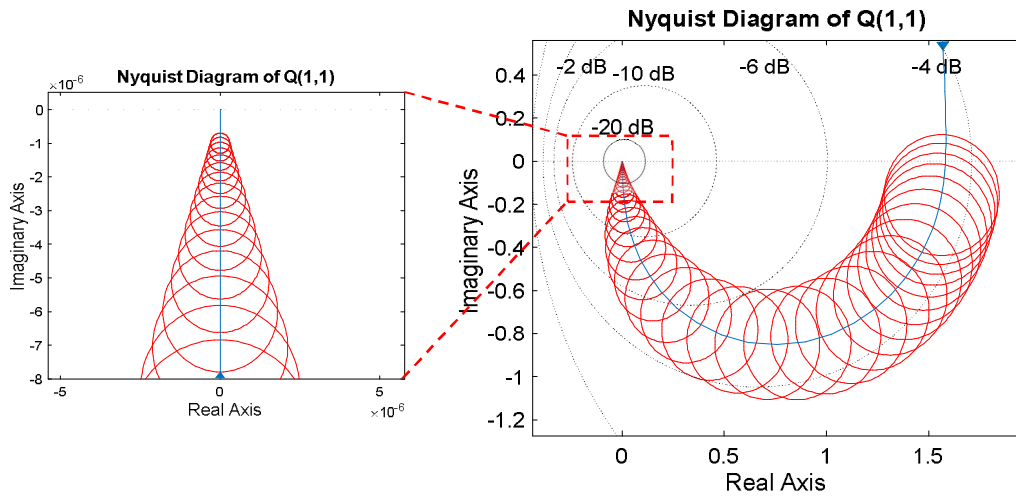


Figure 5.12 a. Gershgorin band and Nyquist diagram for matrix element  $q_{11}(s)$

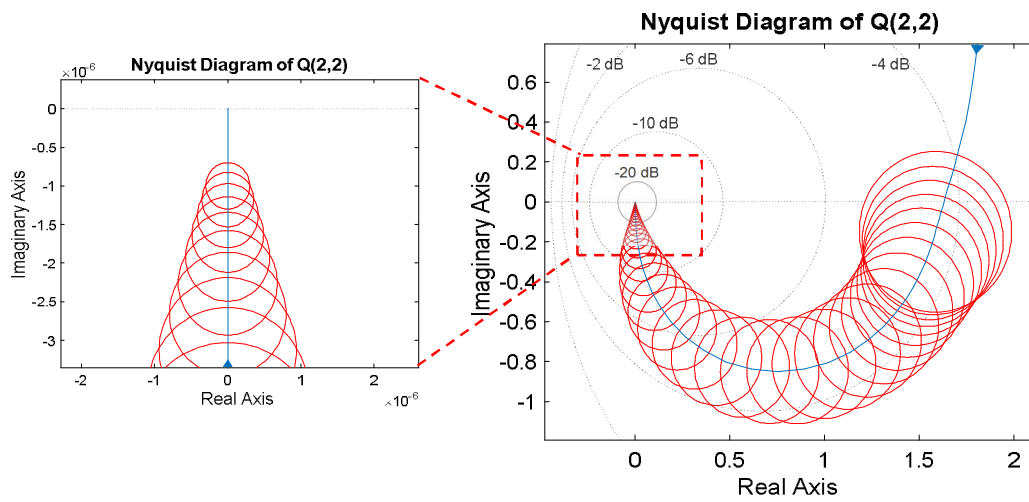


Figure 5.12 b. Gershgorin band and Nyquist diagram for matrix element  $q_{22}(s)$

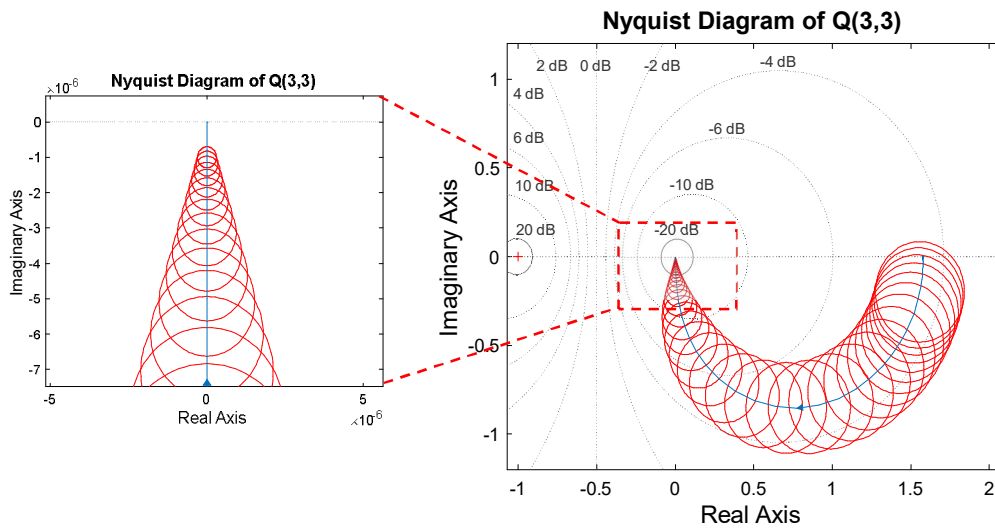


Figure 5.12 c. Gershgorin band and Nyquist diagram for matrix element  $q_{33}(s)$

With the  $Q(s)$  being diagonal dominant matrix, the multiplication product of  $G(s)K(s)$  becomes a transfer function matrix with decoupled and reduced cross interaction between the system loops. Such a situation can provide the possibility to design a controller for each decoupled loop individually. The next step is to configure individual SISO controllers, such as PID which represent the diagonal elements of  $C(s)$  matrix so that the final closed loop Equation built as per Figure 4.11 becomes:

$$G_{cl} = \frac{H(s)}{1+H(s)}, \quad (5.39)$$

where  $H(s) = G_{ol}(s) = G(s)K(s)C(s)$

### 5.2.3 System Stability Test

To assure the stability of the system under the closed loop structure, the Gershgorin bands centred about the diagonal elements of  $H(s)$  and with radii equal to the summation of the off-diagonal elements for the row of  $h_{ii}(s)$  must exclude the point  $(-1, j0)$  of the complex plane and encircle it a number of times equal to the number of the unstable poles of  $G_{ol}(s)$ . The methodology to shape the Gershgorin circles that fulfils the stability criterion depends strongly on selecting the proper PID controllers which are the elements of  $C(s)$  matrix. Identifying such SISO controllers can be done based on PID tuner Toolbox application in MTALAB software. According to such application process, the following PID controllers were identified fulfilling the stability criterion

- i. PID controller for the first loop:

$$PID_1 = -\frac{0.45706 (s+0.0001136)}{s}, \quad (5.40)$$

where:

$$Kp_1 = -0.4571$$

$$Ki_1 = -5.19e-05$$

$$Kd_1 = 0$$

ii. PID controller for the second loop:

$$PID_2 = \frac{-0.3405 s - 2.966e-05}{s}, \quad (5.41)$$

where:

$$Kp_2 = -0.3405$$

$$Ki_2 = -2.9661e-05$$

$$Kd_2 = 0$$

iii. PID controller for the second loop:

$$PID_3 = \frac{0.009463}{s}, \quad (5.42)$$

where:

$$Kp_3 = 0$$

$$Ki_3 = 0.0095$$

$$Kd_3 = 0$$

With the PID SISO controllers, the open loop transfer function  $G_{ol}(s)$  matrix after simplifying

it based on cancelling all pole/zero pair becomes:

$$G_{ol}(s) = \begin{bmatrix} \frac{-0.4571s - 0.8909}{s^2 + 2.25s + 1.265} & \frac{-0.03405s - 0.3405}{s^2 + 4.5s + 5} & \frac{0.001892s + 0.009462}{s^3 + 7s^2 + 12s} \\ \frac{-0.0457s - 0.4613}{s^2 + 4.5s + 5} & \frac{-0.3405s^2 - 1.51s - 1.724}{s^3 + 4.75s^2 + 6.89s + 3.163} & \frac{0.001892s^2 + 0.009226s - 0.001106}{s^4 + 7.006s^3 + 12.04s^2 + 0.07603s} \\ \frac{-0.04571s - 0.457}{s^2 + 4.5s + 5} & \frac{-0.06811s - 0.3406}{s^2 + 7s + 12} & \frac{0.009463s + 0.01893}{s^3 + 2.25s^2 + 1.265s} \end{bmatrix} \quad (5.43)$$

Gershgorin circles can now be plotted and showed in Figures 5.13 a, b and c below for the row elements centred on the diagonal elements of a row and with radii of off-diagonal elements summation for the same row.

It is apparent from Figures 5.13 a, b and c that the Gershgorin bands do not enclose the point  $(-1, j0)$  in the complex plane and the number of encirclements for the same point is zero. Since the number of encirclements ( $N_i$ ) for the point  $(-1, j0)$  is zero, then the system is stable under the closed loop structure as the number of unstable poles of the closed loop system as per Equation (4.45) is also zero. Consequently, the system is stable for the three loops under the closed loop function incorporating the PID controllers as per Equations (5.44), (5.45) and (5.46)

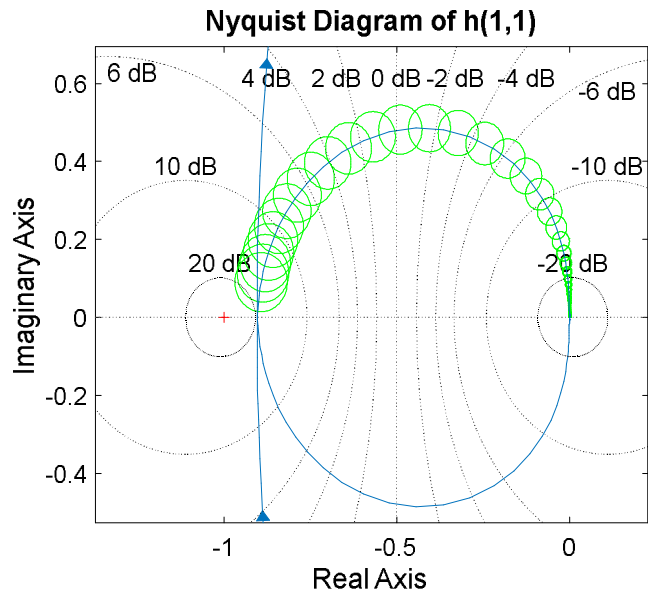


**Figure 5.13 a.** Gershgorin bands centered about the diagonal elements of  $h_{11}(s)$  and with radii equal to the summation of the off-diagonal elements for the row  $h_{11}(s)$

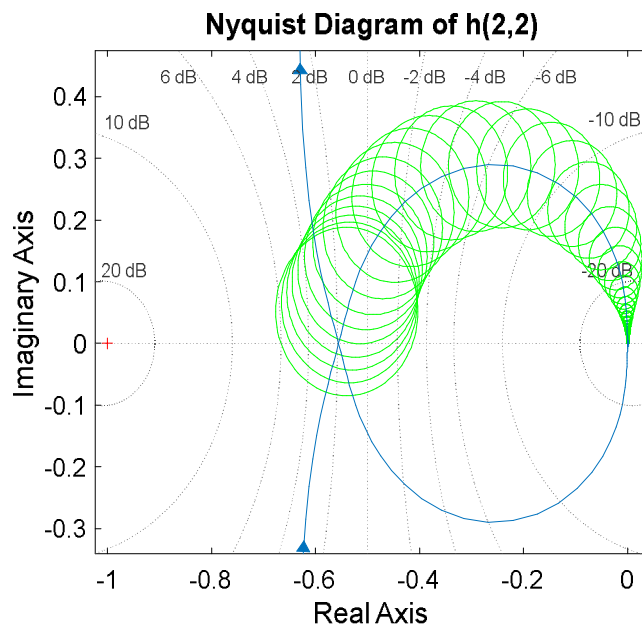


**Figure 5.13 b.** Gershgorin bands centered about the diagonal elements of  $h_{22}(s)$  and with radii equal to the summation of the off-diagonal elements for the row  $h_{22}(s)$

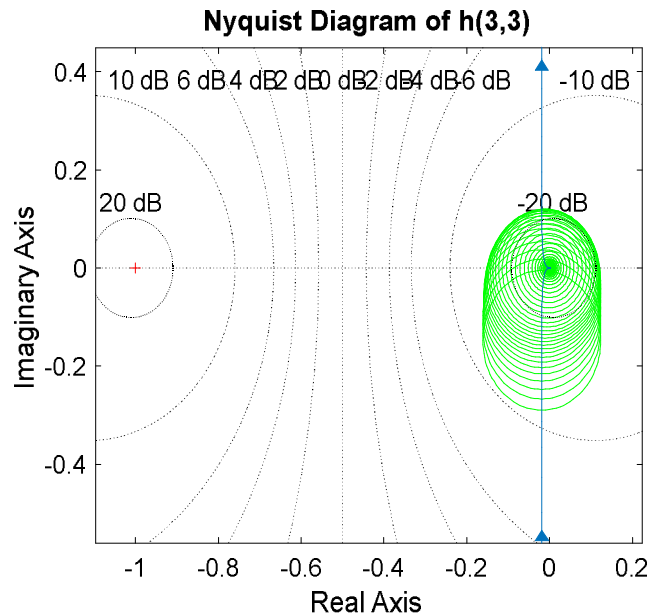


**Figure 5.13 c.** Gershgorin bands centered about the diagonal element of  $h_{33}(s)$  and with radii equal to the summation of the off-diagonal elements for the row  $h_{33}(s)$

#### 5.2.4 System Performance Analysis under DNA Controller

Figure 5.20 illustrates the block diagram of the closed loop system under the Direct Nyquist Array controller. Simulating the block diagram by the MATLAB and SIMULATION software at different step input changes will be investigated. Figure 5.14 shows the response for the air pressure, volume airflow rate, and temperature at the inlet of the ventilated volume following unity step change at  $r_1(t)$  while the change on the other inputs  $r_2(t)$  and  $r_3(t)$  remain zero. The outputs of the system are decoupled and the cross interaction between the loops is almost zero. The pressure response is unity as per the reference input at  $r_1(t)$  while the volume air flow rate and the temperature at the inlet of the ventilated volume are almost zero corresponding to the zero reference input changes at  $r_2(t)$  and  $r_3(t)$ . The steady state of the outputs are reaching

their final values at longer time than 1800 seconds, but cannot be shown in the figure due to the commitment to the uniform time for all controllers for the sake of comparison.

The same pattern of performance can be observed in Figure (5.15) and (5.16) when unity change is applied at  $r_2(t)$  and  $r_3(t)$  respectively with zero change on the other inputs. The output responses in both cases are also decoupled with almost zero cross interaction between the loops.

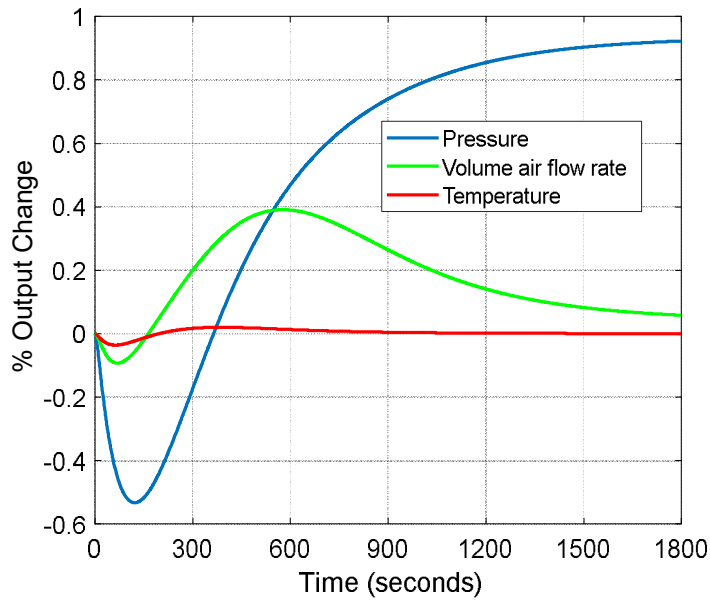


**Figure 5.14.** Direct Nyquist Array closed loop system output responses following a unity step change at  $r_1(t)$  and zero change at  $r_2(t)$  and  $r_3(t)$

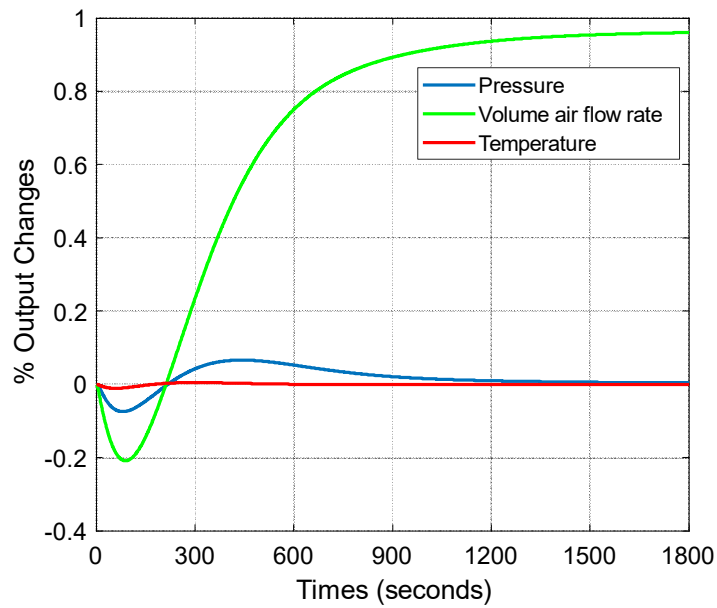


**Figure 5.15.** Direct Nyquist Array closed loop system output responses following a unity step change at  $r_2(t)$  and zero change at  $r_1(t)$  and  $r_3(t)$

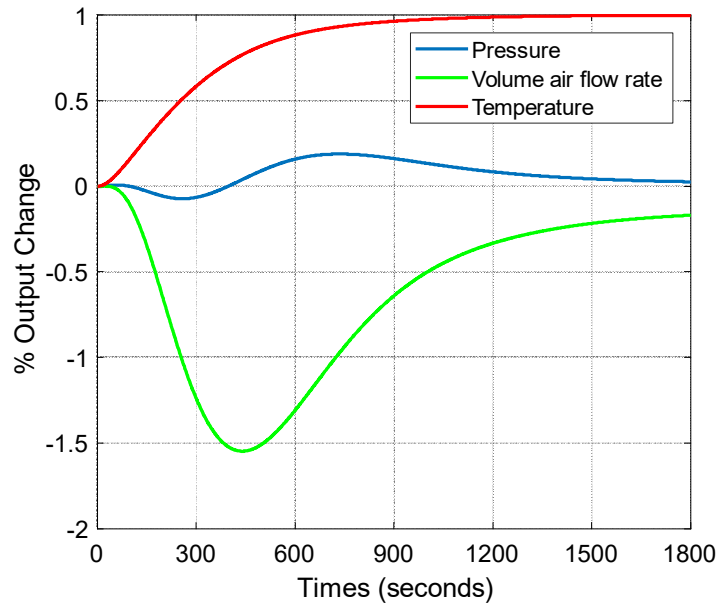


**Figure 5.16.** Direct Nyquist Array closed loop system output responses following a unity step change at  $r_3(t)$  and zero change at  $r_1(t)$  and  $r_2(t)$

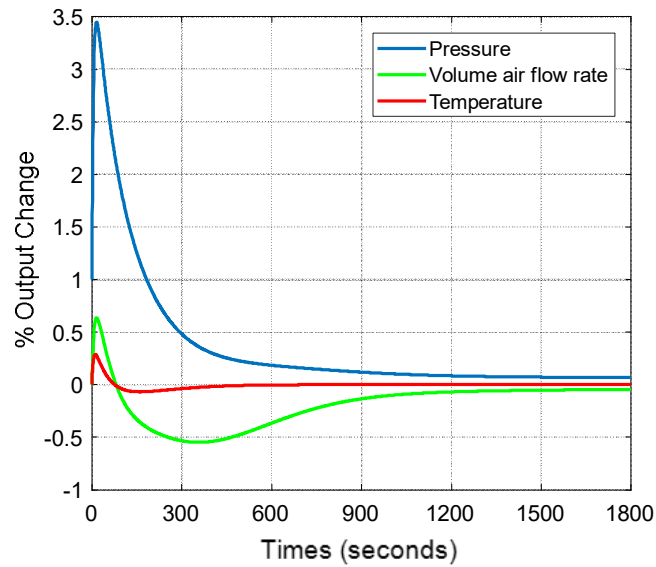
Non minimum phase response is encountered with the system performance under Direct Nyquist Array Controller. The non-minimum phase situation will cause the system to go in the opposite direction for some time before it changes the direction and goes to the desired direction achieving the designed output steady state response. Such situation is adding some delay on the system responses.

### 5.2.5 Disturbance Rejection Analysis for DNA control technique

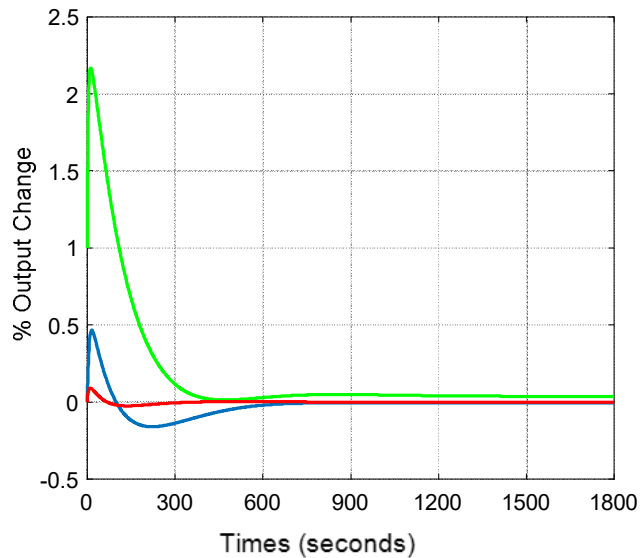
In the last section, the performance of the system was investigated under the DNA control system. Assessment of the system performance, under the disturbance effect on its outputs will be investigated too. A unity step change will be applied as disturbance signal to assess the performance of the system under DNA control system while the changes at the system reference inputs  $r_1(t)$ ,  $r_2(t)$  and  $r_3(t)$  are zero

Figure 5.17 shows the responses for the air pressure, volume airflow rate and temperature at the inlet of the ventilated volume following unity step disturbance change at  $\delta_1(t)$  while the

change on the other disturbance inputs  $\delta_2(t)$  and  $\delta_3(t)$  as well as system reference inputs  $r_1(t)$ ,  $r_2(t)$  and  $r_3(t)$  remain zero. The Figure shows successful disturbance rejection where the system outputs are returned to close to zero change. Same Performance can also be obtained when unity step disturbance change at  $\delta_2(t)$  while the change on the other disturbance inputs  $\delta_1(t)$  and  $\delta_3(t)$  as well as system reference inputs  $r_1(t)$ ,  $r_2(t)$  and  $r_3(t)$  remain zero. Figure 5.18 demonstrates this situation and shows a well-behaved system rejecting the disturbance and making the system responses to return to its original situation which is close to zero change. Same performance can be witnessed in figure 5.19 when unity step disturbance change at  $\delta_3(t)$  while the changes on the other disturbance inputs  $\delta_1(t)$  and  $\delta_2(t)$  as well as system reference inputs  $r_1(t)$ ,  $r_2(t)$  and  $r_3(t)$  remain zero. Well behaved system is also obtained in this condition and the system outputs are recovered to its zero-original reference.



**Figure 5.17.** System air pressure, volume airflow rate and temperature responses at the inlet of the ventilated volume following unity step disturbance change at  $\delta_1(t)$  while the change on the other disturbance inputs  $\delta_2(t)$  and  $\delta_3(t)$  remain zero.



**Figure 5.18.** System air pressure, volume airflow rate and temperature responses at the inlet of the ventilated volume following unity step disturbance change at  $\delta_2(t)$  while the change on the other disturbance

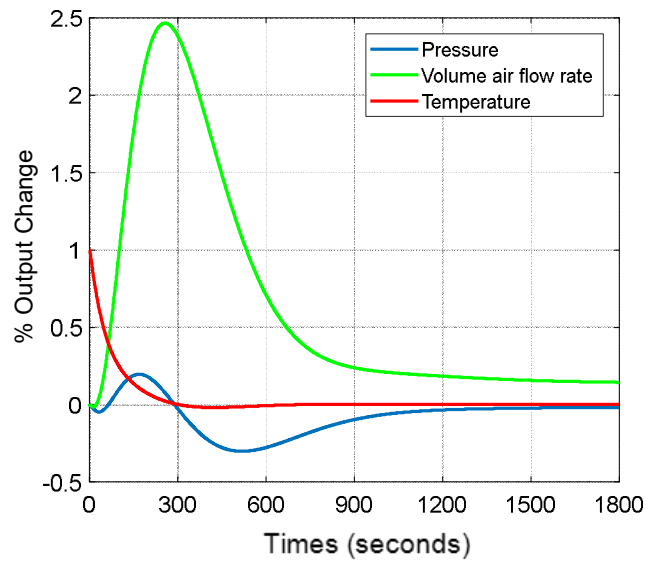


**Figure 5.19.** System air pressure, volume airflow rate and temperature responses at the inlet of the ventilated volume following unity step disturbance change at  $\delta_3(t)$  while the change on the other disturbance inputs  $\delta_1(t)$  and  $\delta_2(t)$

As per Figures 5.17, 5.18 and 5.19 the behaviour of system responses under external disturbance is quite well in terms of steady state suppression values, but obvious unwanted overshoots are also encountered with the responses. The closed loop multivariable DNA controller along with the SISO PID controllers have showed capability in suppressing the external disturbances and restoring the system to original functional values.

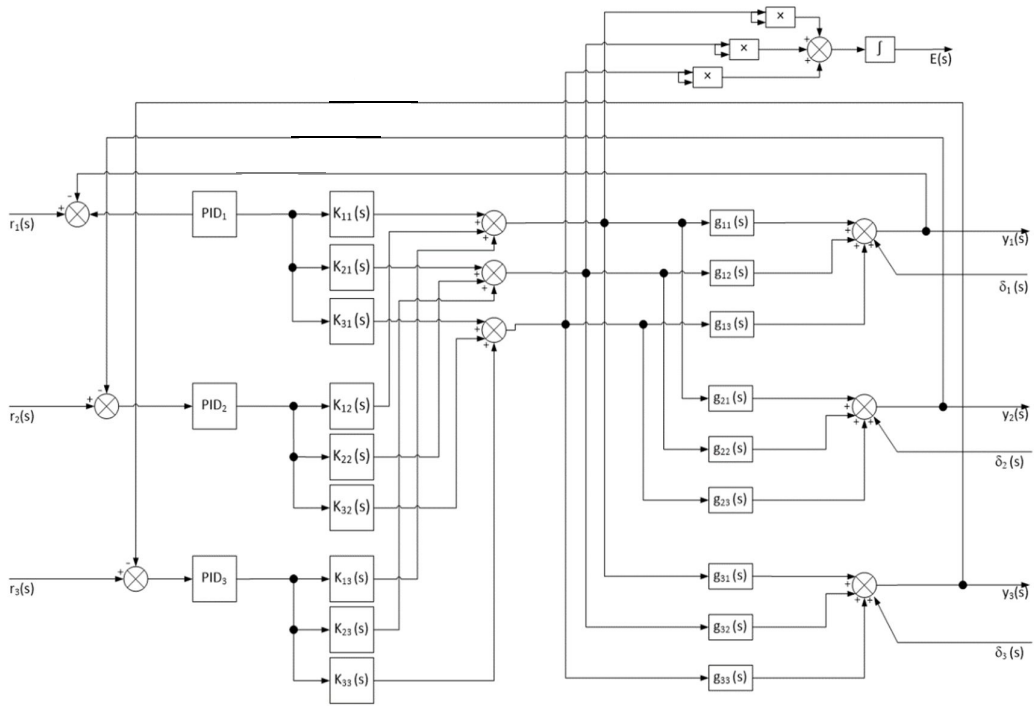


**Figure 5.20**, Block Diagram of Direct Nyquist Array controller

## Chapter Six

### LE and DNA Control Techniques Comparison

Hereafter, a detailed comparison between the LE and Direct Nyquist Array multivariable control techniques will be reviewed in order to highlight their application and performance. The chapter will also review a theoretical validation in order to verify the greatest association of these techniques with the control system energy consumption.

#### 6.1 Mathematical and Algebraic Operations

The LE and DNA multivariable control techniques were applied, demonstrated and investigated in the last chapter and have produced acceptable system performance responses. However, due to the complicated multivariable nature of the HVAC system model with the implementation of both control techniques and maintaining well-behaved system performance achieved with good inner loops decoupling, the technical research work was associated with long mathematical procedures. MATLAB and SIMULATION software played significant role in carrying out all the complicated mathematical operations and procedures to calculate for example the partial differential equations of the complex multivariable Equation  $J(n_1, n_2)$  and solve the Equation aiming to find the roots pairs in LE control technique. The mathematical operations executed by MATLAB were a bit long but not challenging as encountered in finding the proper percentage values of the interaction between the internal loops of the system in the application of LE controller. Such a situation pushed to work on many mathematical procedures to identify the proper interaction percentages that give the required steady state values and maintain closed loop system stability.

In the DNA multivariable control technique, finding a realistic decoupling compensators matrix was a great challenge to decouple the heavy interaction among the internal loops of the

system. Unfortunately, there is no clear systematic approach to find the proper compensator matrix that decouples the plant transfer function. A trial and error approach is a familiar way to find such a decoupling compensator matrix with no guarantee on the time required to do so. This time-consuming and tiring procedure has been witnessed in finally shaping the Gershgorin bands in the DNA technique for making the system transfer matrix diagonal dominant.

Consequently, the mathematical procedures used in the LE Control were very long, but straightforward. However, the DNA mathematical operations were complicated with one major disadvantage against the LE controller which is unsystematic trial and error approach that created a great challenge to find the decoupling compensator matrix with no specific time to have the solution.

## **6.2 The Controller Simplicity**

On one hand, the values of the feedback and forward gains, as well as the pre-compensators forward gains of the outer loop in the LE technique are simple passive gains so that it can cope with the limitation on the mass, inertia and space of power supply. Such gains will lead to avoiding the employment of integral controllers, as its corrective actions are strictly increasing under sustained error conditions and consuming control energy (Whalley and Ebrahimi, 2006)

On the other hand, the controller in the DNA technique was very complicated and was developed with very high order (between 9<sup>th</sup> to 11<sup>th</sup> order) decoupling compensators matrix as shown in Equation (5.41). Although these compensators can be factorised into a combination of lead, lag and lead-lag single compensators, the order of such factorised compensators are of first and second order compensators for one element of the decoupling matrix so that in total

more than 90 single lead, lag and lead-lag compensators for a complete  $3 \times 3$  decoupling matrix.

This is a big number.

Avoiding employing integrators and with the simple passive feedback and forward gains, the LE controller is far simpler than the DNA technique that employs very high order compensators (i.e. 9<sup>th</sup> to 11<sup>th</sup> order).

### **6.3 Closed Loop Responses and Disturbance Rejection**

In this comparison aspect, the system responses under both controllers, as well as disturbance rejection, will be investigated. The system responses for the LE controller when the outer feedback gain is ( $f = 0.8$ ) will be the basis for the comparison of closed loop performance.

Figure 6.1 shows the HVAC system responses under both controllers techniques when unity change is applied on the first input  $r_1(t)$  representing the voltage on the inlet and exit motor fans, and with zero change at  $r_2(t)$  and  $r_3(t)$ .

The Figure shows similar performance in both controllers in terms of very small steady state error for all the output responses and good transient responses but with exception of a significant overshoot for the volume airflow rate in the LE controller. Such overshoot will cause air noise for the blower for some time before it goes to lower steady state value, thus

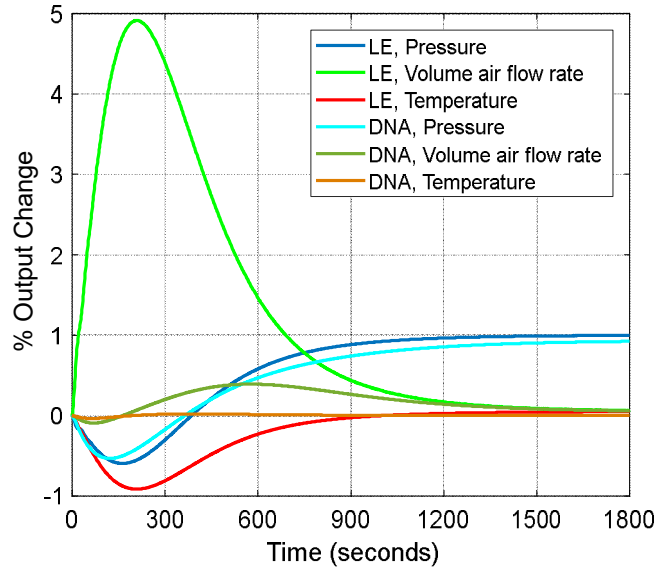


**Figure 6.1.** System responses under both controllers techniques when unity change is applied on the  $r_1(t)$  representing the voltage on the inlet and exit motor fans, and with zero change at  $r_2(t)$  and  $r_3(t)$ .

reducing the air noise. Both controllers have demonstrated a high level of decoupling between the internal control loops. Considering the rise time definition, the LE controller is providing better performance over the DNA by producing faster responses as per the figure 6.1 and an important advantage against DAN controller.

Figure 6.2 shows the HVAC system responses under both controllers when unity change is applied on the second input  $r_2(t)$  representing the voltage on a chilled water pump, and with zero change at  $r_1(t)$  and  $r_3(t)$ . The volume air flow rate in the LE controller, is a also faster than the same response in DNA controller. Moreover, the volume air flow rate response in DNA

controller is taking longer time to reach its final steady state value. Both controllers show very small steady state error for all the output responses and demonstrate a high level of decoupling between the internal control loops.

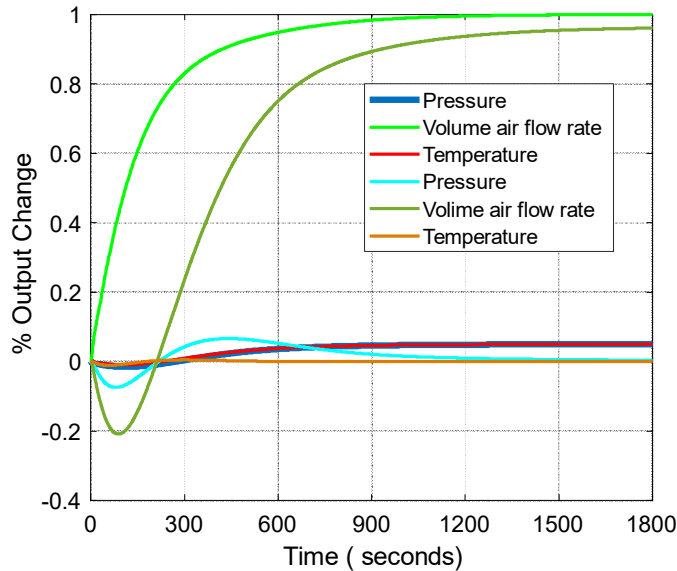


**Figure 6.2.** System responses under both controllers techniques when unity change is applied on the  $r_2(t)$  representing the voltage on the chilled water pump, and with zero change at  $r_1(t)$  and  $r_3(t)$ .

Similarly, in Figure 6.3, the response of the temperature in the LE is faster than the DNA controller. In mean while the dynamic responses of the pressure and volume air flow rate in the LE are better than the same responses in the DNA.

The responses in the LE shows better performance than the performance in DNA in terms of system response speed, however, the comparison between both controllers in terms of disturbance rejection will also be investigated; it is an important aspect of comparison as HVAC systems are exposed to external disturbances very often.

Figure 6.4 shows the output responses at the disturbance unity step change  $\delta_1(t)$  on the volume airflow output, while there is no disturbance change at the other outputs and no change at all reference inputs. The system performance under the DNA controller demonstrates better recovery response than the LE controller. Although the disturbance recovery is improving with the increased value of ( $f$ ) in LE control technique, it is failing to suppress the disturbance to low level in comparison with the DNA control technique. The output response when disturbance step change  $\delta_2(t)$  is applied on the air pressure output at the inlet of the ventilated volume and while there is no disturbance change at the other outputs and no change at the inputs is shown in Figure 6.5. In this case the recovery performance is quite well in both control techniques and suppressed the effect of the disturbance change accrued by  $\delta_2(t)$  signal making all the outputs values close to zero according to zero reference inputs values. However, the dynamics of the LE system responses in this case is better than the system responses dynamics of DNA controller.

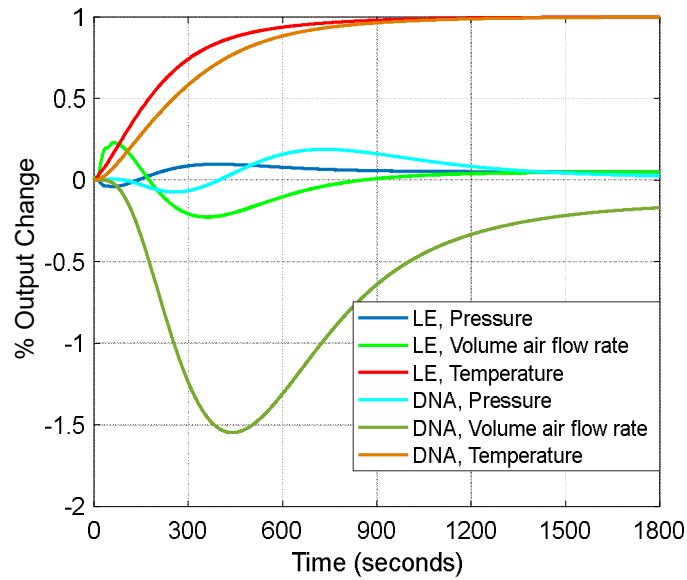


**Figure 6.3.** System responses under both controllers techniques when unity change is applied on the  $r_3(t)$  representing the ambient heat transfer, and with zero change at  $r_1(t)$  and  $r_2(t)$ .

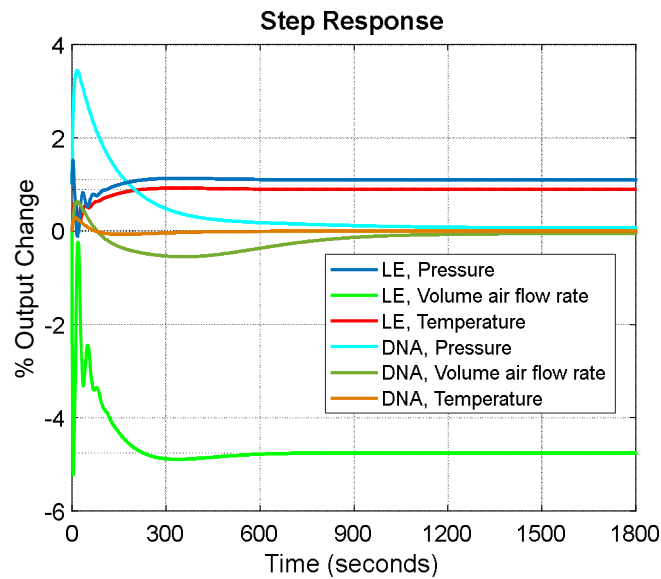


**Figure 6.4.** System responses following unity step change  $\delta_1(t)$  on the Pressure output, while there is no disturbance change at  $\delta_2(t)$  and  $\delta_3(t)$  and no change at all reference inputs  $r_1(t)$ ,  $r_2(t)$  and  $r_3(t)$

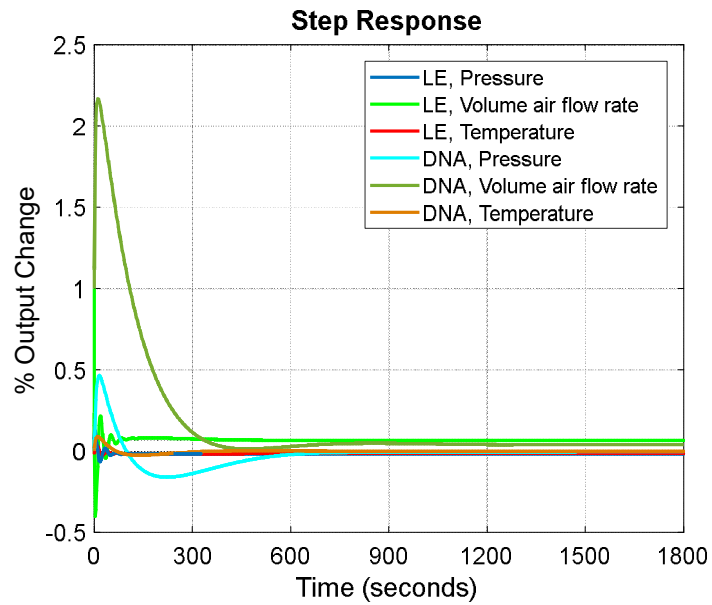


**Figure 6.5.** System responses following unity step change  $\delta_2(t)$  on the Volume Air Flow Rate output, while there is no disturbance change at  $\delta_1(t)$  and  $\delta_3(t)$  and no change at all reference inputs  $r_1(t)$ ,  $r_2(t)$  and  $r_3(t)$

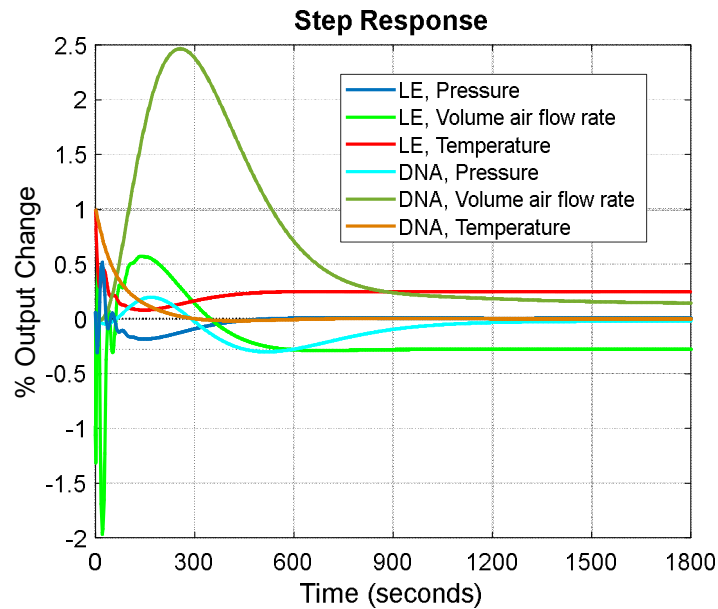


**Figure 6.6.** System responses following unity step change  $\delta_3(t)$  on the Volume Air Flow Rate output, while there is no disturbance change at  $\delta_1(t)$  and  $\delta_2(t)$  and no change at all reference inputs  $r_1(t)$ ,  $r_2(t)$  and  $r_3(t)$

In Figure 6.6, the output responses when step disturbance change  $\delta_3(t)$  is applied on the temperature output at the inlet of the ventilated volume and when there is no disturbance step change at the other outputs and no change at the inputs are shown.

The disturbance recovery performance can be considered as moderate in both control techniques where the influence of the disturbance by  $\delta_3(t)$  is recovered for some of the system outputs to the value of  $\pm 0.25$  while remaining outputs to the zero values. However, the dynamic responses in the LE control technique are better than the dynamic responses in the DNA controller while recovering the influence of the disturbance  $\delta_3(t)$

As an overview, the DNA control technique has showed capability to regulate the performance of the HVAC system, but the system outputs performance in the LE control technique is better than the responses performance of the DNA controller in terms of faster responses and better dynamics with the exception of the disturbance rejection on the pressure output in the LE, where the DNA reacted better than the LE in this case. The DNA control technique design is associated with a big number of decoupling first and second order compensators that makes the control solution complicated. The capability the DNA to regulate and to suppress the disturbance effect would have not been achieved without decoupling the transfer function matrix with the big number of compensators. As a result, the LE controller provided good system performance and good disturbance rejection (apart from the disturbance rejection behaviour at the first output) by using simple passive gains and pre-compensators that are realistic, achievable and simple.

#### **6.4 Control Energy Consumption**

This is the key comparison factor since the study motivation is to find a solution for excess energy consumption caused by HVAC system design and operation, which has to correspond

with the global efforts to reduce the energy consumption inside the buildings and without sacrificing the indoor thermal comfort and air quality.

The control energy costs, under these conditions according to (Whalley and Ebrahimi, 2006), are proportional to

$$E(t) = \int_{t=0}^{t=1800} (u_1^2(t) + u_2^2(t) + u_3^2(t)) dt, \quad (6.1)$$

where  $u_1(t)$ ,  $u_2(t)$ ,  $u_3(t)$  are the control output signals of each system control loop. Those are the voltages on the inlet and exit fans, the voltage on the chilled water pump and the ambient heat transferred into the ventilated volume

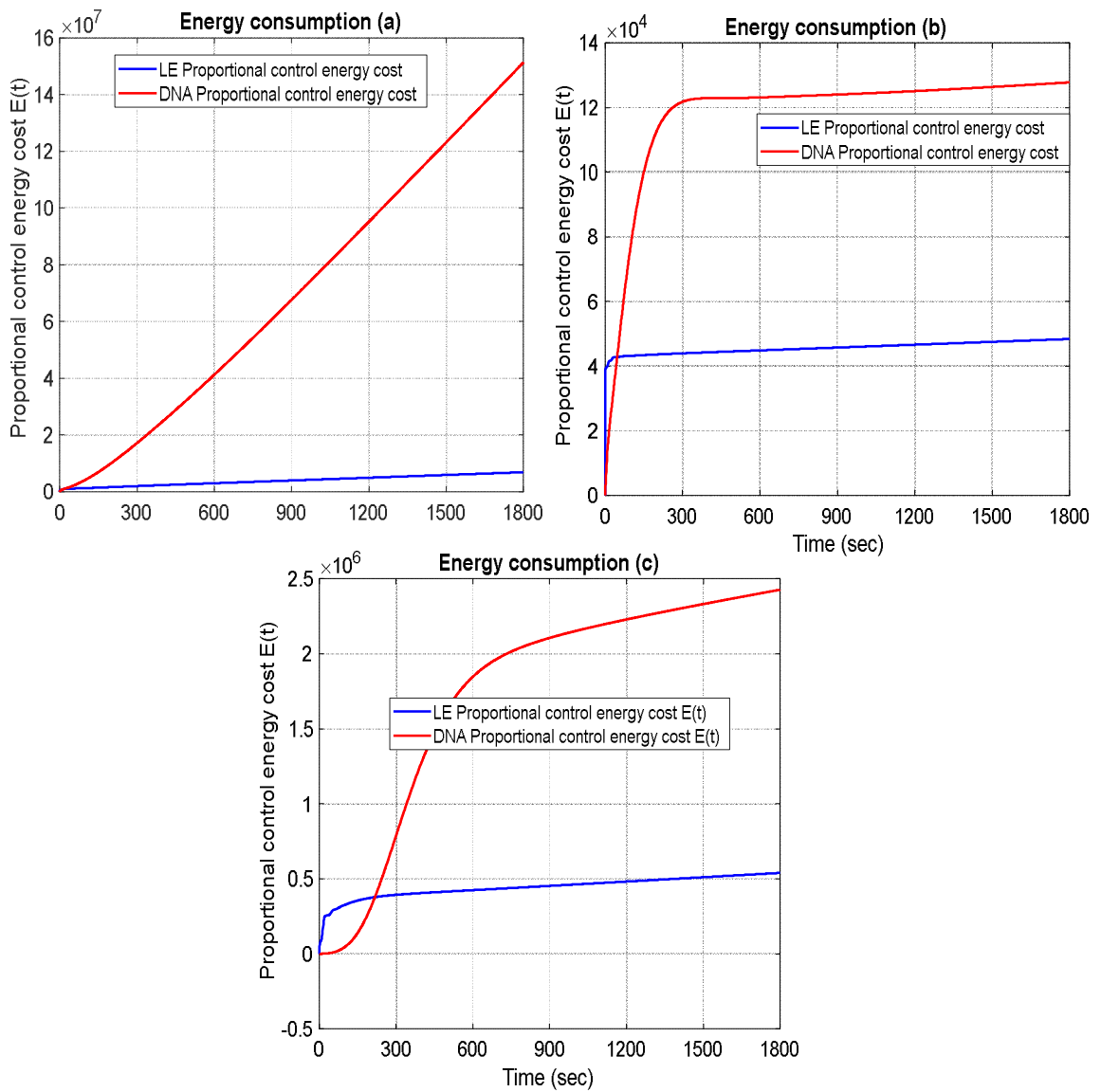
The Equation can be executed, simulated and run by Simulink software for 30 minutes for both controllers and with three different scenarios, a) when  $\delta_1(t)$  is unity step change while the others disturbances are zero, b) when  $\delta_2(t)$  is unity step change while the others disturbances are zero and c) when  $\delta_3(t)$  is unity step change while the others disturbances are zero. The control structure selected for the LE controller in this comparison is when the outer loop gain is equal to 0.8

Figure 6.7 shows the amount the proportional control energy cost to run the HVAC plant under disturbance rejection scenarios in both controllers. The proportional control energy cost to recover the disturbance on the outputs of the system and to run the HVAC plant clearly lower in the LE is clearly than the DNA controller for three conditions. The big difference in the control energy dissipation for both controllers can be recognized from the difference in the control structure and procedure followed in each control technique. In the LE controller, simple passive gains and pre-compensators were used and calculated based on the optimization process, which calculate the gain values that makes the Performance Index representing the control energy Equation minimum and avoiding the utilization of integrators. However, the

individual decoupled loops in the DNA required to have PID controllers have included integrators in order to get well-behaved system. The integrators in these controllers are responsible for the higher energy consumed.

Looking at Figure 6.7 the ratio of the proportional control energy cost in the LE to DNA controller at the time 900 seconds is  $\frac{4.4}{100}$ ,  $\frac{39}{100}$  and  $\frac{22}{100}$  for Figures 6.7 a, 6.7 b and 6.7 c respectively, so that the added value of optimizing the control efforts of a specific control technique can be recognised from the above ratios.

As an overall comparison, both controllers have shown similar performance by showing capability to regulate the HVAC system outputs associated with good decoupling level and zero steady state error. On one hand the, the DNA was able to control the HVAC system in terms of, decoupling the internal loops, zero steady state values and disturbance rejection, but was associated with a high proportional control energy cost and complicated decoupling compensators. On the other hand, LE control technique has shown faster response and better system dynamics behaviour with simple passive forward and feedback gains avoiding employment integrators, but except for the behaviour on suppressing the disturbance effect on the pressure output where the performance was moderate. Most important in the LE control technique is its performance in terms of least proportional control energy cost when recovering the disturbances and running the HVAC plant in comparison with DNA controller as per figures 6.7, which is the crucial aspect of judgment. It is important to mention that the LE controller can be an ideal control strategy solution that achieves least actuator activity, least heat and least wear and maintenance cost minimization without sacrificing the indoor thermal comfort and air quality.



**Figure 6.7.** Proportional control energy cost, **a:** when  $\delta_1(t)$  disturbance is applied. **b:** when  $\delta_2(t)$  disturbance is applied. **c:** when  $\delta_3(t)$  disturbance is applied, and with zero change at all reference inputs  $r_1(t)$ ,  $r_2(t)$  and  $r_3(t)$

# Chapter Seven

## Conclusion and Recommendations for Future Work

### 7.1 Conclusion

HVAC systems are characterized with active designed components, such as fans, heaters, pumps and compressors. They are classified as a building's highest energy consumers. In the current era of climate change caused by global warming, many regions in the world have become hotter than before, which in turn has increased the demand for HVAC systems in buildings to provide acceptable indoor thermal comfort. Further global warming is likely to take place due to the rapidly growing demand for HVAC systems unless governments undertake active steps to mitigate the impacts of HVAC usage. Despite the negative direct and indirect impacts of HVAC system usage on the climate, they provide good filtration, high indoor air quality and thermal comfort that necessitates the need to install HVAC systems as important elements of building services.

This study is motivated by the need to find a solution for excess energy consumption caused by HVAC system design and operation, which must correspond with the global efforts to reduce the energy consumption inside buildings, without sacrificing the indoor thermal comfort and air quality. It concentrates on employing a distinct HVAC system mathematical model and developing an appropriate automatic control strategy to achieve improved HVAC system performance and to fulfil general energy efficiency philosophy. This technical approach has been adopted based on limitations found in the modelling and controlling techniques presented by HVAC related research studies reviewed in chapters 2 and 3. Most research studies in the literature approached each HVAC component separately, thus fragmenting the HVAC system into components, then modelling, and controlling each component individually. Such studies

have neglected the fact that a HVAC plant consists of various components, which have to work together simultaneously and are required to operate under continuous changing dynamics and environmental conditions.

Moreover, the control approach followed in most HVAC system designs was single-variable controllers, such as the proportional-integral-derivative (PID) controller, which measures one controlled variable and applies a corrective control effort in a repetitive manner. The PID controller can be a good solution when it is confined to one specific condition, however, with the variations in the operating condition, which is the nature of HVAC system operation, it has to be tuned repeatedly and it becomes an exhausting process consuming extra efforts.

Consequently, this study has adopted a HVAC system model considering air conditioning function that consists of all the major components, including the chilled water pump, inlet and outlet fans, ventilated volume and ducts networking that work simultaneously as an integral whole so that the resulted mathematical model is a 3 inputs-3 outputs multivariable system model. Another modelling consideration that has been included in the study is the spatial nature of the slender long ventilated volume as a dimensionally dispersed system where the physical properties of the object are distributed and not lumped mass elements. Meanwhile, the fan motors, inlet and exit impedances are of physical properties that can be treated as concentrated lumped mass elements without compromising on the accuracy. The final obtained model based on the aforementioned modelling improvements has been adopted from the HVAC hybrid distributed-lumped parameter model developed by Whalley R. and Abdul-Ameer A. (2011) as a readily derived HVAC system model due to its robustness and accuracy. The four research objectives set in chapter 1, were found to be fulfilled and can be reviewed and explained as follows:

- i. Different nine-time domain responses of the hybrid distributed-lumped parameter HVAC systems mathematical model developed by Whalley R. and Abdul-Ameer A. (2011) have been examined, so that the actual dynamical characteristics of the system were identified and acknowledged. This process was achieved by identifying x-y coordinates of each time domain system response and feeding such coordinates into MATLAB software, so that MATLAB was introduced to the dynamical characteristics of the HVAC open loop system model.
- ii. Necessary frequency domain transfer functions employing MATLAB Tool-Box to handle and process HVAC system time domain mathematical model responses developed in (i) so that  $(3 \times 3)$  transfer function matrix was obtained. Simulating the frequency domain responses gave an approximately 98% fit with the time domain responses so that similar dynamical characteristics were also maintained and acknowledged by the frequency domain representations. The input-output relationship in Laplace (s) variable representation is shown in Equation 4.2 and the open loop system responses are shown in Figure 4.7, 4.8 and 4.9.
- iii. Based on the HVAC open loop transfer function matrix in the frequency domain, designing a controller and enabling system analysis can be a straightforward process. The HVAC system control strategy based on the LE control procedures outlined by Whalley R. and Ebrahimi M. (2004) has and applied so that minimized control system energy dissipation, adequate disturbance suppression, superior system performance in terms of integrity, and closed loop stability have been achieved. The LE controller was the main control technique employed in this study. It employs output feedback, passive compensators and proportional

gains for multivariable process industries. The controller design employs two major control loops. The desired dynamics and transient responses are designed by the inner control loop while the outer loop is configured to improve the system steady state error and disturbance rejection. Good results and well-behaved system performance have been obtained by the LE controller. LE control technique managed to minimize the control system energy dissipation associated with good system performance in terms of integrity and closed loop stability. It has also shown acceptable performance in terms of reducing the coupling between the output signals and adequate disturbance suppression.

- iv. To enable theoretical validation for the performance of the LE controller, a detailed comparison between the LE controller and alternative multi-variable control technique, namely Direct Nyquist Array (DNA) has been explored. The DNA procedure is based on reducing the interactions between system outputs by decoupling them through a decoupling matrix, so that a closed loop control technique can be applied on each loop independently. Contrasting the straightforward procedure used to decouple the interaction between the outputs in the LE controller, the decoupling matrix in the DNA controller was based on a trial and error approach, which was very time consuming. The order of the computed compensators of the decoupling matrix in the DNA control technique were of 9<sup>th</sup> and 11<sup>th</sup> orders that can be very complicated. Although the system under the DNA controller was able to regulate and control the HVAC multivariable system, having high proportional control energy cost makes the solution to contravene with global efforts to minimize energy consumption inside buildings. Moreover, the system responses in the DNA control technique were slower than same responses in the LE controller. With the exception of the LE behaviour in suppressing the disturbance exerted in the pressure output which was not

completely well, the LE control is superior to the DNA control solution when considering the simplicity of each controller, the system behaviour under closed loop control and the control energy dissipated by each controller which is the key judgment.

Minimised control dissipation achieved by the LE controller makes it the ideal solution for HVAC system regulation, especially given the global attention encouraging sustainable technology and least energy consumption. Moreover, using simple gains and pre-compensators calculated based on values that make the Performance Index minimum and based on avoiding employment of the integrators, were the main reasons for achieving minimized control energy dissipation. This would be reflected in lower energy bill values and the operational cost for such a HVAC system under the LE controller, achieving least actuator activity, least heat and wear and achieving maintenance cost minimization.

## **7.2 Recommendations for Future Work**

The selected HVAC mathematical model employed in the study was accurate and close to reality in comparison with the other previous modelling studies. This is evident from the distinctive mathematical modelling approach followed in the study, mainly the hybrid lumped-distributed parameter model. The importance of this model arises also from the integration of the Equations describing the air stream transient temperature variations in the model. However, temperature variations caused by heat that could be transferred through the building envelope to the ventilated volume was integrated in the selected mathematical model as simple first order transfer function which might not represent the actual ambient heat transfer input-output relationship.

Nevertheless, the modelling procedure followed in deriving the mathematical model of the HVAC system, provided a good flexibility and adaptability so that further substantial system complexity and dispersion can be accommodated. Consequently, these modelling features

allow for further model enhancement. Model enhancement can take place by making the model more comprehensive so that major objectives of building energy efficiency, high indoor air quality and thermal comfort can be also enhanced. Such improvement in the comprehensiveness of the mathematical model can be attained by integrating the thermodynamics and fluid mechanics Equations describing the heat transfer from the external environment through a building's envelope to the ventilated volume. Therefore, as recommendations for future work, additional temperature variation from the difference between the indoor and outdoor temperature, which causes heat transfer through the ventilated volume walls and roof, can be integrated in the HVAC hybrid distributed-lumped parameter final model, with the intention of establishing more comprehensiveness in the system mathematical model and replacing the simple first order transfer function of the ambient heat transfer into the ventilated volume..

## References

- Afram, A. and Janabi-Sharifi, F. (2014). Review of modeling methods for HVAC systems. *Applied Thermal Engineering*, 67(1-2), pp.507-519.
- Afram, A. and Janabi-Sharifi, F. (2014). Theory and applications of HVAC control systems – A review of model predictive control (MPC). *Building and Environment*, 72, pp.343-355.
- Agarwal, Y., Balaji, B., Gupta, R., Weng, T. and Dutta, S. (2011). Duty-cycling buildings aggressively: The next frontier in HVAC control. *IEEE*.
- Al-Assadi, S., Patel, R., Zaheer-uddin, M., Verma, M. and Breitingner, J. (2004). Robust decentralized control of HVAC systems using  $\gamma$ -performance measures. *Journal of the Franklin Institute*, 341(7), pp.543-567.
- Alcalá, R., Benítez, J., Casillas, J., Cordón, O. and Pérez, R. (2003). Fuzzy Control of HVAC Systems Optimized by Genetic Algorithms. *Springer Nature Switzerland AG*.
- Allen, M. (2016). How can our homes influence our comfort, health and wellbeing?. [online] Multicomfort.saint-gobain.co.uk. Available at: <https://multicomfort.saint-gobain.co.uk/how-can-a-home-improve-my-comfort-health-and-wellbeing/> [Accessed 14 Oct. 2018].
- Anderson, M., Buehner, M., Young, P., Hittle, D., Anderson, C., Jilin Tu and Hodgson, D. (2008). MIMO Robust Control for HVAC Systems. *IEEE Transactions on Control Systems Technology*, 16(3), pp.475-483.
- Aswani, A., Master, N., Taneja, J., Culler, D. and Tomlin, C. (2012). Reducing Transient and Steady State Electricity Consumption in HVAC Using Learning-Based Model-Predictive Control. *Proceedings of the IEEE*, 100(1), pp.240-253.
- Bahadori, M. (1978). Passive Cooling Systems in Iranian Architecture. *Scientific American*, 238(2), pp.144-154.
- Balan, R., Cooper, J., Chao, K., Stan, S. and Donca, R. (2011). Parameter identification and model based predictive control of temperature inside a house. *Energy and Buildings*, 43(2-3), pp.748-758.
- Bartlett, H. and Whalley, R. (1998). Modelling and analysis of variable geometry exhaust gas systems. *Applied Mathematical Modelling*, 22(8), pp.545-567.
- Belletrutti, J. and MacFarlane, A. (1971). Characteristic loci techniques in multivariable-control-system design. *Proceedings of the Institution of Electrical Engineers*, 118(9), p.1291.
- Bi, Q., Cai, W., Wang, Q., Hang, C., Eng-Lock Lee, Sun, Y., Liu, K., Zhang, Y. and Zou, B. (2000). Advanced controller auto-tuning and its application in HVAC systems. *Control Engineering Practice*, 8(6), pp.633-644.

- Bryson, A. (1996). Optimal control-1950 to 1985. *IEEE Control Systems*, 16(3), pp.26-33.
- Crahmaliuc, R. (2018). *Thermal Comfort in Buildings: How to Better Control and Predict*. [online] SimScale. Available at: <https://www.simscale.com/blog/2016/08/thermal-comfort-in-buildings/> [Accessed 14 Oct. 2018].
- El-Hassan, T. (2012). *A Design Study for Multivariable Feedback Control System Regulation for Aircraft Turbo-Jet Engines*. MSc Systems Engineering. British University in Dubai.
- Ferkl, L. and Siroky, J. (2010). *Ceiling radiant cooling: Comparison of ARMAX and subspace identification modelling methods*. *Building and Environment*, 45(1), pp.205-212.
- Ganji, D., Sabzehmeidani, Y. and Sedighiamiri, A., (2018). *Nonlinear Systems in Heat Transfer. 1st ed. Netherlands: Elsevier Science*.
- García, C., Prett, D. and Morari, M. (1989). Model predictive control: Theory and practice—A survey. *Automatica*, 25(3), pp.335-348.
- Gheji, S., Kamble, K., Gavde, A. and Mane, S. (2016). Basic Classification of HVAC Systems for Selection. *International Journal of Innovative Research in Science, Engineering and Technology*, Volume 5(Issue 4).
- Ghiaus, C. and Hazyuk, I. (2010). Calculation of optimal thermal load of intermittently heated buildings. *Energy and Buildings*, 42(8), pp.1248-1258.
- Hariharan, N. and Rasmussen, B. (2010). Parameter Estimation for Dynamic HVAC Models with Limited Sensor Information. *IEEE*.
- Hawkins, D. (1972). ‘Pseudodiagonalisation’ and the inverse-Nyquist array method. *Proceedings of the Institution of Electrical Engineers*, 119(3), p.337.
- He, X. and Asada, H. (2003). A new feedback linearization approach to advanced control of multi-unit HVAC systems. *IEEE*.
- Hiyama, K. and Kato, S. (2011). Optimization of variables in air conditioning control systems: Applications of simulations integrating CFD analysis and response factor method. *Building Simulation*, 4(4), pp.335-340.
- Homod, R. (2013). Review on the HVAC System Modeling Types and the Shortcomings of Their Application. *Journal of Energy*, 2013, pp.1-10.
- Homod, R., Mohamed Sahari, K., Almurib, H. and Nagi, F. (2012). RLF and TS fuzzy model identification of indoor thermal comfort based on PMV/PPD. *Building and Environment*, 49, pp.141-153.

- Hong, T. and Jiang, Y. (1995). Stochastic weather model for building HVAC systems. *Building and Environment*, 30(4), pp.521-532.
- House, J. and Smith, T. (1995). Optimal control of building and HVAC systems. *IEEE*.
- Hughes, A. (2017). What is data mining? - Definition from WhatIs.com. [online] SearchSQLServer. Available at: <https://searchsqlserver.techtarget.com/definition/data-mining> [Accessed 15 Oct. 2018].
- Jetté, I., Zaheer-uddin, M. and Fazio, P. (1998). PI-control of dual duct systems: manual tuning and control loop interaction. *Energy Conversion and Management*, 39(14), pp.1471-1482.
- Jin, G., Tan, P., Ding, X. and Koh, T. (2011). Cooling Coil Unit dynamic control of in HVAC system. *IEEE*.
- Kalman, R. (1959). On the general theory of control systems. *IRE Transactions on Automatic Control*, 4(3), pp.110-110.
- Kim, T., Kato, S. and Murakami, S. (2001). Indoor cooling/heating load analysis based on coupled simulation of convection, radiation and HVAC control. *Building and Environment*, 36(7), pp.901-908.
- Kusiak, A. and Xu, G. (2012). Modeling and optimization of HVAC systems using a dynamic neural network. *Energy*, 42(1), pp.241-250.
- Kusiak, A., Li, M. and Zhang, Z. (2010). A data-driven approach for steam load prediction in buildings. *Applied Energy*, 87(3), pp.925-933.
- Layton, J. and Macfarlane, A. (1970). Commutative controller: a critical survey. *Electronics Letters*, 6(12), p.362.
- Li, J., Poulton, G., Platt, G., Wall, J. and James, G. (2010). Dynamic zone modelling for HVAC system control. *International Journal of Modelling, Identification and Control*, 9(1/2), p.5.
- Lienhard, J., (2017). A Heat Transfer textbook. 4th ed. U.S.A: Phlogiston Press.
- Lim, D., Rasmussen, B. and Swaroop, D. (2009). Selecting PID Control Gains for Nonlinear HVAC&R Systems. *HVAC&R Research*, 15(6), pp.991-1019.
- Liu, S. and He, X. (1994). A distributed parameter model approach to optimal comfort control in air conditioning systems. *IEEE*.
- Lopes dos Santos, P., A. Ramos, J. and Martins de Carvalho, J. (2012). Identification of a Benchmark Wiener–Hammerstein: A bilinear and Hammerstein–Bilinear model approach. *Control Engineering Practice*, 20(11), pp.1156-1164.

- Lü, X. (2002). Modelling of heat and moisture transfer in buildings. *Energy and Buildings*, 34(10), pp.1033-1043.
- Ma, Y., Matusko, J. and Borrelli, F. (2015). Stochastic Model Predictive Control for Building HVAC Systems: Complexity and Conservatism. *IEEE Transactions on Control Systems Technology*, 23(1), pp.101-116.
- MacFarlane, A. (1970). Commutative controller: a new technique for the design of multivariable control systems. *Electronics Letters*, 6(5), p.121.
- MacFarlane, A. (1970). Return-difference and return-ratio matrices and their use in analysis and design of multivariable feedback control systems. *Proceedings of the Institution of Electrical Engineers*, 117(10), p.2037.
- MathWorks (2018). *Time-Delay Approximation- MATLAB & Simulink*. [online] Mathworks.com. Available at: <https://www.mathworks.com/help/control/ug/time-delay-approximation.html> [Accessed 15 Oct. 2018].
- Matlabtips.com. (2015). *What is Matlab – Where and Why to Use It*. [ONLINE] Available at: <http://www.matlabtips.com/what-is-matlab-where-how-and-when-to-use-it/>. [Accessed 5 September 2019].
- Mirinejad, H., Conn Welch, K. and Spicer, L. (2012). A review of intelligent control techniques in HVAC systems. *IEEE*.
- Miskovic, N. and Vukic, P. Z. (2009) ‘Lecture : Feedback Linearization’, (June), pp. 1–16.
- Moradi, H., Saffar-Avval, M. and Bakhtiari-Nejad, F. (2011). Nonlinear multivariable control and performance analysis of an air-handling unit. *Energy and Buildings*, 43(4), pp.805-813.
- Mudi, R. and Pal, N. (2000). A self-tuning fuzzy PI controller. *Fuzzy Sets and Systems*, 115(2), pp.327-338.
- Mustafaraj, G., Chen, J. and Lowry, G. (2010). Development of room temperature and relative humidity linear parametric models for an open office using BMS data. *Energy and Buildings*, 42(3), pp.348-356.
- Nejat, P., Jomehzadeh, F., Taheri, M., Gohari, M. and Abd. Majid, M. (2015). A global review of energy consumption, CO<sub>2</sub> emissions and policy in the residential sector (with an overview of the top ten CO<sub>2</sub> emitting countries). *Renewable and Sustainable Energy Reviews*, 43, pp.843-862.

- Nicol, J. and Humphreys, M. (2002). Adaptive thermal comfort and sustainable thermal standards for buildings. *Energy and Buildings*, 34(6), pp.563-572.
- Noh, K., Jang, J. and Oh, M. (2007). Thermal comfort and indoor air quality in the lecture room with 4-way cassette air-conditioner and mixing ventilation system. *Building and Environment*, 42(2), pp.689-698.
- Palermo, E. (2014). *Who Invented Air Conditioning?*. [online] Live Science. Available at: <https://www.livescience.com/45268-who-invented-air-conditioning.html> [Accessed 14 Oct. 2018].
- Pérez-Lombard, L., Ortiz, J. and Pout, C. (2008). A review on buildings energy consumption information. *Energy and Buildings*, 40(3), pp.394-398.
- Piper, J. (2004). *Closing Gaps in HVAC Design - Facilities Management Insights*. [online] Facilitiesnet. Available at: <https://www.facilitiesnet.com/hvac/article/Closing-Gaps-in-HVAC-Design-Facilities-Management-HVAC-Feature--1527> [Accessed 15 Oct. 2018].
- Pita, E. (2008). *Air conditioning principles and systems*. New Delhi: PHI Learning Private Limited.
- Qin, S. and Badgwell, T. (2003). A survey of industrial model predictive control technology. *Control Engineering Practice*, 11(7), pp.733-764.
- Rasmussen, B. and Alleyne, A. (2010). Gain Scheduled Control of an Air Conditioning System Using the Youla Parameterization. *IEEE Transactions on Control Systems Technology*, 18(5), pp.1216-1225.
- Satyavada, H. and Baldi, S. (2016). An integrated control-oriented modelling for HVAC performance benchmarking. *Journal of Building Engineering*, 6, pp.262-273.
- Semsar-Kazerooni, E., Yazdanpanah, M. and Lucas, C. (2008). Nonlinear Control and Disturbance Decoupling of HVAC Systems Using Feedback Linearization and Backstepping With Load Estimation. *IEEE Transactions on Control Systems Technology*, 16(5), pp.918-929.
- Tahersima, F., Stoustrup, J., Rasmussen, H. and Nielsen, P. (2010). Thermal analysis of a HVAC system with TRV controlled hydronic radiator. *IEEE*.
- Tashtoush, B., Molhim, M. and Al-Rousan, M. (2005). Dynamic model of a HVAC system for control analysis. *Energy*, 30(10), pp.1729-1745.
- Thosar, A., Patra, A. and Bhattacharyya, S. (2008). Feedback linearization based control of a variable air volume air conditioning system for cooling applications. *ISA Transactions*, 47(3), pp.339-349.

- VanDoren, V. (2018). Multivariable controllers balance competing objectives, *Control Engineering*. [online] Controleng.com. Available at: <https://www.controleng.com/single-article/multivariable-controllers-balance-competing-objectives/4648178963a5022682456c951c55f6d8.html> [Accessed 15 Oct. 2018].
- Vhora, H. and Patel, J., 2016. Design of Static and Dynamic Decoupler for Coupled Quadruple Tank Level System. *NIRMA UNIVERISTY JOURNAL OF ENGINEERING AND TECHNOLOGY*, VOL. 5, NO. 2, 2.
- Virk, G. and Loveday, D. (1994). Model-based control for HVAC applications. *IEEE*.
- Wang, J., Zhang, C. and Jing, Y. (2007). Hybrid CMAC-PID Controller in Heating Ventilating and Air-Conditioning System. *IEEE*.
- Wang, Q., Zou, B., Lee, T. and Bi, Q. (1997). Auto-tuning of multivariable PID controllers from decentralized relay feedback. *Automatica*, 33(3), pp.319-330.
- Watson, I. (2001). A Case Study of Maintenance of a Commercially Fielded Case-Based Reasoning System. *Computational Intelligence*, 17(2), pp.387-398.
- Whalley, R. (1988). The Response of Distributed—Lumped Parameter Systems. *Proceedings of the Institution of Mechanical Engineers, Part C: Journal of Mechanical Engineering Science*, 202(6), 421–429.
- Whalley, R. (1990) ‘Interconnected spatially distributed systems’, *IMechE 1990*, (1), pp. 262–270.
- Whalley, R. and Abdul-Ameer, A. (2010). Ventilation system airflow dynamics. *Proceedings of the Institution of Mechanical Engineers, Part I: Journal of Systems and Control Engineering*, 224(3), pp.305-320.
- Whalley, R. and Abdul-Ameer, A. (2011). Heating, ventilation and air conditioning system modelling. *Building and Environment*, 46(3), pp.643-656.
- Whalley, R. and Abdul-Ameer, A. (2014). Ventilation system modeling and turbulence minimization. *International Journal of Modeling, Simulation, and Scientific Computing*, 05(01), p.1350017.
- Bartlett, H., and Whalley, R. (1998). Analogue solution to the modelling and simulation of distributed-lumped parameter systems. *Proceedings of the Institution of Mechanical Engineers, Part I: Journal of Systems and Control Engineering*, 212(2), 99–114.
- Whalley, R. and Ebrahimi, M. (1999). Multivariable system regulation with minimum control effort. *Proceedings of the Institution of Mechanical Engineers, Part I: Journal of Systems and Control Engineering*, 213(6), pp.505-514.

- Whalley, R. and Ebrahimi, M. (2000). Process system regulation with minimum control effort. *Proceedings of the Institution of Mechanical Engineers, Part E: Journal of Process Mechanical Engineering*, 214(4), pp.245-256.
- Whalley, R. and Ebrahimi, M. (2004). Automotive Gas Turbine Regulation. *IEEE Transactions on Control Systems Technology*, 12(3), pp.465-473.
- Whalley, R. and Ebrahimi, M. (2006). Multivariable System Regulation. *SAGE Journals*.
- Wu, S. and Sun, J. (2012). A physics-based linear parametric model of room temperature in office buildings. *Building and Environment*, 50, pp.1-9.
- Xi, X., Poo, A. and Chou, S. (2007). Support vector regression model predictive control on a HVAC plant. *Control Engineering Practice*, 15(8), pp.897-908.
- Yang, R. and Wang, L. (2012). Optimal Control Strategy for HVAC System in Building Energy Management. *IEEE*.
- Yiu, J. and Wang, S. (2007). Multiple ARMAX modeling scheme for forecasting air conditioning system performance. *Energy Conversion and Management*, 48(8), pp.2276-2285.
- Yiu, J. and Wang, S. (2007). Multiple ARMAX modeling scheme for forecasting air conditioning system performance. *Energy Conversion and Management*, 48(8), pp.2276-2285.
- Zlatanović, I., Gligorević, K., Ivanović, S. and Rudonja, N. (2011). Energy-saving estimation model for hypermarket HVAC systems applications. *Energy and Buildings*, 43(12), pp.3353-3359.

## Appendix

### 8.1 Performance Index Equation

$$\begin{aligned} J(n_1, n_2) = & (1.3318628564369766600231966788422e74 * n_1^6 + \\ & 5.9609519461060418074441522713909e74 * n_1^5 * n_2 - \\ & 4.7015915278917765097154074186046e74 * n_1^5 + \\ & 5.9426007634729908576845414109705e74 * n_1^4 * n_2^2 - \\ & 3.2602639780975353696992166404717e75 * n_1^4 * n_2 - \\ & 2.7893353953188743972285294278074e73 * n_1^4 + \\ & 1.0476889425673104339047601376401e74 * n_1^3 * n_2^3 - \\ & 4.7653734104919980543508941680539e75 * n_1^3 * n_2^2 + \\ & 3.2285589334792119544906640912491e75 * n_1^3 * n_2 - \\ & 3.0259298071190453035801094374429e75 * n_1^3 + \\ & 5.5015917648212160827302915952208e74 * n_1^2 * n_2^4 - \\ & 1.5492622575510659086960630962302e75 * n_1^2 * n_2^3 + \\ & 9.0247412518043834754730521563045e75 * n_1^2 * n_2^2 + \\ & 2.626275118959780926817117287568e75 * n_1^2 * n_2 + \\ & 1.4927408005906085739882101259053e76 * n_1^2 - \\ & 4.9132630035387313735393921337508e74 * n_1 * n_2^5 - \\ & 4.2952142577028204033793534261934e75 * n_1 * n_2^4 + \\ & 2.1411374385147346363923096507351e75 * n_1 * n_2^3 - \\ & 6.8509849120326880559879221217753e75 * n_1 * n_2^2 + \\ & 2.6324637388686077737462488640884e75 * n_1 * n_2 - \\ & 2.5557706543298676526085686956236e75 * n_1 + \\ & 8.9085385778520188506894686309247e73 * n_2^6 + \end{aligned}$$

1.7110017205464694610031535442415e75\*n2^5+  
 8.8138324864761886541884173315632e75\*n2^4+  
 7.5975408176037857575194874722844e75\*n2^3+  
 2.3813234746200640615538228866479e76\*n2^2+  
 5.8865390970573162965163339280335e75\*n2+  
 1.5088487645502972149856706221226e76) / (-  
 3.8621676118038409267902074427861e34\*n1^3+  
 8.5686784049303800605742195030733e33\*n1^2\*n2-  
 4.6372726326283271489582066825713e35\*n1^2+  
 830071357387678100170459246343699.0\*n1\*n2^2+  
 1.1263437460032191514508929409445e35\*n1\*n2+  
 3.8594807294670045551070064077302e36\*n1+  
 111790015733316707803254166798844.0\*n2^3+  
 1.2614385821302693411519434889755e34\*n2^2+  
 6.9179091021217221137436899327834e35\*n2-  
 2.5233752832330744631027704553201e35)^2

## 8.2 Partial differential Equation of ( $J$ ) in respect to ( $n_1$ ).

$$\frac{\partial J}{\partial n_1} = (3.0318229438852237495217621453702e112*n1-  
 n2^7*(2.5225355902166563540289676949654e108*n1+  
 2.9586602053980958486098381811377e109) -  
 n2^5*(1.0395480528089414033536609559595e110*n1^3+  
 1.7425412494569258595266811450655e110*n1^2-  
 5.9740588629318580643197149387542e111*n1+$$

1.8026417213625267169436075842389e112)+  
 n2^3\*(1.3712788927458957293278614923107e109\*n1^5+  
 1.5866523277434202499501942341284e109\*n1^4+  
 1.721271806688663846319575927242e110\*n1^3-  
 4.9326717032150079583353516758944e111\*n1^2+  
 1.9120285140559929363686639141294e112\*n1-  
 6.9266092068015990257836433488032e112)+  
 n2^2\*(5.1452604902113730639625485961981e109\*n1^6-  
 3.4180811476207126413851614226527e110\*n1^5+  
 5.0415055534799253565763492104572e111\*n1^4-  
 2.0651592603995493499529842838188e112\*n1^3+  
 6.1130066562884448858608075857566e111\*n1^2+  
 6.9572189957738347217148272219597e112\*n1-  
 1.8164690795263681134317297728354e113)+  
 n2^6\*(3.3308949026192748219797182106772e109\*n1^2+  
 1.7904021562103500915666059516948e110\*n1-  
 1.4815512972148616222819773764225e111)+  
 2.2315814497790190646168044926417e111\*n1^2+  
 1.70058777283249391125852180579e111\*n1^3+  
 1.2807661894048658070498819819473e111\*n1^4-  
 5.9959574015718592896588631393842e111\*n1^5+  
 2.2719906525410020679803331139472e111\*n1^6-  
 1.4168255801434260383497733283123e110\*n1^7-  
 2.6637257128739533200463933576844e76\*n1^8-  
 2.0281982903991418324031506943523e107\*n2^8-

$n^2 \cdot 4 \cdot (-8.5414291140461037696809374085941e109 \cdot n^1 +$   
 $2.5627196836900708020940923555681e110 \cdot n^1^3 +$   
 $3.9498536192685818693925019277336e111 \cdot n^1^2 -$   
 $3.0237359532742087754184449438953e112 \cdot n^1 +$   
 $6.7305718670658080065461586854541e112) +$   
 $n^2 \cdot (2.5304656441025911964800715504471e109 \cdot n^1^7 -$   
 $4.7228253870779621898647957346527e110 \cdot n^1^6 +$   
 $7.6698849461813460822212462991362e111 \cdot n^1^5 -$   
 $2.562165696930855148500369153687e112 \cdot n^1^4 +$   
 $1.8021584856392946849004515133015e112 \cdot n^1^3 -$   
 $3.6319695654659225744482366396496e111 \cdot n^1^2 +$   
 $1.9857640425954002286033883956507e112 \cdot n^1 -$   
 $5.1269261456444704046886456027405e112) -$   
 $1.1582253775936455298581012749034e113) / (-$   
 $3.8621676118038409267902074427861e34 \cdot n^1^3 +$   
 $8.5686784049303800605742195030733e33 \cdot n^1^2 \cdot n^2 -$   
 $4.6372726326283271489582066825713e35 \cdot n^1^2 +$   
 $830071357387678100170459246343699.0 \cdot n^1 \cdot n^2^2 +$   
 $1.1263437460032191514508929409445e35 \cdot n^1 \cdot n^2 +$   
 $3.8594807294670045551070064077302e36 \cdot n^1 +$   
 $111790015733316707803254166798844.0 \cdot n^2^3 +$   
 $1.2614385821302693411519434889755e34 \cdot n^2^2 +$   
 $6.9179091021217221137436899327834e35 \cdot n^2 -$   
 $2.5233752832330744631027704553201e35) ^3$

### 8.3 Partial differential Equation of ( $J$ ) in respect to ( $n_2$ ).

$$\frac{\partial J}{\partial n_2} = (2.2191867890352990519342214412922e112*n1+n2^7*(2.0281982903991418324031506943523e107*n1+2.0562419452400695652034644944976e108)+n2^5*(-3.3308949026192748219797182106772e109*n1^3-3.6938597792049056896379977692902e110*n1^2+1.6206895253747034408650846629028e111*n1+3.4135408089292204933306008187375e111))-n2^3*(8.5414291140461037696809374085941e109*n1^5+3.6367521957415250716120134100556e110*n1^4-1.5118689093124851808410070611696e112*n1^3+8.4196623991720747382914410912819e112*n1^2-1.4287144236070167800098422141331e113*n1+4.2444020841630623064685281679618e111)+n2^2*(-1.3712788927458957293278614923106e109*n1^6+1.9628723091495305341822705425741e109*n1^5+3.2356406649813115163508696529458e111*n1^4-2.2003044790256977938739486718781e112*n1^3+1.5278332290851395019700024095515e112*n1^2+8.6234253919102573126460910566738e112*n1-5.98431969334382680691484795929e111))+n2^4*(1.0395480528089414033536609559595e110*n1^4+8.612185696023243969295163548895e110*n1^3-1.3490123992164548987051866143388e112*n1^2+$$

2.9650239674014301932522596723372e112\*n1+  
 9.9294220322417331917467695221247e111)+  
 n2^6\*(2.5225355902166563540289676949654e108\*n1^2+  
 3.6319104995510917760924439989051e109\*n1+  
 2.6612647935651784743987667224891e110)-  
 1.3568645247585349686055895585855e112\*n1^2+  
 8.7410205131960952817234222251167e111\*n1^3+  
 1.2428126249236017138395058511213e112\*n1^4-  
 1.3623301533795271362493010148753e112\*n1^5+  
 3.6099149102351511182434238507365e111\*n1^6-  
 1.7245415663837612487421796097298e110\*n1^7-  
 2.5304656441025911964800715504471e109\*n1^8-  
 2.2358003146663341560650833359767e73\*n2^8-  
 n2\*(5.1452604902113730639625485961981e109\*n1^7+  
 2.274196269507352976947291208743e110\*n1^6-  
 8.26063226214061947649259169192e111\*n1^5+  
 4.3043761072220744996477858101821e112\*n1^4-  
 7.4132422298763915353583683368858e112\*n1^3+  
 8.24312361206443363040551302666e112\*n1^2-  
 1.8486568110400089045780884930602e113\*n1+  
 1.6851527852912099707136787444481e112)-  
 2.2361551930145189794242729530769e112)/(-  
 3.8621676118038409267902074427861e34\*n1^3+  
 8.5686784049303800605742195030733e33\*n1^2\*n2-  
 4.6372726326283271489582066825713e35\*n1^2+

```

830071357387678100170459246343699.0*n1*n2^2+
1.1263437460032191514508929409445e35*n1*n2+
3.8594807294670045551070064077302e36*n1+
111790015733316707803254166798844.0*n2^3+
1.2614385821302693411519434889755e34*n2^2+
6.9179091021217221137436899327834e35*n2-
2.5233752832330744631027704553201e35)^3

```

#### 8.4 Script file to find list of roots pairs

```

%-----Computing & differentiating J-----%
J=simplify(vpa((1+(n1*n1)+(n2*n2))*(transpose(b))*(transpose(inv(Q))
)*(inv(Q))*b)), 'Steps', 50);
dJ_dn1=simplify(vpa(diff(J,n1)), 'Steps', 50);%first      partial
derivative in respect to n1;
dJ_dn2=simplify(vpa(diff(J,n2)), 'Steps', 50);%first      partial
derivative in respect to n2;
% The above equations are the system of equations for which we need
to find
% the roots of n1 & n2 %
dJ2_dn1dn1=simplify(vpa(diff(dJ_dn1,n1)), 'Steps', 50);%      second
partial derivative in respect to n1;      df1/dx
dJ2_dn1dn2=simplify(vpa(diff(dJ_dn1,n2)), 'Steps', 50);%      second  mix
partial derivative in respect to n1 and then n2% df1/dy
dJ2_dn2dn1=simplify(vpa(diff(dJ_dn2,n1)), 'Steps', 50);%      second  mix
partial derivative in respect to n2 and then n1% df2/dx
dJ2_dn2dn2=simplify(vpa(diff(dJ_dn2,n2)), 'Steps', 50);%      second
partial derivative in respect to n2%      df2/dy%
eqns=[dJ_dn1==0,dJ_dn2==0]
vars=[n1 n2];
[soln1, soln2]=solve(eqns, vars)
%-----%

```

#### 8.5 List of roots pairs

```

[-1.707224297e62,      128.3006638]

[3.217531148,      1.064370365]

[655360.0,      6.253705797]

[4.312422106e93,      502.834547]

[8.806856763e57,      102.2124131]

```

[8.367005307e52, 84.65391354]  
 [-3.461022444, 0.9162545417]  
 [3.633893826, -1.77785253]  
 [Inf, -2.997426291e29]  
 [1.005398901e62, -121.5049929]  
 [0, -5.944045915]  
 [-4.382909873e34, -32.84011291]  
 [-34359738377.0, -8.86542806]  
 [Inf, 4.753065613e28]  
 [4.813641995, -2.349099765]  
 [Inf, 2.894534321e34]  
 [8589934592.0i, - 2.87929908 - 7.642566902i]  
 [-8589934592.0i, - 2.87929908 + 7.642566902i]  
 [2.857242982e30 + 5.099926106e30i, 9.886427517 + 24.35636159i]  
 [2.857242982e30 - 5.099926106e30i, 9.886427517 - 24.35636159i]  
 [45056.0 + 2048.0i, - 5.331286928 + 0.6124005219i]  
 [45056.0 - 2048.0i, - 5.331286928 - 0.6124005219i]  
 [-1.414297864e160-7.053855162e158i,-40.86835261- 8562.863908i]  
 [-1.414297864e160+7.053855162e158i,-40.86835261+ 8562.863908i]  
 [1.809289561 - 0.03652238823i, - 0.03197099192 - 2.067174379i]  
 [1.809289561 + 0.03652238823i, - 0.03197099192 + 2.067174379i]  
 [0.1368925591 + 1.480532329i, 0.04308054658 - 1.085556776i]  
 [0.1368925591 - 1.480532329i, 0.04308054658 + 1.085556776i]  
 [- 0.6543769215 + 0.01900614236i, 0.01040793377 + 1.194971233i]  
 [- 0.6543769215 - 0.01900614236i, 0.01040793377 - 1.194971233i]

[Inf - Inf\*1i, - 2.873461635e28 + 4.4024589e28i]  
 [Inf + Inf\*1i, - 2.873461635e28 - 4.4024589e28i]  
 [5.961987685e22 - 3.073227563e23i, 1.444724298 - 17.47140123i]  
 [5.961987685e22 + 3.073227563e23i, 1.444724298 + 17.47140123i]  
 [1048576.0-0.0009765625i, 6.253705794 + 0.000000001507007685i]  
 [1048576.0+0.0009765625i, 6.253705794 - 0.000000001507007685i]  
 [3.20703125 - 1.028808594i, - 1.066686021 - 3.217881891i]  
 [3.20703125 + 1.028808594i, - 1.066686021 + 3.217881891i]  
 [-7.461869654e54-1.585115147e48i, 84.65391282+ 0.0000004200678616i]  
 [-7.461869654e54+1.585115147e48i, 84.65391282 - 0.0000004200678616i]  
 [4.813816577-0.00000000600240635i,-2.349099765+0.000000002140993478i]  
 [4.813816577+0.00000000600240635i, - 2.349099765 - 0.000000002140993478i]  
 [0.07354725222-0.2660041202i, - 0.1142579213 + 1.442152834i]  
 [0.07354725222+0.2660041202i, - 0.1142579213 - 1.442152834i]  
 [4.813815124+3.364627095e-15i,-2.349099765 - 8.764022543e-18i]  
 [4.813815124 -3.364627095e-15i, -2.349099765+8.764022543e-18i]  
 [0.8635565466-1.550086864i, - 1.306457357 - 1.024593293i]  
 [0.8635565466 + 1.550086864i, - 1.306457357 + 1.024593293i]  
 [Inf - Inf\*1i, 1.703883414e32 - 1.233607613e33i]  
 [Inf + Inf\*1i, 1.703883414e32 + 1.233607613e33i]  
 [-4.752490085e54 + 5.778183829e40i, 84.65391306 - 2.005075598e-14i]  
 [-4.752490085e54-5.778183829e40i, 84.65391306 + 2.005075598e-14i]  
 [- 98304.0 + 147456.0i, - 1.68973715 - 5.341709484i]  
 [- 98304.0 - 147456.0i, - 1.68973715 + 5.341709484i]  
 [5505024.0 - 0.000000002444721758i, 6.253705795 - 8.884358524e-17i]

```

[5505024.0 + 0.000000002444721758i, 6.253705795 + 8.884358524e-17i]
[1.260728547 + 0.7630078557i, - 0.7322523701 + 1.762603129i]
[1.260728547 - 0.7630078557i, - 0.7322523701 - 1.762603129i]
[- 0.1788647159 - 0.7021875341i, - 0.105043051 - 0.8995697895i]
[- 0.1788647159 + 0.7021875341i, - 0.105043051 + 0.8995697895i]
[1.89969641 - 1.384419304i, - 0.4636379537 + 0.07363292789i]
[1.89969641 + 1.384419304i, - 0.4636379537 - 0.07363292789i]
[0.0577691304 - 0.1808459717i, 0.01060357259 + 0.9852636412i]
[0.0577691304 + 0.1808459717i, 0.01060357259 - 0.9852636412i]

```

### 8.6 Script file : roots making $J(n_1, n_2)$ only local minimum:

```

%-----%
for j=1:length(soln1)
    aa=isreal(soln1(j,1));bb=isreal(soln2(j,1));
    if (aa==1 && bb==1);
        roots_real{j}=[soln1(j,1) soln2(j,1)];

J_at_n1_n2{j}=subs(subs(J,n1,soln1(j,1)),n2,soln2(j,1));%value of J
at pairs of roots%
    else
        roots_complex{j}=[soln1(j,1) soln2(j,1)];
    end
end
Roots_Real_vec=vertcat(roots_real{:});
Real_roots_num=vpa(Roots_Real_vec,numeric)
Roots_complex_vec=vertcat(roots_complex{:});
Complex_roots_num=vpa(Roots_complex_vec,numeric)
J_vec=vertcat(J_at_n1_n2{:});
J_vec_num=vpa(J_vec,numeric)
%=====segregating true from false real roots=====
for c=1:length(Real_roots_num)
    J_value(c)=isnan(J_vec_num(c,1));
    if J_value(c)==1;
        false_roots_real{c}=[Roots_Real_vec(c,1)
Roots_Real_vec(c,2)];
    else
        true_roots_real{c}=[Roots_Real_vec(c,1)
Roots_Real_vec(c,2)];
    end
end
true_roots=vertcat(true_roots_real{:});
true_roots_num=vpa(true_roots,numeric)

```

```

>false_roots=vertcat(false_roots_real{:});%
>false_roots_num=vpa(false_roots,numeric)%
%=====
for i=1:length(true_roots_num)
    root{i}=[true_roots_num(i,1) true_roots_num(i,2)];
    dJ_dn1_at_n1{i}=subs(dJ_dn1,n1,true_roots_num(i,1));
dJ_dn1_at_n1_n2{i}=subs(dJ_dn1_at_n1{i},n2,true_roots_num(i,2));%To
prove that pairs of roots make dJ_dn1=0%
dJ_dn2_at_n1{i}=subs(dJ_dn1,n1,true_roots_num(i,1));
dJ_dn2_at_n1_n2{i}=subs(dJ_dn2_at_n1{i},n2,true_roots_num(i,2));%To
prove that pairs of roots make dJ_dn2=0%
dJ2_dn1dn1_at_n1{i}=subs(dJ2_dn1dn1,n1,true_roots_num(i,1));
dJ2_dn1dn1_at_n1_n2{i}=subs(dJ2_dn1dn1_at_n1{i},n2,true_roots_num(i,
2));% A required condition for local minimum%
dJ2_dn2dn2_at_n1{i}=subs(dJ2_dn2dn2,n1,true_roots_num(i,1));
dJ2_dn2dn2_at_n1_n2{i}=subs(dJ2_dn2dn2_at_n1{i},n2,true_roots_num(i,
2));%second derivative in respect to n2%
dJ2_dn1dn2_at_n1{i}=subs(dJ2_dn1dn2,n1,true_roots_num(i,1));
dJ2_dn1dn2_at_n1_n2{i}=subs(dJ2_dn1dn2_at_n1{i},n2,true_roots_num(i,2))
;%mixed derivative in respect to n1 & n2%
D{i}=(dJ2_dn1dn1_at_n1_n2{i}*dJ2_dn2dn2_at_n1_n2{i})-
((dJ2_dn1dn2_at_n1_n2{i})^2);% should be positive if
dJ2_dn1dn1_at_n1_n2{i,j} to prove that pairs of roots is making J
local minimum%
    end
dJ_dn1_vec=vertcat(dJ_dn1_at_n1_n2{:});
dJ_dn1_num=vpa(dJ_dn1_vec, numeric)
dJ_dn2_vec=vertcat(dJ_dn2_at_n1_n2{:});
dJ_dn2_num=vpa(dJ_dn2_vec, numeric)
dJ2_dn1dn1_at_n1_n2_vec=vertcat(dJ2_dn1dn1_at_n1_n2{:});
dJ2_dn1dn1_at_n1_n2_num=vpa(dJ2_dn1dn1_at_n1_n2_vec,numeric)
D_vec=vertcat(D{:});
D_vec_num=vpa(D_vec,numeric)
ROOTS_vec_num=true_roots_num
for k=1:length(true_roots_num);
if(D_vec_num(k,1))>0 && dJ_dn1_num(k,1)<1e-5 && dJ_dn2_num(k,1)<1e-5
&& dJ2_dn1dn1_at_n1_n2_num(k,1)>0;
Data_Mat_yes{k}=[J_vec_num(k,1) D_vec_num(k,1) dJ_dn1_num(k,1)
dJ_dn2_num(k,1) dJ2_dn1dn1_at_n1_n2_num(k,1) k ROOTS_vec_num((k),1)
ROOTS_vec_num(k,2)];
    else
Data_Mat_no{k}=[J_vec_num(k,1) D_vec_num(k,1) dJ_dn1_num(k,1)
dJ_dn2_num(k,1) dJ2_dn1dn1_at_n1_n2_num(k,1) k ROOTS_vec_num((k),1)
ROOTS_vec_num(k,2)];
    end
end
end
Data_Mat_yes=vertcat(Data_Mat_yes{:})
Data_Mat_no=vertcat(Data_Mat_no{:})
[Aa,Bb]=size(Data_Mat_yes)
J_min=Data_Mat_yes(1,1)
for p=1:Aa
if Data_Mat_yes(p,1)<=J_min
J_min=Data_Mat_yes(p,1);

```

```

Final_Data=[Data_Mat_yes(p,1) Data_Mat_yes(p,2) Data_Mat_yes(p,3)
Data_Mat_yes(1,4) Data_Mat_yes(1,5) Data_Mat_yes(1,6)
Data_Mat_yes(1,7) Data_Mat_yes(1,8)]
else
    'not minimum'
end
end
J_min
n1=Final_Data(1,7)
n2=Final_Data(1,8)

```

### 8.7 Script file : Proper compensators to decouple $G(s)$ :

```

for k=1:1e6
s=sym('s');
s=sym('s');
num1=[-0.007734 0.004677 7.761e-8];
den1=[1 0.08749 0.001259 3.132e-7];
G11=tf(num1,den1);
g11=poly2sym(num1,s)./poly2sym(den1,s);
%-----%
num2=[-0.1314 -0.001673];
den2=[1 0.0385 0.000147];
G12=tf(num2,den2);
g12=poly2sym(num2,s)./poly2sym(den2,s);
%-----%
num3=[0.02071 6.281e-5];
den3=[1 0.009175 1.64e-5];
G13=tf(num3,den3);
g13=poly2sym(num3,s)./poly2sym(den3,s);
%-----%
num4=1.05*[0.001335 -1.943e-7];
den4=[1 0.03509 3.44e-9];
G21=tf(num4,den4);
g21=poly2sym(num4,s)./poly2sym(den4,s);
%-----%
num5=[-0.02075 -2.227e-5 -2.162e-7];
den5=[1 0.2141 8.726e-5 2.189e-6];
G22=tf(num5,den5);
g22=poly2sym(num5,s)./poly2sym(den5,s);
%-----%
num6=[0.001252 2.159e-5];
den6=[1 0.06249 0.0005558];
G23=tf(num6,den6);
g23=poly2sym(num6,s)./poly2sym(den6,s);
%-----%
num7=[-0.002809 -8.36e-5];
den7=[1 0.06943 0.001082];
G31=tf(num7,den7);
g31=poly2sym(num7,s)./poly2sym(den7,s);
%-----%
num8=[-0.004665 -4.227e-5 -3.085e-7];
den8=[1 0.4551 0.003889 2.48e-5];

```

```

G32=tf(num8,den8);
g32=poly2sym(num8,s)./poly2sym(den8,s);
%-----%
num9=[0.000137 1.657e-6];
den9=[1 0.05461 0.0003927];
G33=tf(num9,den9);
g33=poly2sym(num3,s)./poly2sym(den3,s);
%-----%
G_sym=[g11 g12 g13;g21 g22 g23;g31 g32 g33];
G_tf=[G11 G12 G13;G21 G22 G23;G31 G32 G33];
%-----%
%-----First column of K-----%
A11=randperm(a,b);
a11=vpa(poly2sym(A11/d,s));
B11=randperm(a,c);
b11=vpa(poly2sym(B11/d,s));K11=(a11./b11);
A21=randperm(a,b);
a21=vpa(poly2sym(A21/d,s));
B21=randperm(a,c);
b21=vpa(poly2sym(B21/d,s));K21=(a21./b21);
A31=randperm(a,b);
a31=vpa(poly2sym(A31/d,s));
B31=randperm(a,c);
b31=vpa(poly2sym(B31/d,s));K31=(a31./b31);
%-----Second column of K-----%
A12=randperm(a,b);
a12=vpa(poly2sym(A12/d,s));
B12=randperm(a,c);
b12=vpa(poly2sym(B12/d,s));K12=(a12./b12);
A22=randperm(a,b);
a22=vpa(poly2sym(A22/d,s));
B22=randperm(a,c);
b22=vpa(poly2sym(B22/d,s));K22=(a22./b22);
A32=randperm(a,b);
a32=vpa(poly2sym(A32/d,s));
B32=randperm(a,c);
b32=vpa(poly2sym(B32/d,s));K32=(a32./b32);
%-----%
%-----Third column of K-----%
A13=randperm(a,b);
a13=vpa(poly2sym(A13/d,s));
B13=randperm(a,c);
b13=vpa(poly2sym(B13/d,s));K13=(a13./b13);
A23=randperm(a,b);
a23=vpa(poly2sym(A23/d,s));
B23=randperm(a,c);
b23=vpa(poly2sym(B23/d,s));K23=(a23./b23);
A33=randperm(a,b);
a33=vpa(poly2sym(A33/d,s));
B33=randperm(a,c);
b33=vpa(poly2sym(B33/d,s));K33=(a33./b33);
%-----%
K=[K11 K12 K13;K21 K22 K23;K31 K32 K33];

```

```

Q=K*G_sym;
%-----%
ww=10;
www=10;
w=logspace(-1,6,ww);
%-----G(1,1)-----%
Center11=(subs(Q(1,1),complex(0,w)));
Radius1=(abs(subs(Q(1,2),complex(0,w)))+(abs(subs(Q(1,3),complex(0,
w)))));
%-----%
for j=1:ww
    xj=real(Center11(1,j));% x coordinate of center %
    yj=imag(Center11(1,j));% y coordinate of center %
    rj=Radius1(1,j);% radius %
    th=0:pi/www:2*pi;
    aj=rj*cos(th)+xj;
    bj=rj*sin(th)+yj;
    if (rj<sqrt(((aj).^2)+((bj).^2)))
        'not encircling'
    else
        break
    end
end
j
%-----G(2,2)-----%
Center22=subs(Q(2,2),complex(0,w));
Radius2=(abs(subs(Q(2,1),complex(0,w)))+(abs(subs(Q(2,3),complex(0,
w)))));
%-----%
for i=1:ww
    xi=real(Center22(1,i));% x coordinate of center %
    yi=imag(Center22(1,i));% y coordinate of center %
    ri=Radius2(1,i);% radius %
    th=0:pi/www:2*pi;
    ai=ri*cos(th)+xi;
    bi=ri*sin(th)+yi;
    if (ri<sqrt(((ai).^2)+((bi).^2)))
        'not encircling'
    else
        break
    end
end
i
%-----G(3,3)-----%
Center33=(subs(Q(3,3),complex(0,w)));
Radius3=(abs(subs(Q(3,2),complex(0,w)))+(abs(subs(Q(3,1),complex(0,
w)))));
for h=1:ww
    xh=real(Center33(1,h));% x coordinate of center %
    yh=imag(Center33(1,h));% y coordinate of center %
    rh=Radius3(1,h);% radius %
    th=0:pi/www:2*pi;
    ah=rh*cos(th)+xh;

```

```

        bh=rh*sin(th)+yh;
        if (rh<sqrt(((ah).^2)+((bh).^2)))
            'not encircling'
        else
            break
        end
    end
end
h
%|%
if(j==ww)
    'now culomnn dominance achieved'
    break
else
end
end

end
K
'number of iterations:'
k

```

## 8.8 Script file for Executing Newton Raphson Algorithm

```

%-----Newton Raphson methodology-----%
% n10, n02 are the starting points%
%(n1 n2)T=(n10 n20)T - [Jac(n10,n02)]-1 x [dJ/dn1(n10,n20)
dJ/dn2(n10,n20)]T%
% Jac(n1,n2)=[dJ2/dn1n1 dJ2/dn1n2;dJ2/n2n1 dJ/n2n2]
aa=[-6 -3 -1 0 1 3 6];
bb=[-6 -3 -1 0 1 3 6];
for i=1:length(aa)
    for j=1:length(bb)
        N1=[aa(1,i);bb(1,j)]
syms n1 n2
for u=1:200
    N0=N1;
    Jac_mat11=dJ2_dn1dn1;
    Jac_mat12=dJ2_dn1dn2;
    Jac_mat21=dJ2_dn2dn1;
    Jac_mat22=dJ2_dn2dn2;
    Jac_mat=[Jac_mat11 Jac_mat12;Jac_mat21 Jac_mat22];
    Jac_mat_inv=inv(Jac_mat);

    Jac_mat_inv11_n1_0_n2_0=subs(subs(Jac_mat_inv(1,1),n1,N0(1,1)),n2,N0
(2,1));

    Jac_mat_inv12_n1_0_n2_0=subs(subs(Jac_mat_inv(1,2),n1,N0(1,1)),n2,N0
(2,1));

    Jac_mat_inv21_n1_0_n2_0=subs(subs(Jac_mat_inv(2,1),n1,N0(1,1)),n2,N0
(2,1));

```

```

Jac_mat_inv22_n1_0_n2_0=subs(subs(Jac_mat_inv(2,2),n1,N0(1,1)),n2,N0
(2,1));
    JAC_INV=[Jac_mat_inv11_n1_0_n2_0
Jac_mat_inv12_n1_0_n2_0;Jac_mat_inv21_n1_0_n2_0
Jac_mat_inv22_n1_0_n2_0];
    Jn1_n1_0_n2_0=subs(subs(dJ_dn1,n1,N0(1,1)),n2,N0(2,1));
    Jn2_n1_0_n2_0=subs(subs(dJ_dn2,n1,N0(1,1)),n2,N0(2,1));
    F_N0=[Jn1_n1_0_n2_0;Jn2_n1_0_n2_0];
    N1=vpa(N0-(JAC_INV*F_N0));
    ERR=N1-N0;
    if
        (0<ERR(1,1))&&(ERR(1,1)<1e-
10)&&(0<ERR(2,1))&&(ERR(2,1)<1e-10)
        break
    end
end
uu{i,j}=u% Number of iterations required for finding the root%
NN1{i,j}=[N1(1,1);N1(2,1)]%roots of J function%
J_at_n1_n2{i,j}=subs(subs(J,n1,N1(1,1)),n2,N1(2,1));%value of J at
pairs of roots%
dJ_dn1_at_n1{i,j}=subs(dJ_dn1,n1,N1(1,1));
dJ_dn1_at_n1_n2{i,j}=subs(dJ_dn1_at_n1{i,j},n2,N1(2,1));%To prove
that pairs of roots make dJ_dn1=0%
dJ_dn2_at_n1{i,j}=subs(dJ_dn1,n1,N1(1,1));
dJ_dn2_at_n1_n2{i,j}=subs(dJ_dn2_at_n1{i,j},n2,N1(2,1));%To prove
that pairs of roots make dJ_dn2=0%
dJ2_dn1dn1_at_n1{i,j}=subs(dJ2_dn1dn1,n1,N1(1,1));
dJ2_dn1dn1_at_n1_n2{i,j}=subs(subs(dJ2_dn1dn1_at_n1{i,j},n1,N1(1,1))
,n2,N1(2,1));% A required condition for local minimum%
dJ2_dn2dn2_at_n1{i,j}=subs(dJ2_dn2dn2,n1,N1(1,1));
dJ2_dn2dn2_at_n1_n2{i,j}=subs(dJ2_dn2dn2_at_n1{i,j},n2,N1(2,1));%sec
ond derivative in respect to n2%
dJ2_dn1dn2_at_n1{i,j}=subs(dJ2_dn1dn2,n1,N1(1,1));
dJ2_dn1dn2_at_n1_n2{i,j}=subs(dJ2_dn1dn2_at_n1{i,j},n2,N1(2,1));
D{i,j}=(dJ2_dn1dn1_at_n1_n2{i,j}*dJ2_dn2dn2_at_n1_n2{i,j})-
((dJ2_dn1dn2_at_n1_n2{i,j})^2);% should be positive if
dJ2_dn1dn1_at_n1_n2{i,j} to prove that pairs of roots is making J
local minimum%

    end
end
J_vec=vertcat(J_at_n1_n2{:});
dJ_dn1_vec=vertcat(dJ_dn1_at_n1_n2{:});
dJ_dn2_vec=vertcat(dJ_dn2_at_n1_n2{:});
dJ2_dn1dn1_at_n1_n2_vec=vertcat(dJ2_dn1dn1_at_n1_n2{:});
D_vec=vertcat(D{:});
ROOTS_vec=vertcat(NN1{:});
for k=1:length(bb)^2;
    if
        (D_vec(k,1))>0
        &&(dJ_dn1_vec(k,1)<1e-
30)&&(dJ_dn2_vec(k,1)<1e-30)&&(dJ2_dn1dn1_at_n1_n2_vec(k,1)>0);
        Data_Mat_yes{k,1}=[ J_vec(k,1) D_vec(k,1) dJ_dn1_vec(k,1)
dJ_dn2_vec(k,1) dJ2_dn1dn1_at_n1_n2_vec(k,1) k ROOTS_vec((2*k)-1,1)
ROOTS_vec(2*k,1)];
    end
end

```

```

else
    Data_Mat_no{k,1}=[J_vec(k,1)    D_vec(k,1)    dJ_dn1_vec(k,1)
dJ_dn2_vec(k,1) dJ2_dn1dn1_at_n1_n2_vec(k,1) k ROOTS_vec((2*k)-1,1)
ROOTS_vec(2*k,1)];
end
end
Data_Mat_yes=vertcat(Data_Mat_yes{:})
Data_Mat_no=vertcat(Data_Mat_no{:})

```